Real Time NMR analysis of Melamine Formaldehyde Resin Reactions

THE UNIVERSITY OF
WAIKATO
Te Whare Wānanga o Waikato

A thesis submitted in partial fulfilment

of the requirements for the degree

of

Master of Science

in Chemistry

at

The University of Waikato

by

Yuan Wang

_____

The University of Waikato
2012

Abstract

This investigation was carried out on behalf of the Momentive Specialty Chemicals Pty Ltd, Mt Maunganui. The aim of the investigation was to develop a method to analyse the formation of melamine formaldehyde resins *via* an *in situ* real time NMR experiment leading to quantitative NMR intensities of the resin up to the stages of its Industrial Resin Endpoint (IRE).

In order to run an *in situ* reaction for the melamine formaldehyde resin system and monitor it in real time, both qualitative and quantitative NMR acquisition methods were required. The qualitative method was power gated and used to obtain results *in situ* and in real time. However to render it quantitative, it was necessary to develop a quantitative method which was initially executed to obtain a conversion factor for relating the qualitative results obtained in the *in situ* experiment to quantitative results performed by doing inverse gated NMR spectra on a final form of the resin. The development of this technique required the determination of the longitudinal relaxation times (T_1) of the species within the melamine reaction as these were required to derive the necessary repetition rates employed in the NMR acquisition methods.

In general, this project involved the development of the above mentioned NMR analytical protocols with tailoring to run this type of experiment in a 5 mm NMR tube using a 400 MHz NMR spectrometer whereby previous research on urea and phenol formaldehyde resins and employing identical NMR methodologies had relied on analyses conducted in a 10 mm NMR tube on a 300 MHz NMR instrument.

As a result, reaction profiles of the melamine resin reaction were obtained during a real time experiment. The reaction profiles of the addition stage of the melamine resin reaction showed that the increase in the methylol melamine species occurs very fast and is justified by the exponential decay of the methylene glycol species corresponding to the formaldehyde solution. The condensation stages of the resin

reaction were also observed until the IRE. The reaction profiles of the ether and methylene bridge links are clearly given showing that ether linkages predominate in the addition stage and plateaus, and methylene linkages only increase after the addition stage of the reaction. They provided insight to the reaction progress corresponding to addition and condensation stages of the melamine resin reaction.

Acknowledgements

Table of Contents

List of Figures

x

List of Tables

List of Equations

List of Abbreviations

NMR	Nuclear Magnetic Resonance
FID	Free Induction Decay
ESI - MS	Electrospray Ionisation mass spectrometry
FT	Fourier Transform
FT - IR	Fourier Transform Infrared Spectroscopy
ATR - IR	Attenuated Total Reflection Infrared Spectroscopy
MCT	Mercury Cadmium Telluride
MALDI - TOF	Matrix Assisted Laser Desorption Ionisation Time of Flight
NOE	Nuclear Overhauser Effect
CP	Cross Polarisation
r.f.	Radiofrequency
HMMM	Hexakis Methoxymethyl Melamine
VTU	Variable Temperature Unit
M:F	Melamine to Formaldehyde ratio
IRE	Industrial Resin Endpoint
RPI	Relative Peak Intensity
S/N	Signal to noise ratio
NS	Number of scans

DEPT   Distortionless Enhancement by Polarisation Transfer

HMBC   Heteronuclear Multiple Bond Correlation

HSQC   Heteronuclear Single Quantum Coherence

D1   Relaxation delay

VD   Variable delay

T1   Longitudinal relaxation time

T2   Transverse relaxation time

MPa   Mega Pascal

Hz   Hertz

MF   Melamine formaldehyde

Introduction

1.1 General Background

Resins are hydrocarbon secretions from plants dating back as far as 320 million years ago.[1] Ambers are a well known group of fossilized remains of tree resin which has been precious to many cultures since the Neolithic times.[2] Since then the uses of resin were well documented by Theophrastus in ancient Greece,[3] as well as in ancient Egypt.[4] Resins in contemporary times are useful components of varnishes, adhesives and laminates, polishes, perfume, incense and are valued for their ability to form enamel-like finishes.

Due to the vast applications of resins and their limited natural resources, alternative methods were required to produce resins more economically. This led to the production of the well known synthetic resins. Synthetic resins are the liquid material which have a property of interest similar to natural plant resins that are replicated by scientists, i.e. they are viscous and can harden permanently.

Synthetic resins can be typically classified as either thermoplastic resins or thermosetting resins. Thermoplastic resins are those which after being physically set can be reformed and softened upon pressure and heating. These thermoplastic resins include polyethylene resin, polypropylene resin and polyvinyl chlorine (PVC). Thermosetting resins are those which are typically softened during formation stages and set to their final shape, then cured by introducing a chemical curing agent or heat treatments. Once it is cured a thermosetting resin cannot be melted and reformed into a new shape.[5]

Since the development of thermosetting resins, the market for these resins increased rapidly and is now a multibillion dollar industry. Thermosetting resins include epoxy resins, phenolic resins and amino resins.

Epoxy resins were initially produced by the Devoe Raynolds company around 1947. They are often used in industrial and construction materials for high strength properties[6]

Phenolic resins were initially proposed by Baekeland, and they are commonly applied to moulding compounds in foundries, lacquers varnishes and spray insulators.[7,8]

Amino resins are comprised of urea formaldehyde resins, melamine formaldehyde resins and composite of melamine urea formaldehyde resins, of which urea formaldehyde resins are the most cost effective due to the relatively high cost of melamine in other resins.

Melamine formaldehyde resins, commonly known simply as melamine resins were produced industrially by Henkel and its condensation production patented around 1935. Furthermore, this was around the same time as the first feasible route to commercial production of melamine was developed by Ciba AG (Switzerland).[9, 5] This resin was initially invented by Talbot[10] for the use of casting and molding which was the building block of developing this resin for the vast range of applications melamine resins now contribute to.

A substantial improvement in chemical resistance properties and high water resistance occurred with melamine resins compared to urea formaldehyde resins. This resulted in the interest for the determination of the mechanism of the formation reaction and it is commonly covered within many textbooks related to plastics and polymers.[5, 9, 11] Accounts of chemical reaction, applications and their importance in the industrial field of melamine resins are described in these textbooks.

Melamine resins were initially invented for the purpose for moulding and casting,[10] but at present, due to the relatively high cost of production, melamine resins are generally used for surface coatings, laminates, moulding compositions, textile finishes and adhesives. [5,9,11-15] For the purposes of this project the melamine resins of

interest are those involved in the wood adhesive industry to produce plywood and laminated veneer lumber(LVL).

A major consideration for formaldehyde based resins is the release of formaldehyde upon hydrolysis. This is a significant problem associated with urea formaldehyde resins. Formaldehyde in melamine-based resins is tightly bound compared with the formaldehyde in urea based resins. Consequently, formaldehyde emissions are reduced and thus melamine resins are preferred in cabinets, furniture and timber.

The dominant limitation to the wider use of melamine resins in production is the cost of manufacturing.[16] The raw material, melamine is expensive in terms of the industrial revenue the resin is expected to produce, limiting the applications of melamine resins to materials which require relatively less of the material for example in coatings and laminates rather than the use as a bulk material.

The commercial production of melamine resins needs to be improved to be more efficient, economical and eco-friendly resin to be produced commercially whilst preserving or strengthening the physical properties in the final state of the resin product to improve its desirability for manufacture and utilization of these resins. Using spectroscopic characterization techniques of the reaction while it is progressing can provide valuable insights into the resin reaction and its evolution,

In previous studies, the use of NMR allowed Woolley[7] and Zeng[17] to develop *in situ* NMR methods which followed the formation reactions of phenolic- and urea-based formaldehyde resins in real time. These studies helped to account for the changes over time for those resins quantitatively. Being able to quantitate the NMR intensities observed allowed for a complete understanding of the reactions between the reactants used up to the commercial endpoints of the resins (i.e. the final product).

1.2 The chemistry of melamine formaldehyde resins

1.2.1 Raw materials

Melamine

Melamine was first synthesized in 1834 by a German chemist called Justus von Liebig, by heating ammonium thiocyanate. The material had no documented uses until Henkel's 1935 patent as mentioned earlier. [5,9,18] There are several methods to synthesize melamine, [12-14] the method used in early commercial production involved a two step reaction via the production of dicyanodiamide. The production of dicyanodiamide from calcium carbide is shown below:
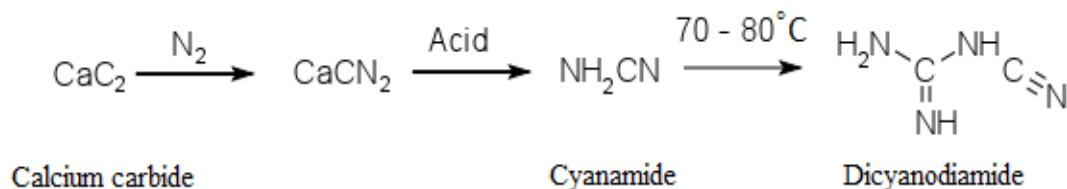
Figure 1.1 The production of dicyanodiamide from calcium carbide. Adapted from reference 9.

Dicyanodiamide is the product of treating calcium carbide with nitrogen gas to form calcium cyanamide. The acid treatment of calcium cyanamide removes the calcium component and produces cyanamide. The heating of cyanamide between 70 - 80 ℃ dimerises and produces dicyanodiamide (Figure 1.1). [5]
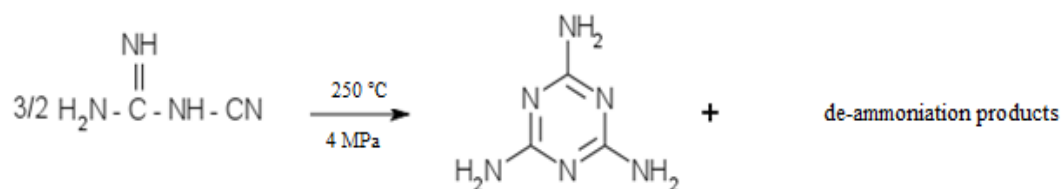
Figure 1.2 The dimerisation of dicyanodiamide under high yield melamine production conditions. Adapted from reference 9.

4

The heating of dicyanodiamide to just above its melting point of 209 °C results in an exothermic reaction which produces melamine plus a number of water insoluble de-ammoniation products. To maximise the yield of melamine the reaction was carried at 250 - 300 °C under approximately 4 MPa of pressure (Figure 1.2).

In modern commercial production, melamine is produced from urea (shown below).

$$6\ CO(NH_2)_2 \xrightarrow[-3\ H_2O]{NH_3} 3\ C(NH_2)N + 3\ CO\ (NH_2)ONH_4$$

Ammonia carbamate
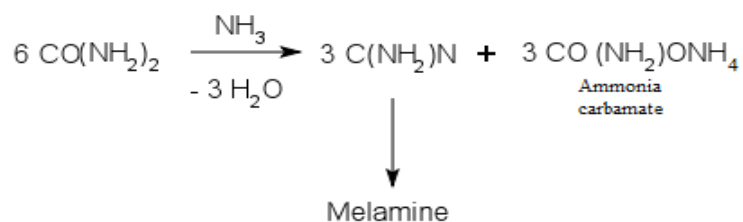
Melamine

Figure 1.3 The modern commercial synthesis for melamine. Adapted from reference 5.

This process requires six urea molecules to form one molecule of melamine. The three ammonia carbamate molecules can potentially be recycled to form urea. Thus this process is normally carried out parallel to the production of urea.

Formaldehyde

In 1859 Butlerov described the possibility of formaldehyde forming polymers during its isolation.[5] In 1872 Bayer reported that the reaction between phenols and aldehydes was found to produce a resin type material.[19] In 1899, Smith lodged the first patent involving phenol and aldehyde resins. It was British patent 16,274 for making a substitute for electrical insulation. What truly established the industrial utilisation of formaldehyde was when Baekeland patented the phenolic resins.[5] The production of formaldehyde is effected by the catalytic vapour phase oxidation of methanol over a metal catalyst, commonly silver.[7] The basic equation is shown in Equation 1.1.
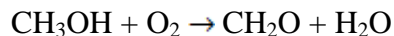
$$CH_3OH + O_2 \rightarrow CH_2O + H_2O \qquad \text{Equation 1.1}$$

In the process the methanol is vapourised and passed over the metal catalyst at 300 - 600 °C. The formaldehyde formed is absorbed into the aqueous reaction medium and passed through a fractioning column. A 37% solution of formaldehyde is removed at the bottom of the column and excess methanol is recycled from the top of the column.[5,9]

Aqueous formaldehyde solution (a.k.a. formalin) is known to undergo a rapid acid/base catalysed hydration reaction of formaldehyde to form methylene glycol shown in the equations below (Equation 1.2 and Equation 1.3):

$$nCH_2{=}O + H_2O \rightleftharpoons HOCH_2OH \text{ (methylene glycol)} \qquad \text{Equation 1.2}$$

$$nHOCH_2OH \text{ (methylene glycol)} \rightleftharpoons HO(CH_2O)_nH \text{ (polymeric methylene glycol)} + nH_2O$$

Equation 1.3

The equilibrium of the hydration reaction (Equation 1.2) of formaldehyde to form methylene glycol lies to the right thus in aqueous formaldehyde solution the primary constituents are methylene glycol and its polymeric species with less than 0.1% of monomeric formaldehyde present.[7,17]

$$HO(CH_2O)_nH + H_2O \rightleftharpoons HO(CH_2O)_{n-1}H + HOCH_2OH \qquad \text{Equation 1.4}$$

The depolymerisation of polymeric methylene glycol (Equation 1.4) becomes an important reaction relative to the overall reaction for the resin formation. In the

presence of methanol this is slightly stabilised due to the reaction with the methylene glycol species to form hemiacetals and their associated polymeric derivatives (Equation 1.5). In acidic conditions, the below equilibrium lies to the right but in basic conditions it lies to the left shown as the reversed equilibrium.[7]

$$CH_3OH + HO(CH_2O)nH \rightleftharpoons CH_3OCH_2O(CH_2O)_{n-1}H + H_2O$$ **Equation 1.5**

The reaction of formaldehyde in basic condition undergoes a base-induced disproportionation redox reaction of an aldehyde where the oxidation product is a salt and the reduction product is an alcohol:[7]

$$2CH_2=O + NaOH \rightleftharpoons CH_3OH + H(CO)O^- Na^+$$ **Equation 1.6**

This is called the Cannizzaro reaction and means that small amounts of formate (HCOO⁻) are usually present.[13]

1.2.2 Reactions between melamine and formaldehyde

The main practical application of melamine formaldehyde resins is in a network polymer form. Just like urea formaldehyde polymers, the resin preparation is carried out via two operations. [9, 14] The first operation is that the resin formation process produces resins of a low molecular weight, aqueous, semi-soluble polymer resin made in batches of approximately 16 tonnes each. The second operation consists of curing of the resin which involves the application of heat and pressing to produce the final condensed and cross-linked product. Both the modified resins and unmodified resin have commercial importance.

1.2.2.1 Modified resins

Methylol melamines reacting with alcohols under acidic conditions to produce methylated and butylated products are modified melamine formaldehyde resins in which their production requires the approximate melamine to formaldehyde (M:F) mole ratio of 1 : 3.3.[9] The resin is heated briefly for 15 minutes at 70 ℃ or until all the melamine is dissolved, and then spray-dried or allowed to crystallise into a solid composed mainly of monomeric methylol melamine.

The methylated product, trimethyl ether of trimethylol melamine (Figure 1.4) is used for textile finishing. It is made by heating methylol melamine at 70 ℃ in a solution at twice its weight of methanol and oxalic acid (0.5%) at 70 ℃ to form a clear solution. The solution is adjusted to a pH of 9 and concentrated to 80% solids under reduced pressure.
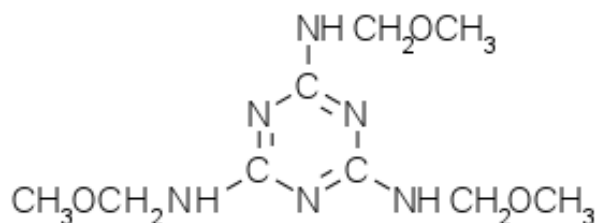
Figure 1.4 The structure of trimethyl ether of trimethylol melamine.

The butylated products are preferred for utilisation in surface coating formulations due to their compatibility with hydrocarbon solvents and with film-forming materials. The preparation of the butylated melamine formaldehyde resin involves using a melamine to formaldehyde (M:F) mole ratio Between 1:4 and 1:6 and a melamine to butanol (n- or iso) mole ratio between 1:4 and 1:8. The esterified groups are bound to half of the methylol groups. The rest of these methylol groups interact with each other to produce resin with a molecular weight between 800-1500. The butylated product is

brittle when used by itself thus it is more commonly mixed with other film-forming material such as alkyd resins and acts as a plasticizer.[9]

1.2.2.2 Unmodified resins

Unmodified melamine formaldehyde resins are primarily used in moulding compositions, laminates and various textile finishes. The methods for each application vary, but the example below for a laminating resin for the illustration of the general principles. The formaldehyde solution is made slightly alkaline (pH 7.5 - 8.5) with aqueous sodium carbonate then the addition of melamine is made to give an M:F ratio of approximately 1:3. This mixture is heated to 80 °C for 1 to 2 hours until the predetermined endpoint.[9] The end point is dictated by the degree of water tolerance required in the resin.[5,9,14] This research is ultimately directed to unmodified resins commonly employed for the plywood and LVL industries. There are three stages of reactions involved in the synthesis:[20]

(i) Addition stage reactions

The addition stage reactions are considered to be those which form the methylol melamines. Under alkaline conditions melamine reacts to produce methylol derivatives, each melamine has six possible positions to substitute methylol compounds at any of the three amine groups of the melamine.
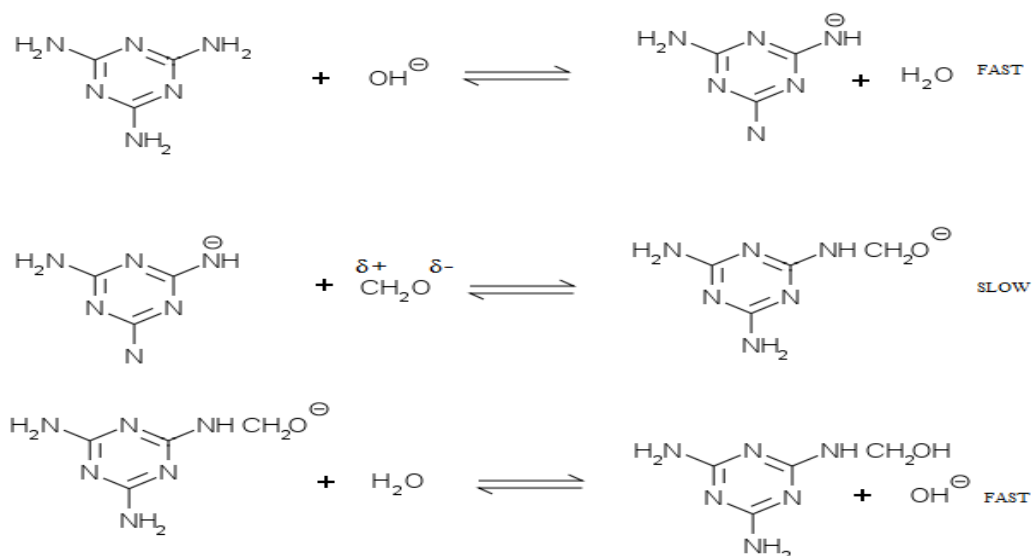
Figure 1.5 The mechanism of which formaldehyde reacts with melamine under basic conditions. Adapted from reference 18.

This can give six possible products when reacted, examples of possible products are as follows (Figure 1.6):
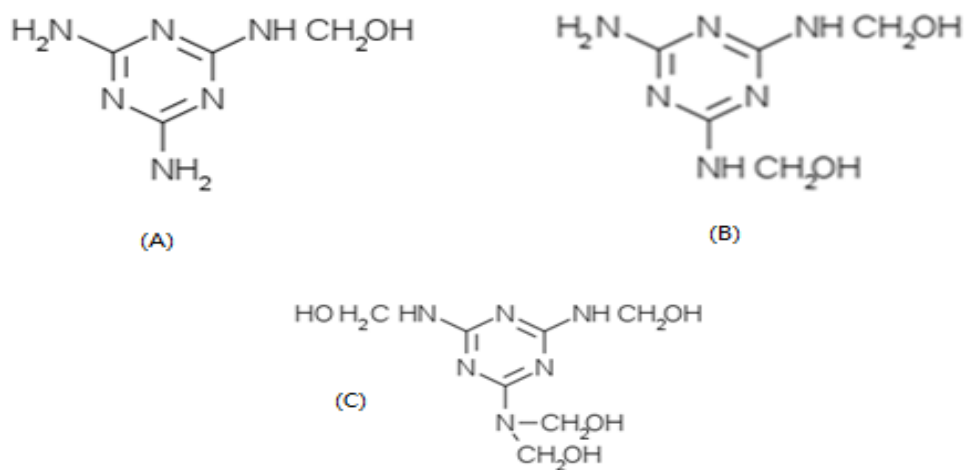
Figure 1.6 Possible methylol melamine products: (A) monomethylol melamine (B) dimethylol melamine (C) tetramethylol melamine.

10

The reactions, in reality, between melamine and formaldehyde are much more complicated than the idealized monomeric structures shown above as the resins could also contain dimeric, trimeric and oligomeric structures within the resin and when the MF resin is in a solution or liquid state. They are described as "living structures"[18] in that the methylol groups can change their position on different N-H groups i.e. they can cross link or hydrolyse again.

A generalised scheme of the pathways of methylolated melamines is shown below: (Figure 1.7)
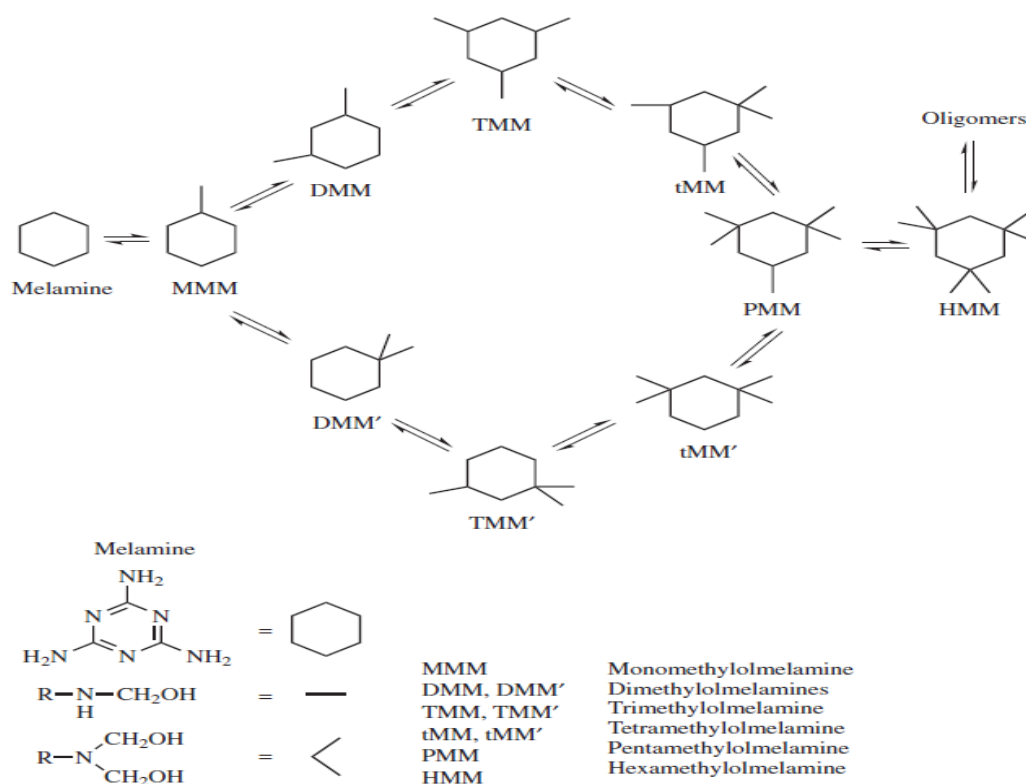
Figure 1.7 A generalised scheme of the pathways of methylolated melamine. Adapted from reference 15.

(ii) Condensation stage reactions

The methylol melamines undergo condensation reaction on heating, to form a more viscous resinous product. This resin increases in hydrophobicity as the reaction time increases until eventually the product forms an insoluble gel. The rate of resinification is highly dependent on pH. [5, 9] The minimum pH is 10 - 10.5 and either increasing or decreasing the pH will result in a increase in reaction rates. [9, 11, 21] It is envisaged that the methylol undergoes reaction with amino, imino, and other methylol groups (Figure 1.8):

(a) $R-NH\,CH_2OH\ +\ H_2N-R\ \longrightarrow\ R-NH\text{-}CH_2\text{-}NH-R\ +\ H_2O$

(b) $R-NH\,CH_2OH\ +\ R-NH-CH_2OH\ \longrightarrow\ R-NH-\underset{R-N-CH_2OH}{CH_2}\ +\ H_2O$

(c) $R-NH\,CH_2OH\ +\ HO-CH_2-NH-R\ \longrightarrow\ R-NH-CH_2\text{-}O\text{-}CH_2-NH-R\ +\ H_2O$

(d) $R-NH\,CH_2OH\ +\ HO-CH_2-NH-R\ \longrightarrow\ R-NH\text{-}CH_2-NH-R\ +\ CH_2O\ +\ H_2O$
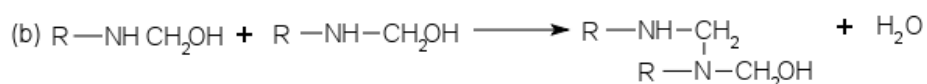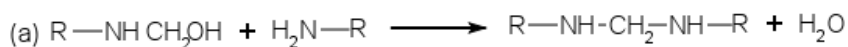
Figure 1.8 The reactions of methylol with amino, imino and other methylol groups where R is the melamine moiety. Adapted from reference 9.

The proposed mechanisms are in good concordance with many studies by which heating the methylol melamines produces water and formaldehyde, however the various reactions proposed have not been fully investigated with certainty in the literature. [5, 9] Elemental analysis of the products of heating hexamethylol melamine indicates ether, rather than methylene linkages. Thus it is believed that preparing resins with less formaldehyde produces more ether linkages.

(iii) Curing stage reaction

Curing is where the reactions of the unmodified resins convert from low molecular weight melamine formaldehyde resins into high molecular weight network polymers via the direct application of heat. The rate at which this occurs, however, may be accelerated in the presence of acidic compounds. Under the curing conditions, it is thought that the reaction involves the formation of methylene and dimethylene ether links. These are formed through the methylol groups of the methylol melamine positions and the reaction undergone is shown in Figure 1.8 (c) and (d). There are six positions in which the methylol group can be on the methylol melamine, this increases the complexity of the combinations of cross linking with either methylene or dimethylene ether as there is a high number of possible interactions with each methylol on each melamine moiety. Investigations show that during curing stages, there is less formaldehyde produced compared to water. The general assumption is that the dimethylene ether links predominate over the methylene links in the final product.

A proposed structure of a final liquid state resin is shown in (Figure 1.9):
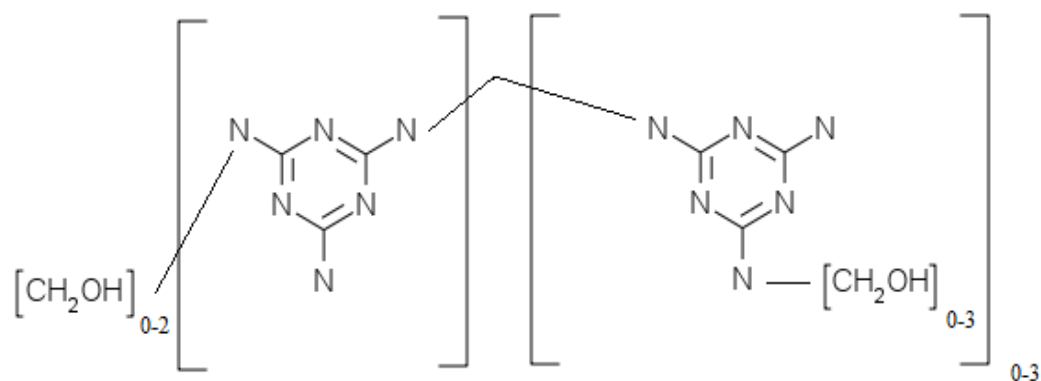
Figure 1.9 A proposed structure of a final liquid state melamine resin

13

These reactions become more complex when dealing with the various polymeric forms of formaldehyde and their reactions with dimers and trimers. Further complexity can be seen since the reactions shown above are mostly in the mono methylol melamine and not in longer chain linkage groups. Despite the diverse reactions achievable, a large number of synthesis parameters such as temperature and pH contribute to the reaction progress of a melamine formaldehyde reaction. These parameters affect the reaction pathways and hence the final structure and properties of the resin.

Nuclear Magnetic Resonance (NMR) spectroscopy has been used previously as a structural analysis technique of many resin species including melamine resin systems. NMR has provided the structural elucidation of the various isomers and the effect of synthesis conditions on the final resin structure. Therefore NMR is a common analytical technique for resins and is the paramount technique for this investigation.

1.3 NMR Spectroscopy

1.3.1 Introduction

NMR Spectroscopy is a technique used for structural elucidation.[22] It was independently discovered between 1945 - 1946 by two groups; Bloch *et al* at Stanford and Purcell *et al* at Harvard. In 1952 they received a joint Nobel Prize for the discovery and development of this technique. The importance of NMR methods has increased steadily since then and this was highlighted in 1991 when Richard R. Ernst received a Nobel Prize in chemistry for his contributions to the development of the methodology of high resolution NMR spectroscopy. The importance of NMR methodologies is furthermore demonstrated in 2002 and 2003 when K. Wüthrich, P.

Lauterbur and P. Mansfield were awarded the Nobel Prize for their contributions to NMR research in medicine, chemistry and biochemistry. [23,24]

The theory behind NMR is well documented in the literature. [23,25,26] Section 1.3.2 - 1.3.6 (see below) include a brief description of the NMR concepts and techniques that were important for the current investigation. Application of these techniques allow for the determination of the species in the mixtures and their interactions with each other throughout a polymerisation reaction.

1.3.2 Nuclear magnetism

NMR spectroscopy utilises the magnetic properties of the atomic nucleus and observes the response of the perturbation to the system from equilibrium via the use of a magnetic field (B_0).

Certain nuclei of natural isotopes possess an intrinsic quantized nuclear spin or angular momentum (ρ), as defined in Equation 1.7:[24, 27]

$$\rho = \hbar\sqrt{I(I+1)}$$

Equation 1.7

where I is the spin quantum number and $\hbar$ is the reduced Planck's constant ($= h/2\pi$).

The spin quantum number (I) is dependent on the isotope . Allowed values of I, range from values of I, I - 1, I - 2, down to -I. There are 2I + 1 allowed spin states.

A nucleus with a spin also has a magnetic moment, μ. The magnetic moment (μ) and angular momentum (ρ) arising from it behave as vectors which are either aligned with (same direction) or opposite (opposite direction) to the applied magnetic field (B).

The ratio (γ) between the aligned or opposed energies is referred to as the magnetogyric ratio or gyromagnetic ratio and is given by Equation 1.8. The gyromagnetic ratio is different for each magnetically active nucleus.

$$\gamma = \mu / \rho \qquad \qquad \textbf{Equation 1.8}$$

A large γ value indicates a sensitive nucleus (easy to observe) and vice versa.

The resonant frequency of an NMR active species is directly proportional to the strength of the magnetic field. The intensity of the detected NMR signal(s) is directly related to the applied magnetic field.

With no external magnetic field applied, the two spin states present (+1/2 and -1/2) have the same energy, but when exposed to a magnetic field (B_0) their degeneracy is destroyed due to the interaction between the magnetic moment (μ) and magnetic field (B_0). The potential energy of the magnetic dipole is μB_0 or $-\mu B_0$ and since the spin axis aligns with the z axis in the same direction as B_0, what results is an energy difference between the two spin states of:

$$\Delta E = 2\,\mu B_0 = E_{-1/2(a)} - E_{+1/2(b)} \qquad \qquad \textbf{Equation 1.9}$$

Since the lower energy state (a) is preferred. ΔE follows the Bohr model:

$$h\nu_0 = \Delta E = \gamma \hbar B_0 \qquad \qquad \textbf{Equation 1.10}$$

thus the rearrangement of these equations will allows the frequency of precession (ν_0) or Larmor frequency of the nucleus to be calculated (Equation 1.11).[28]

$$\nu_0 = \gamma B_0 / 2\pi \qquad\qquad \textbf{Equation 1.11}$$

The energy difference between the aligned and opposite spin states can be expressed as:

$$\Delta E = 2\,\mu B_0 = \gamma \hbar B_0 = \gamma h B_0/2\pi = E_{-1/2} - E_{+1/2} \qquad\qquad \textbf{Equation 1.12}$$

If thermal equilibrium is reached the population of the energy levels will mimic those of the Boltzmann's distribution. In this case, the net or equilibrium magnetisation(M_0) should be in parallel with the applied magnetic field direction which is defined using Cartesian coordinates as the z axis. If this is applied to a single nucleus then the observed magnetisation would be shown as Figure 1.10(a). If the magnetisation of the z axis of an entire sample was considered, a macroscopic magnetisation would be observed (Figure 1.10b). To simplify the system, a set of coordinates are chosen and rotated with the nuclear precession so only the equilibrium magnetisation (M_0) is observed, This choice of rotating axis is known as the rotating frame of reference (Figure 1.10c)
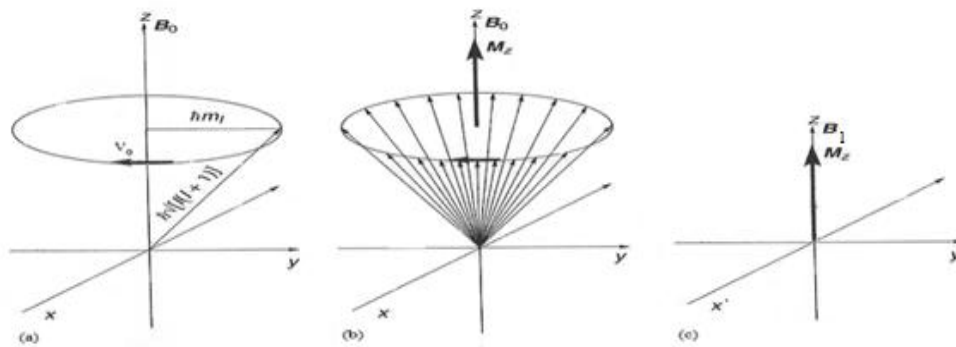
Figure 1.10 (a) Larmor precession of a single nucleus, (b) excess low energy nuclei in a sample and (c) excess low energy nuclei presented as a rotating frame. Adapted from reference 27.

1.3.3   Pulse

In a rotating frame, the sample magnetisation (M) and the B_1 field vector are static, one on the z axis and one at right angles to it (x axis) . The application of a radio frequency (r.f.) pulse on the B_1 field vector allows the nucleus to absorb the energy causing the degeneracy of the spin states to be destroyed, thus causing the nucleus to resonate. The applied pulse causes the sample magnetisation to be rotated around the B_1 field vector (x axis) at a speed depending on the field strength and in theory it can be rotated by a defined angle. When the pulse applied causes the magnetisation to turn and be rotated into the y axis direction, it is said that a $\pi/2$ or 90 °pulse has been applied. (Figure 1.11)
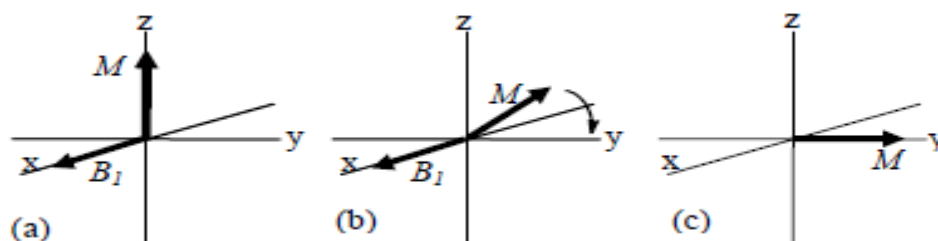
Figure 1.11 The magnetisation from equilibrium to a 90 °pulse. (a) r.f. radiation perpendicular to static field, (b) sample magnetisation driven around the x axis, (c) the position of the sample magnetisation after a 90 °pulse. Adapted from reference 7.

The generation of a detectable signal arises from the voltage created in the receiver coil. This only occurs when the sample magnetisation is in the x-y plane. When a π or 180 °pulse is applied the sample magnetisation is aligned in the z axis direction, and no x-y axis signal is generated, in contrast when the sample is subjected to a $\pi/2$ or 90 °pulse the sample magnetisation is completely aligned along the x-y plane, with no residual magnetisation in the z axis, thus providing maximum x-y axis signal intensity. The component of the magnetisation in the z axis after a pulse of angle θ is given by the Equation 1.13:

$$M_z = M_0 \cos \theta \qquad\qquad\qquad \textbf{Equation 1.13}$$

When the r.f. pulse is applied, NMR active nuclei undergo resonance, and the net sample magnetisation rotates about the x axis. When the r.f. pulse is turned off the resonant energy used to disrupt the degeneracy dissipates and decays back to equilibrium, and the consequential precessing magnetisation will induce an oscillating current within the receiver coil which is detected. This is the so called free induction decay (FID) NMR signal, induced in the coil as induced alignment magnetism decays back to equilibrium.

A useful analogy of this behaviour is that of a plucked string on a musical instrument. Little can be heard from the initial impulse but the resulting sound lasts for a significant time as the system (string) returns to equilibrium during which time the amplitude of the sound decreases but the frequency remains the same.

1.3.4 Relaxation

When a system is interrupted from equilibrium in the static field B_0, the nuclear spins will relax back to its original equilibrium condition along the z axis exponentially (Bloch theory). This does not happen instantly. Rather it takes a finite amount of time, characterised by a definable time constant (T_1) for it to readjust to the changed conditions. This time constant is known as the longitudinal (or spin-lattice) relaxation time and is given by the expression:

$$M_z = M_0(1-e^{-t/T1}) \qquad\qquad\qquad \textbf{Equation 1.14}$$

Where M_z is the sample magnetisation and M_0 is the magnetisation at thermal equilibrium. This relaxation is what is observed in the FID period.

1.3.5 The NMR experiment

When a sample is subjected to the NMR technique, a short r.f. pulse is applied and the radiation from the pulse excites all the nuclei within the analyte to undergo resonance. The response decays over a period of time and can be observed as the FID. This experiment can be repeated (number of scans), accumulated and the individual FID's summed to increase the signal-to-noise of the signals. Once the desired number of scans (NS) is reached the data collected in the time domain (more commonly known as the FID) is converted into a signal in the frequency domain using a mathematical operation known as the Fourier Transformation (FT). The function of frequency produced is the conventional NMR spectrum.
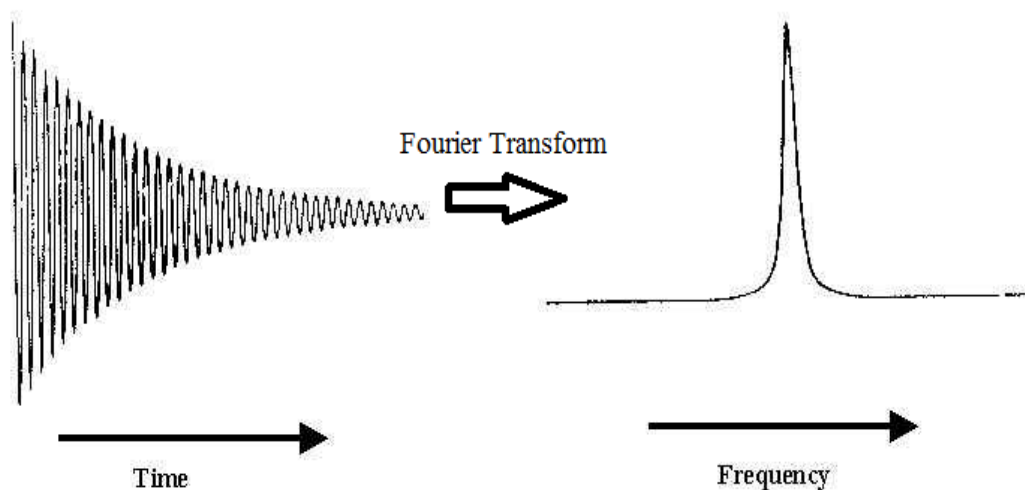
Figure 1.12 The Fourier transformation from an FID (time domain) to an NMR spectrum (frequency domain). Adapted from reference 29.

1.3.6 The NMR spectra

Every molecule has a unique structure and shape, which is dictated by the outer electron clouds of the atoms and their associated neighbouring atoms. The interactions between the atoms with a molecule can produce unique environments called "chemical environments". These interactions of the outer electron clouds have small influences on the magnetic field applied on the nucleus, their differences in the nuclear precession frequency are called chemical shifts. Thus a unique spectrum of discrete frequencies for a given NMR active nucleus is produced instead of a single Larmor frequency.

The effective magnetic field experienced by the nucleus therefore dictates the chemical shift of a nucleus since the magnetic field and the frequencies are proportional to each other. A consequence for nuclei with spin is coupling, the interaction between two nuclei through a bond may cause a shielding effect or deshielding of the nucleus from external magnetic field. The signal arising from the nucleus coupled to n amounts of equivalent nuclei with I number of spins will be split into a multiplet, with the number of resonances observed following the multiplicity rule of $2nI + 1$. Their relative intensities can be defined by Pascal's triangle.[28]

Carbon -13 (^{13}C) NMR

The element carbon consists predominantly of two stable isotopes ^{12}C and ^{13}C with the natural abundance of 98.9% and 1.1% respectively. While the ^{12}C nucleus of the major isotope is NMR inactive, the low abundant ^{13}C nucleus is NMR active. This makes NMR spectroscopy of organic chemistry limited to carbon - 13. The magnetic moment of ^{13}C is smaller than ^{1}H by a factor of four, and as a consequence the sensitivity of the ^{13}C NMR experiment is less than that of ^{1}H NMR. The detection of

^{13}C is further rendered challenging by the low natural abundance of the ^{13}C nucleus thus making it more difficult to detect.

For many ^{13}C NMR experiments it is desirable and necessary to completely ignore the coupling between different nuclei (e.g. between C and H), thus producing signal which normally would be multiplets as a single discrete resonance. This "ignoring of the coupling" referred to as "decoupling" results in a remarkable increase in signal intensity and simplicity in the analysis of the NMR spectrum. Decoupling occurs when the r.f. field is exactly tuned to the frequency of a nucleus such as the ^{1}H nucleus while obtaining data of the nuclei coupled to it i.e. ^{13}C. The proton decoupled ^{13}C - NMR spectrum thus simply illustrates the single discrete resonance of the individual carbon atoms.

As a consequence of the ^{13}C nucleus's insensitivity and low natural abundance the amount of time required to carry out an NMR analysis in greatly increased compared to that of a proton spectrum. This means that the majority of ^{13}C NMR analysis is routinely carried out under *qualitative* conditions where the observed intensities of peaks are not able to be correlated to the quantity of that nucleus in the sample. To perform a highly precise ^{13}C quantitative NMR analysis of a system (as will be the subject of the present study), considerable difficulties in choosing appropriate experimental conditions are experienced. Factors such as the relaxation time (T_1) and the NOE factor are two of the key parameters required to be determined for quantitative experiments to be successful (see Section 3.6.1 and 3.8.2 respectively).

1.4 Previous Studies of Melamine Formaldehyde resins

Melamine resins have been formulated primarily on an empirical basis due to the complexity and instability of the resin. The chemical analysis was difficult and the commercial drive for the immediate supply allowed the industry to be satisfied with incomplete fundamental research on these systems. Improved analytical techniques were required to investigate the chemistry of melamine resins throughout the formation reaction.

Many techniques have been used in the past for the characterisation of melamine resins including Matrix Assisted Laser Desorption Ionisation - Time of Flight - mass spectrometry (MALDI-TOF-MS),[29] Raman spectroscopy,[30] high performance liquid chromatography (HPLC),[31-32] Ultraviolet spectroscopy (UV),[32-33] Fourier transform infrared spectroscopy (FT-IR). [29,34 -35] The technique of primary importance to resin analysis, mainly for its ability to elucidate the structure determining properties is ^{13}C NMR.

Extensive research on the physical and chemical properties of melamine resins and their application to the wood industry has been done by Pizzi.[16] He described the chemistry of the reactions between melamine and formaldehyde, the possible structures they can form and the kinetics of the acid condition reactions of melamine resins.

Saito and Naito carried out research on acid[36] and base[37] hydrolysis of the reactions of (hydroxymethyl) melamine, products of reaction between melamine and formaldehyde and obtained kinetic information deduced from the rate of hydrolysis of di - substituted methylol melamine using acid and base catalysts. In their studies of the basic conditions it was revealed that between the pH of 8 and10, first order kinetics are followed and when the pH was increased to the range of 11 - 13.5, the slope of the rate constant increased and was found to follow third order kinetics overall.

In 1949, Widmer[38] devised a method for characterising the melamine and urea resin in technical products by preparing crystalline compounds and observing them under the microscope. Melamine crystals and long crystalline needles of urea dixanthate were able to be visualised and allowed for the urea and melamine to be distinguishable even in a cured resin. In this investigation, Widmer[38] also developed a method of quantifying the melamine in the condensation products of the resin. During this procedure, the resin is destroyed by aminolysis under pressure leaving the melamine unchanged. The melamine is then converted to melamine picrate to be crystallised and weighed. This method allowed for the species within a mixed cured resin of melamine and urea to be quantitatively identified.

Hirt *et al.*[39] described a rapid method for detecting melamine by ultraviolet spectroscopy. The melamine formaldehyde resin in this case is hydrolysed to melamine by boiling with hydrochloric acid under reflux. The detection of the melamine is aided by its characteristic strong absorption at 235 nm.

Snyder and Vuk[21] investigated the self condensation of commercial hexakis (methoxymethyl) melamine (HMMM) resins and reported that condensation of HMMM is pH sensitive and is also dependent on alcohol content.

Blank[40] conducted GPC analysis of the melamine resins and showed that upon self condensation, demethylolation of the resin occurred. According to Blank's studies, water and high reaction temperatures were factors promoting the demethylolation and elimination of methanol.

Chang[41] used HPLC methods to separate different components of HMMM and the different components of the resin were characterised by liquid chromatography - mass spectrometry (LC-MS). This technique afforded identification of twenty monomeric compounds and thirteen dimeric compounds.

^{13}C NMR has been utilised for investigations of melamine resins and the ability to assign all the signals was an advantage in terms of characterisation of the

functionalities within the resin.[42] This was a major advancement into understanding the polymer structure and relating this to the properties of the resin.

Subraya *et al.*[43] published a paper on highly methylolated melamine resins describing the structure with ^{13}C NMR spectroscopy and applied the technique of DEPT to justify the assignment of signals. Their advancements also included carrying out quantitative NMR experiments on the resins with moderate success. They concluded from the results of ^{13}C NMR and GPC that the self condensation of HMMM predominantly produced methylene linkages. The result of this study were consistent with the results of Blank[40] and Chang.[41]

Another interesting paper regarding the advancement of quantitative studies Scheepers *et al.,*[44] where the authors described the basic criteria required to obtain quantitative results. They quantitatively described the curing stages of the resin with the use of ^{1}H and ^{13}C NMR by regulating experiments. This was achieved by methylolating the melamine then placing the resin in a sealed (*in vacuo*) tube and regulating the temperature at 90 °C for different reaction times (stages). This provided mechanistic details of the curing stage however this was only achievable under isothermal conditions. This meant that the kinetic studies of the addition stages and some of the condensation stages were undescribed.

There is a need for quantitative *in situ* reaction monitoring under the commercial conditions of resin production. The ability to monitor the reaction in real time and provide quantitative analysis of the reaction can provide insight to the reaction pathways.

The significant advancement towards the quantitative real time reaction monitoring was proposed by Zeng,[17] regarding urea formaldehyde resins. The research provided a novel NMR acquisition method where the real time qualitative NMR data obtained from an *in situ* resin reaction, could be converted to quantitative data. In addition, maintaining the synthesis conditions similar to those applied industrially produced data corresponding closely to the commercial process.

Seven years later Woolley[7] conducted the real time analysis of phenolic formaldehyde resins by adapting the method developed by Zeng to better suit phenolic resins. The advantage of Woolley's method was that it allowed for reaction profiles to be built quantitatively. The monitoring of the relative concentrations of each individual species and intermediates within the resin was also possible, thus providing kinetic information about the resin formation process.

The NMR data obtained at specific time intervals during the synthesis correlates effectively to "snapshots" of the reactions progress. This meant that the conditions of the experiment were completely controlled by Zeng and Woolley. This allowed them to carry out investigations of different reaction parameters such as temperature and pH. This allowed the effects of different parameters to be investigated and its effects on the structure of the resin to be monitored. This led to the proposal of the optimum conditions of the formation of the urea and phenolic formaldehyde resins.

1.5 Objectives of present investigation

Two principal goals for this research were:

1. Adoption and adaption of the methods utilised by Zeng and Woolley and expansion on their methods so that the analysis of melamine formaldehyde resin was possible. Several factors needed to be addressed:

2. Determination of whether the parameters derived from previous research on urea formaldehyde or phenol formaldehyde resins could be applied to melamine formaldehyde resins.

3. Determination of the logistics of carrying out this investigation in a 5 mm NMR tube with a 400 MHz NMR instrument. In the past the methods used by Zeng and Woolley were conducted in a 10 mm probe (associated with a 300 MHz NMR instrument) which obviously allows for greater sensitivity, however for this research this was not an available option due to the malfunctioning of the 10 mm NMR probe associated with the 300 MHz NMR instrument.

4. Determination of the main parameters required for this particular investigation.

5. The investigation of transient species and products as a result of the synthesis by monitoring their concentrations of a commercial melamine resin process.

This investigation will give insight to the melamine resin reaction and form the basis for further work. The information is intended to aid the optimisation of these adhesives supplied to the plywood and LVL industries, and thus develop new, cost effective and original resins.

2 Materials and Methods

Methodology, parameters and experimental conditions of the Nuclear Magnetic Resonance (NMR) technique used on the commercial resin reaction are discussed.

In addition to the NMR methodologies mainly used, Infrared spectroscopy (IR), Matrix Assisted Laser Desorption Ionisation Time-of-Flight mass spectrometry (MALDI TOF), and Electrospray Ionisation mass spectrometry (ESI-MS) methods employed for the analysis of the melamine resin are also described.

The preparation of melamine formaldehyde resins used for the *in situ* real time NMR monitoring is also briefly described. Due to commercial confidentiality not all details of this process can be divulged.

2.1 Nuclear Magnetic Resonance
2.1.1 General NMR conditions

NMR Spectra were acquired using a 5 mm multinuclear probehead installed in a Bruker Avance DRX400 Fourier Transform Nuclear Magnetic Resonance spectrometer, operating at 400.13 MHz for proton (^{1}H) and 100.62 MHz for carbon (^{13}C).

Unless otherwise stated, NMR spectra were recorded at 303.15 K (30 ℃), with the chemical shifts reported relative to the acetic acid methyl group ($\underline{C}$H$_3$COOH) in the internal solvent tube kept separate from the reaction mixture (described below) which gave a resonance peak at 21.3 ppm with an SR (spectral reference correction) = 0.06. The Free induction decay (FID) was processed using the Bruker supplied

Topspin software (version 3.0, Bruker BioSpin 2010) on both online and offline terminals.

As stated above, an internal insert (see Figure 2.1 below) in the form of a small capillary tube was used. This was arranged concentrically within the 5 mm NMR tube and contained a mixture of deuterated Dimethyl Sulfoxide (150 µL, DMSO-d_6; Dimethyl-d_6 Sulfoxide,) and non-deuterated glacial acetic acid (50 µL, CH_3COOH, acetic acid; 99.7 atom %, analytical grade Ajax Finechem Pty Ltd, NSW, Australia) Its purpose was to provide a sufficient deuterium lock and integration reference (see Section 3.5.2) but at the same time remain completely isolated from the reaction mixture so it did not interfere with the reaction mixture.
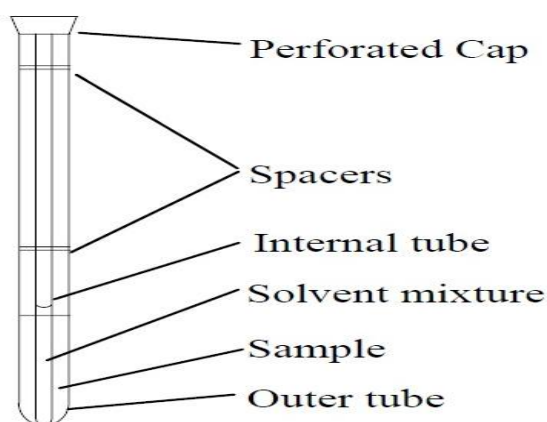
Figure 2.1 The concentric arrangement of the internal solvent tube and sample used for NMR analyses in the current investigation.(adapted from reference 7)

2.1.2 Standard Acquisition Method

The NMR methods employed throughout the analysis consisted of two methods known as "**The Quantitative Method**" and "**The Qualitative Method**". The major differences between the two methods are the *acquisition times* and the *repetition delays* (D1 values).

The following is a table of parameters and acquisition conditions for the NMR methods used for the resin analyses.(see Table 2.1)

Table 2.1 Typical NMR acquisition conditions for the Quantitative and Qualitative NMR methods.

Parameter	Quantitative	Qualitative (rapid)
Pulse angle	90 °	90 °
Number of FID points	32 k	32 k
Repetition Delay (D1)	10 s	1s
Decoupling mode	Inverse gated	Power gated
NOE Enhancement	No enhancement	Enhancement present
Number of scans	3200	640
Typical acquisition time	9 hr 32 min 9 s	18 min 43 s
Analysis temperature	303.15 K	Variable
FID acquisition time	0.68 s	0.68 s
Receiver gain	912	912

The different NMR methods produce two sets of independent spectral data. The specifications of the differences between the methods are derived in detail and explained thoroughly in Section 2.1.3 and Section 2.1.4 (to follow).

2.1.3 The Qualitative (rapid) NMR Acquisition Method

The pulse program utilised for the Qualitative method is shown in Figure 2.2:
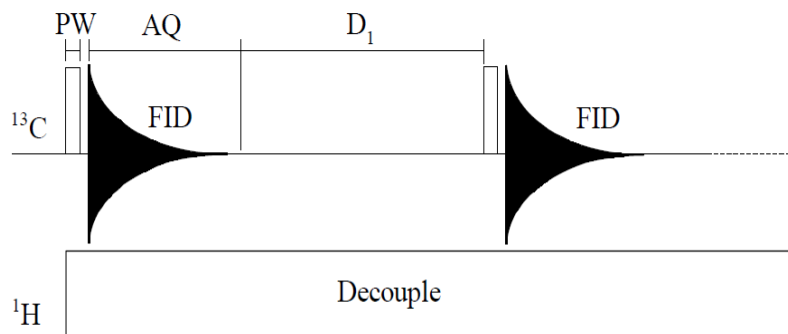
Figure 2.2 Schematic of the Qualitative analysis pulse program

This schematic shows the sequence followed in the ^{13}C channel of the Qualitative NMR pulse program: Pulse (PW), acquisition (AQ), pulse delay (D1), repeated by the chosen number of repetitions.

Broadband proton (^{1}H) decoupling in this qualitative analysis procedure is applied *throughout* the duration of the experiment. This means that any enhancement in sample signals brought about by the Nuclear Overhauser Effect (NOE) is <u>not</u> suppressed and hence (in the case of ^{13}C NMR spectra) maximizes intensities of signals acquired in the experiment. This is also known as power gated decoupling.

31

NOE effects occur via through space interactions between spatially close NMR active nuclei in the molecule. This essentially consists of a transfer of nuclear spin polarity from one nucleus to another. Three effects could arise out of these interactions depending on the nuclei involved. They can act to either 1) enhance signal intensity, 2) decrease signal intensity or 3) have no effect on signal intensity arising from the neighbouring nucleus.

As mentioned earlier, the constant application of proton decoupling in the case of acquisition of ^{13}C NMR spectra causes the protons to experience a significant enhancement from the decoupling leading to an NOE effect increasing the signal on protonated carbons, this in turns causes the method to produce qualitative results because the changes in the observed signal intensity cannot be purely attributed to changes in concentration of the NMR active nuclei within the sample. This means that integrals of NMR signals in ^{13}C NMR spectra must be regarded with caution. NMR acquisition methodologies can, however be modified to remove this NOE effect from spectra so that signal intensities observed are more quantitative. This forms the basis of the quantitative acquisition method (Section 2.1.4).

2.1.4 The Quantitative (slow) NMR Acquisition Method

The schematic for the pulse program used for the Quantitative method is shown below in Figure 2.3
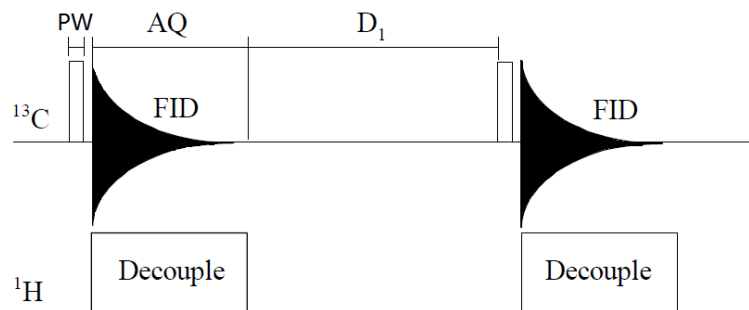
Figure 2.3 Schematic of the quantitative analysis pulse program

The pulse program of the Quantitative NMR pulse program follows a similar series of actions as the Qualitative pulse program (see Figure 2.2): Pulse (PW), acquisition (AQ), and pulse delay (D1), repeated by the chosen number of repetitions.

However the main difference between the Quantitative NMR method as shown above and the Qualitative method is that the Quantitative method only applies proton decoupling in the duration of *acquiring the FID* and <u>not</u> over the entire excitation/acquisition period as in the qualitative method. The selective period of proton decoupling used essentially removes the NOE effects by saturating the signals arising from protons within the sample, essentially removing any proton to carbon couplings. This is known as inverse gated decoupling.

33

Inverse gated decoupling removes the NOE effect of all protonated carbons and effectively provides decoupled spectra with quantitative intensities when suitable delay times are used. This means that the peaks can be integrated and the difference in intensities can be realistically related to the concentration of each NMR active nucleus in the sample.

2.1.5 Temperature Management.

The current investigation required the NMR experiments to be carried out at different temperatures. This means there is the requirement of temperature ramping in the NMR instrument. This is achieved in the Bruker 400 MHz NMR instrument by the means of a variable temperature unit (VTU) installed in the instrument. However, in the past it was discovered (Woolley, 2008)[7] that taking at face value the temperature set on the VTU unit for the temperature monitoring in the NMR spectrometer was ill advised due to its unreliability.[7] Before any experiments at temperatures higher than the usual 30 ℃ were run, there was thus a need to check the accuracy of the variable temperature unit (VTU, Bruker) within the NMR. Woolley (2008) had previously checked this in his work and found the VTU to be in error as the temperature actually reached in the NMR cavity as determined by means of a separately installed thermocouple *deviated f*rom the intended temperature set through the VTU unit.

To measure how much the true temperature in the NMR cavity deviated from that which was set, the strategy devised by Woolley, 2008 was repeated for the sake of the present set of experiments to gain a measure of the true temperature as it is essential that this is well known for studying the melamine resins. After a series of heating experiments executed by setting the VTU to specific temperatures and allowing the temperature to equilibrate, the temperature inside the probe itself was measured using a long thin thermocouple placed inside a sample tube(CHY 502 K/J free standing thermometer with a K type thermocouple wire) (See Section 3.4).

34

2.1.6 Additional NMR Investigations

^1H

1-D Proton NMR spectra were initially obtained to aid in the identification of the species within the melamine resin sample. The internal reference was the same as the one used for the kinetic studies. (See Section 2.1.1) 500 scans were employed to obtain each spectrum.

DEPT135

Distortionless Enhancement by Polarisation Transfer (DEPT) spectra were additionally recorded to help distinguish relatively close peaks such as the linear methylene signal and the methanol signal in the spectra. DEPT-135 has the capability to suppress the quaternary carbons and show methine and methyl carbons (CH and CH_3) as positive signals and methylene carbons (CH_2) as negative signals.

2D NMR

2D NMR spectroscopic techniques of Heteronuclear Single Quantum Coherence (HSQC) and Heteronuclear Multiple Bond Correlation (HMBC) were also acquired under the same conditions as the kinetic experiments (i.e. with same internal insert with 600 mg of sample) and processed as described previously (Section 2.1.1) for the express purpose of signal confirmation.

Relaxation studies

T_1 relaxation investigated for each of the resin species for the important purpose of determining the correct quantitative parameters for this particular resin. (see Section 3.6)

T_2 relaxation experiments was carried out using the Spin Echo technique to give an insight to the molecular size of the resin polymer sample. 280 scans were used to obtain the data (details of this investigation can be found in Section 3.6.2). The parameters used are shown in Table 1.2

Table 2.2 Experimental parameter values used for T_1 and T_2 experimental parameters (D1 = relaxation delay, D20 = Fixed echo time to allow elimination of diffusion)

Parameter	T_1 experiment (s)	T_2 experiment (s)
D1	10	20
D20	-	0.006
VD list - 1	30	0.024
2	25	0.048
3	20	0.096
4	15	0.1923
5	10	0.3606
6	5	0.7212
7	2.5	1.202
8	1.5	2.885
9	0.8	4.808
10	0.4	9.616
11	0.15	14.42
12	0.05	19.23

Solid state NMR studies

Solid state NMR spectra were acquired using a solid state broadband probehead equipped with a MAS spinning unit installed in a Bruker Avance 300 MHz Fourier Transform Nuclear Magnetic Resonance spectrometer, operating at 300.13 Hz for (^{1}H) and 75.47 Hz for ^{13}C. Freeze dried solid final resin samples were ground and packed into a 4 mm zirconia rotor which was spun at 5 - 10 kHz during acquisitions at the magic angle to average out dipolar interactions. A cross Polarisation (CP) pulse program using a ramp for variable amplitude. CP was employed which had D1 set to 1.5 s and the contact time between ^{13}C and ^{1}H set to 2000 μs. Cross polarisation operates by the transfer of energy between the ^{1}H nucleus and the ^{13}C nucleus. Excitation of the ^{1}H nucleus provides additional sensitivity to the ^{13}C nucleus being measured thus spectrum can be acquired faster.

In addition to a CP, solid state NMR spectrum of the final melamine resin products , a ^{13}C spectrum was also acquired by high power decoupling (HPDEC). This represents the solid state NMR spectrum acquired by classical Bloch decay where the nucleus is directly excited by the r.f. pulse (rather than the protons in the sample as in the CP pulse programme), with a D1 delay time of 10 s. Both pulse programs (CP and HPDEC) utilised high power ^{1}H decoupling to generate ^{13}C spectra.

2.2 Additional Techniques used to study the resins.

Although this was a mainly NMR-based study, some use of other techniques was made to see if any further information could be gained on the resin systems studied.

2.2.1 Infrared Spectroscopy

Four IR-based methods were employed for the analysis of the melamine resins. IR transmission spectra of thin film (liquid) samples, Attenuated Total Reflection Infrared Spectroscopy (ATR-IR), analysis via a microscope (Perkin Elmer Spotlight 200 optical bench attached to a Perkin Elmer Spectrum 400 instrument) and IR spectra obtained of solid samples by pressing them into semi-transparent KBr disks. All analysis was carried out at room temperature in absorbance mode on the Perkin Elmer Spectrum 400 FT-IR spectrometer except for the analysis with the KBr disk technique which was operated on a Perkin Elmer Spectrum 100 FT - IR spectrometer with each spectrum obtained after acquisition of 10 scans. All IR data were processed using Spectrum software Version 6.1.1.0132.

Resin was analysed directly from sub samples (without further preparation) obtained every 10 min in a commercial resin production process as a surface film in between calcium fluoride (CaF_2) windows using a Press Lok cell from SpectraTech.

ATR-IR spectra were recorded using a Spectratech ATR cell fitted with a ZnSe multi-pass crystal mount. Samples of the resin were introduced onto the ATR mount without further preparation and subsequently analysed.

Resin sub samples obtained from a commercial process were frozen with liquid nitrogen immediately upon collection. All samples were stored frozen until the entire reaction process completed after which the frozen samples were subsequently freeze dried. The freeze dried samples were then ground to fine powders which were pressed into KBr disks for IR analysis.

Microscope FT - IR analysis was carried out in reflectance mode with focusing on the sample done to maximize reflected IR intensity coming off the specimen. A single beam spectrum obtained from the reflectance of a gold mirror was acquired as the background. A liquid nitrogen cooled MCT detector with a spectral observation window from 4000 - 750 cm^{-1} was used to detect IR peaks in samples examined on the microscope stage.

2.2.2 MALDI-TOF Spectrometry

Preparation of the MALDI-TOF sample[45]

Samples examined by Matrix Assisted Laser Desorption ionization time of flight spectrometry were prepared as follows: the liquid resin sample was dissolved in water to a concentration of 4 mg/mL. This was then mixed with the acetone solution of the matrix (10 mg/mL of dithranol/acetone) to a 1 : 1 mixture. A 0.5 - 1 μL aliquot of the mixture was then spotted onto the MALDI target. After evaporation of the solvent via air drying, the MALDI target was inserted into the spectrometer and the analysis commenced.

Mass analysis was carried out on an Autoflex II MALDI - TOF/TOF™ Proteomics Analyzer (Bruker Daltonics), in the positive ion reflector mode using a 10 Hz frequency pulsed nitrogen laser operating at 327 nm. The ions generated were accelerated at 20 kV with the detector voltage being 1.6 kV. Mass spectra were obtained at the laser power of 45% and each spectrum was the result of at least 300 shots.

2.2.3 Electrospray Ionisation Time of Flight mass spectrometry (ESI-MS or MicrOTOF)

Sample preparation for ESI-TOF

Resin samples examined by ESI-MS were dissolved in a solvent (isopropyl alcohol: distilled water (1:1)) to a concentration of 0.1 mg/mL and 1 mg/mL, then injected into the instrument for analysis.

High resolution mass spectra were obtained of samples using a Bruker Daltonics Electrospray Ionisation (ESI) mass spectrometer. The analysis was carried out using the positive ion mode.

2.3 The Preparation of Melamine Formaldehyde Resins

Due to the commercial sensitivity of this work, the details of the series of additions, and temperature controls could not be revealed in this thesis. It is possible only to give a broad outline.

Several methods were used for preparing the melamine formaldehyde resins, each of which provided information for the main purpose of investigating the real time NMR studies of the reaction.

Under industrial conditions the progress of the melamine formaldehyde resin reaction is monitored as changes in viscosity over time. However, when subjected to real time NMR experiments in a 5 mm NMR tube it is difficult to monitor the viscosity due to the small reaction volume and the location of the reaction mixture to be sampled.(i.e. inside the NMR spectrometer). To deal with this problem, a series of *time allocations*, predetermined by control experiments corresponding to viscosity measurements were used instead throughout this investigation.

The methods used to prepare the melamine resins used throughout the project are presented below in Sections 2.3.1 - 2.3.3.

2.3.1 Preliminary reagent preparations.

A premade formaldehyde solution mixture consisting of aqueous formaldehyde and methanol (prepared to predetermined compositions and remaining stable over an extended period of time) was used throughout the investigation as the "formaldehyde reagent". This allowed easier transportation of formaldehyde in sealed Schott bottles and the reduction of the concentration of formaldehyde decreased the potential hazards associated with the flammability of formaldehyde, and allowed the reaction to be continued at a later time and place.

2.3.2 Commercial Resin Synthesis on a laboratory scale

The representative commercial laboratory scale resin was prepared with the formaldehyde/melamine mole ratio (F:M) of 1.27.

In the previous study on phenolic formaldehyde resin by Woolley, 2008[7] spectral data corresponding to different stages of the reaction could be obtained from sub samples of the resin synthesis. Sub samples are samples collected every 5 minutes after the temperature ramp until the Industrial Resin Endpoint (IRE) of the synthesis is reached. The resin sub samples obtained from preliminary resin synthesis gave insight into the reaction as a function of time (i.e. progress of reaction. This provided information on the reactions taking place during the resin synthesis. Due to the nature of the melamine resin however, sub samples obtained prematurely from the IRE would tend to solidify due to the precipitation of melamine and this prevents such samples from being examined via liquids NMR analytical techniques. This eliminates the ability for the sub samples to be analysed for at specific time frames during the reaction leading up to the IRE. Consequently preliminary sub samples of the resin could not give insight to the reaction as a function of time by the use of liquid state NMR. In the past, conversion factors have been calculated for different time frames of the reaction (i.e.

conversion factors (see Section 3.7) used for the conversion of intensities corresponding to the reaction at 35 min would be determined from the sub sample acquired at 35 min). The conversion factor for this investigation therefore must be determined from the stable final liquid resin (control) obtained at the IRE. This is used as a representative conversion factor for the entire synthesis of the commercial resin.

Preparation of the Laboratory Scale resin (Control for determining conversion factors

The premade formaldehyde mixture was added directly into a five necked 1 L round bottom flask fitted with an overhead stirring device (Global Science, IKA-RW20 digital), condenser, and a custom temperature control unit consisting of a thermocouple probe, cooling coil and heating mantle. Stirring was maintained throughout the entire reaction. The mixture was adjusted to a predetermined pH with 10 molL^{-1} caustic (NaOH aqueous solution) and melamine was added over a predetermined amount of time, upon which the melamine -formaldehyde mixture was put through a temperature ramp and held until the IRE was reached. This final liquid resin is stored at 25 ℃ and has a shelf life of ~2 weeks.

NMR procedure for the Laboratory Scale Resin(Control)

The final resin was taken out of the containers from a 25 ℃ oven and from it 600 mg of resin was directly added into a 5 mm NMR tube (Wilmad Lab Glass, 5 mm thin wall 7" length) without further treatment. A concentric internal tube containing solvents for deuterium locking and referencing (see Section 2.1.1 for description) was

inserted and the cap was secured (see Figure 2.1) before the sample was placed into the NMR spectrometer, where it was locked and shimmed for NMR analysis to work out the conversion factors (see Section 3.7).

2.3.3 Resin synthesis for real time analysis

For real time monitoring of the melamine formaldehyde resin, the reaction was scaled down to NMR dimensions so that the entire reaction could be carried out within a 5 mm NMR tube located inside the spectrometer (i.e. *in situ*) which contained also the insert tube containing reference solvent. For this analysis the overall reaction mixture weight was taken to be 600 mg (c.f. industrial resin production ~ 16 tonnes).

Preparation of the sample used for Real Time NMR Analysis of resins

The initial approach had been to add the solid (powdered) melamine into the bottom of the NMR tube with the subsequent addition of the formaldehyde solution mixture (pH adjusted to industrial condition) to a weight of ~ 600 mg. The internal tube is then inserted into the 5 mL NMR tube (as shown in Figure 2.1) and thoroughly mixed, before being applied to the predetermined time scheme of the kinetics experiment within the NMR. However due to the size of the 5 mL NMR tube and presence of insoluble melamine powder, it was found difficult to then insert the internal tube so it reaches the bottom of the tube and at the same time mix the formaldehyde solution mixture and the melamine thoroughly. The results of this initial approach showed a lack of reaction between the formaldehyde and melamine despite the increase of temperature which would have otherwise aided the solvation of melamine in the reaction mixture. The physical observation also showed that most of the melamine had not reacted. This is a limitation regarding the amount of mixing available within

the NMR sample tube. The mixing of the sample during the kinetics experiment was hence reliant on what little amount of mixing within the tube could be achieved with the NMR tube spin (ca. 20 Hz and a normal part of any acquisition in the NMR) within the probe, this is preset and unable to be adjusted. This challenge in mixing tube contents is obviously a consequence of the "crowded" nature of the sample tube with its containing the insert tube and sample under investigation around it. Hence, instead of relying on mixing of the reagents *from the outset* within the NMR tube, another method (optimised) was used whereby vigorous *premixing* of all the reactants together within a sealed container was carried out first with subsequent sonication in an ultrasonic bath for 5 min. After this premixing, a total of 600 mg of the mixture was transferred into the 5 mm NMR tube with the internal tube inserted and capped (see Figure 2.1). This was then transferred into the spectrometer where it was tuned, locked, and shimmed before NMR acquisition was begun.

Within the NMR, the reaction mixture was heated at a constant rate to the final temperature of 90 ℃. The temperature was held for the predetermined period of time until it reached the IRE of the resin. A total of 12 experiments were carried out corresponding to approximately 225 minutes for each kinetic real time NMR experiment. This was the predetermined period of time for a commercial resin reaction and any longer was deemed unnecessary for this particular resin in terms of commercial resin production.

2.4 Summary of the steps leading up to the deduction of the quantitative NMR intensities of species observed in real time NMR analyses of resin reaction.

The essential steps in summary are hence:

1) Deduce the time allocations of the resin synthesis

2) Make a control resin for deducing the conversion factors (see Section 3.7) to enable the determination of quantitative NMR intensities.

3) Run real time NMR experiments in a NMR tube as a function of time after premixing the alkaline adjusted formaldehyde solution and melamine.

4) Carry out conversion of qualitative real time NMR intensities to quantitative intensities.

3 Development of the Rapid NMR Method

3.1 Introduction

In this section the procedures for carrying out the rapid NMR method will be described. Spectrometer parameters, spectral information and calibration factors necessary for the application of this method are obtained. These parameters have been adopted from, and adapted where necessary from the study of real time analysis of phenolic resins by Woolley[7] who in turn had adapted methodology for his study from the earlier study of urea formaldehyde resins by Zeng.[17]

3.2 Deducing the NMR spectrometer parameters

The first step in the development of the rapid NMR method is determining the acquisition parameters for recording ^{13}C NMR spectra of the samples. In order to achieve the maximum signal intensity in a NMR spectrum it is essential that the radiofrequency (r.f.) pulses are of the correct duration and the relaxation delays are optimised for the system being studied.

3.2.1 The ^{13}C pulse: Theory

A sinusoidal function shows the relationship between the excitation pulse angle (θ) and the intensity of signal detection (I) in pulsed NMR spectroscopy as illustrated in Equation 3.1, where I_0 is the maximum possible signal intensity obtained. [7, 25]

$$I = I_0 \sin \theta$$ **Equation 3.1**

The pulse angle is the pulse used to adjust the sample magnetisation about the x axis. For example a 90 ° or π/2 (radians) pulse angle is the pulse which turns the sample magnetisation by 90 ° around the x axis. (See Section 1.3.2 and Section 1.3.3) As this angle decreases the time required for the re-equilibration of the magnetisation vector via relaxation is also reduced. For example when comparing two r.f. pulses applied to a sample, namely a 70 ° pulse and a 90 ° pulse. The sample magnetisation would be rotated corresponding to the angle of the pulse applied towards the y axis from the z axis. (See Figure 3.1) It can be seen that the amount of time it needed for the re-equilibration of the magnetisation back to the z axis with a 90 ° pulse would be longer than that of the 70 ° pulse. Thus the time required for an NMR acquisition is less when using a 70 ° pulse.
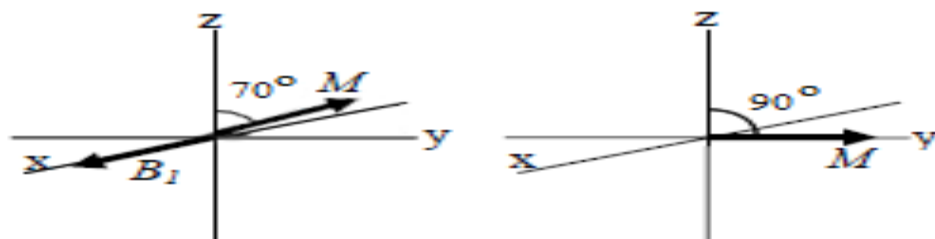
Figure 3.1 Position of the sample magnetisation when a 70 ° and a 90 ° pulse is applied.

A 90 ° rotation of the sample magnetisation causes the magnetisation to be along the y axis, meaning that the field vector is completely in the x-y plane. The more the magnetisation vector deviates from the x-y plane, the more sample magnetisation associated with the z plane where no signal is generated, reduces the intensity of the signal observed. Therefore an investigation of the pulse angles will afford spectra of the maximum intensity within the shortest time period.

48

Determining the optimum pulse angle

A sample of representative resin was placed into the NMR to carry out a series of experiments under three different pulse angles, 45 °, 70 ° and 90 ° to deduce the optimum pulse angle for the current system under investigation (Figure 3.2).
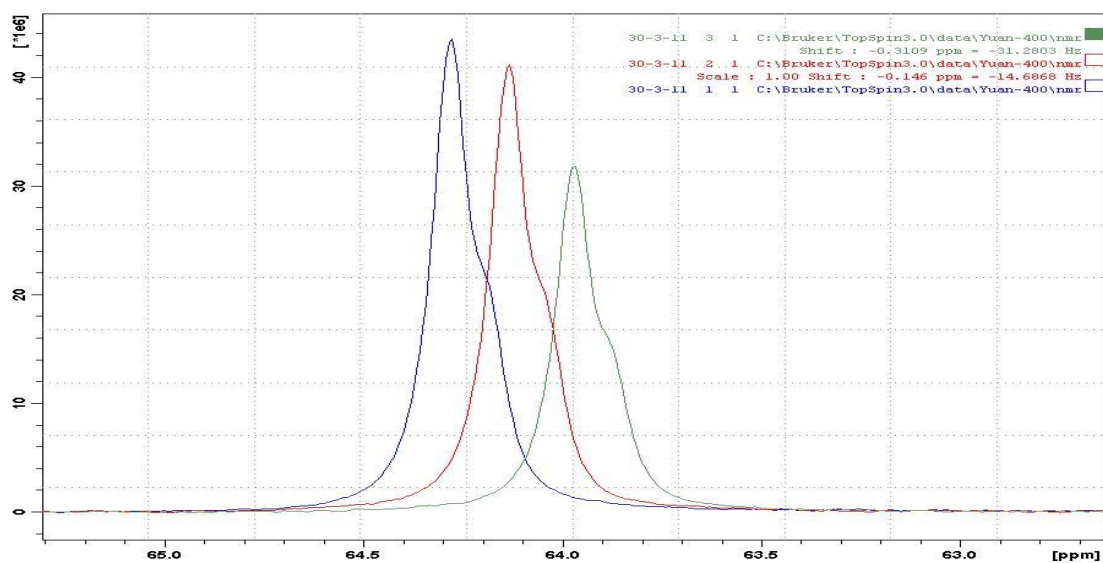
Figure 3.2 An overlaying spectrum of linear methylol species (from a prepared sample of melamine formaldehyde resin) subjected in experiments under different pulse angles. From left to right 90 ° (blue), 70 ° (red) and 45 ° (green). (Note the x axis is offset for clarity).

From the results of the experiment shown above, it can be deduced that even though using a pulse angle less than 90 ° reduced the acquisition time for obtaining each spectrum, the associated loss of signal intensity had even greater disadvantages for the analysis. Thus it was decided that a 90 ° pulse angle would be applied to the two pulse programs (see Section 2.1.2) executed for this investigation.

In NMR spectrometers the required r.f. pulse to adjust the sample magnetism to the intended pulse angle is measured and calculated in lengths of time (μs) required to turn the sample magnetisation to the preferred angle. Due to the importance of the 90 ° pulse in maintaining spectral quality, investigations into the pulse length were carried out to ensure the pulse length utilised in the investigation corresponded to a 90 ° pulse. Not only does this ensure that the pulse parameters are set correctly but also that the spectral quality is the highest possible.

Determination of the 90 ° pulse length

In order to derive the 90 ° pulse length, the signal intensity obtained from analysing a sample of aqueous formaldehyde was employed. A correctly phased spectrum was acquired initially to ensure it produced a positively phased absorption spectrum. A series of experiments was conducted with the increment of pulse lengths ranging from 2 - 36 μs. This series was carried out using Topspin 3.0's internal program 'POPT' "pulse optimization program", which measures the pulse length via measuring pulse lengths from less than 90 ° to pulse lengths greater than 180 °. The result is a set of intensities following a sinusoidal curve. A 90 ° pulse would generate the maximum signal intensity thus the peak of the sinusoidal curve directly represents the 90 ° pulse. Another way of determining this is the fact that the 90 ° pulse is exactly half of the pulse length of the 180 ° signal (Figure 3.3). The pulse length of a 90 ° pulse angle can hence be easily determined as 9.5 μs (from the Figure 3.3 below). This was then employed throughout the investigation.
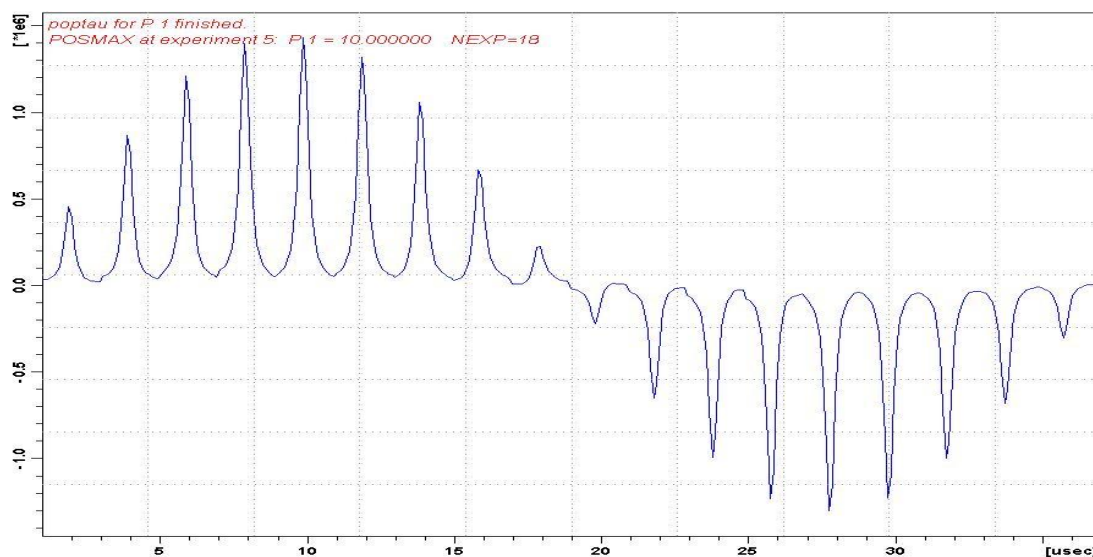
Figure 3.3 Spectra of methylene glycol species obtained after executing the POPT program

When using pulse optimization programs as above it is important to ensure the relaxation time used are long enough. In the series of experiments above, a relaxation time of 20 s was purposely employed to allow the complete relaxation of the nucleus subjected under the conditions of 'POPT'.

This is because an insufficient delay time would not result in the true maximum intensity observed for the pulse angle used due to saturation of the signal. In fact you may get a "flattening" of the curve or lack of a true maximum instead. Thus application of this exceedingly long delay assured the maximum intensity signal intensity of each pulse length was recorded. This extremely long delay clearly increases the length of the time it takes for acquisition of each NMR spectrum. To now find out how to achieve maximum signal intensity with minimal time, an investigation of the optimum repetition rate was subsequently carried out.

51

3.2.2 Repetition rate

Each NMR experiment produces a series of FIDs corresponding to the different nuclei in the sample. The Fourier transformation of these FIDs converts the FID time domain signal to a frequency domain signal known as an NMR spectrum. In order to obtain a reasonable quality spectrum with a good signal to noise ratio (S/N), multiple NMR experiments (scans) can be carried out with the result of multiple FIDs for each experiment. These FIDs can then be accumulated and Fourier transformed to achieve greater S/N, (Equation 3.2), the S/N of a spectrum is related to the square root of the number of scans (NS). Therefore the accumulation of adequate numbers of FIDs is the key to greater resolution and signal intensity.

$$S/N = \sqrt{NS}$$ **Equation 3.2**

A problem arises with the limitation of the time required for the opposite and aligned spin states to re-establish equilibrium (relaxation) after each application of the 90 ° pulse, before the experiment is repeated. This is known as the saturation effect, i.e. when a nucleus is excited with an r.f. pulse, a signal is generated by the current within the receiver coil (FID). This signal decays back to equilibrium after the excitation. However if another excitation pulse is immediately applied (i.e. no delay employed) the nucleus essentially re-establishes equilibrium immediately. This phenomenon is called the saturation effect and as a consequence the signal intensities will be reduced. This means that a delay must be introduced between the application of the 90 ° pulse to allow this relaxation to occur.

The excitation of a sample with the r.f. pulse (90 °) will cause the sample magnetisation to turn to the x-y plane (see Section 1.3.2) from the z axis. In the absence of external influences this magnetisation will return to the z axis with the

longitudinal relaxation time (T_1) exponentially (see Section 3.6). Using a short delay would essentially mean that the re-equilibration would not be complete and produce inaccurate relative signal intensities. Relaxation times of each species are influenced by changes of conditions such as temperature, structure, sample viscosity and molecule size.[25, 28]

The general rule of thumb for obtaining good quantitative NMR results is to obtain signals which have a 99% re-establishment to equilibrium. This corresponds to 5 x T_1 and the accepted value is 3 x T_1 which is when the equilibrium has reached 95%.

The determination of the T_1 values for all the resin species under the investigation was seen as a necessary exercise, in order to determine the optimum repetition rates for constructing the two NMR acquisition methods. A melamine formaldehyde resin as prepared for this investigation was experimentally analysed and the T_1 relaxation times of each resin species are reported in Section 3.6.

As a result of measuring the T_1 values, the repetition rates of the Qualitative and Quantitative NMR acquisition methods used in this study were able to be deduced (Section 2.1.3-2.1.4).

3.3 Signal assignment of the ^{13}C NMR spectrum

There is a goodly amount of previously reported NMR- related literature on the characterization of species observed in melamine resin reactions, of which ^{13}C NMR is a commonly used analysis technique. The chemical shifts of the species obtained in this investigation were skewed in terms of their ppm values compared with other studies reported in the literature. This is due to the solvent effects between the internal solvent used in the insert tube during spectral acquisition and resin reaction solvent. Therefore the elucidation of the patterns of chemical shift observed in this study was compared with the literature,[46-48] taking into account differences in conditions (e.g. concentration, solvents, temperature etc) and the referencing of signals. The chemical shifts in this investigation, are reported relative to the acetic acid methyl group (<u>C</u>H$_3$COOH) peak resonating at 21.3 ppm with an SR (spectral reference adjustment) value of 0.06 in the internal insert. Spectra of the resin obtained using 2D and DEPT NMR techniques were also employed to aid in the resin signal assignment.

Representative spectra of a melamine resin sample obtained via qualitative (rapid) (Figure 3.4) and quantitative (slow) (Figure 3.5) methods are presented below:

54
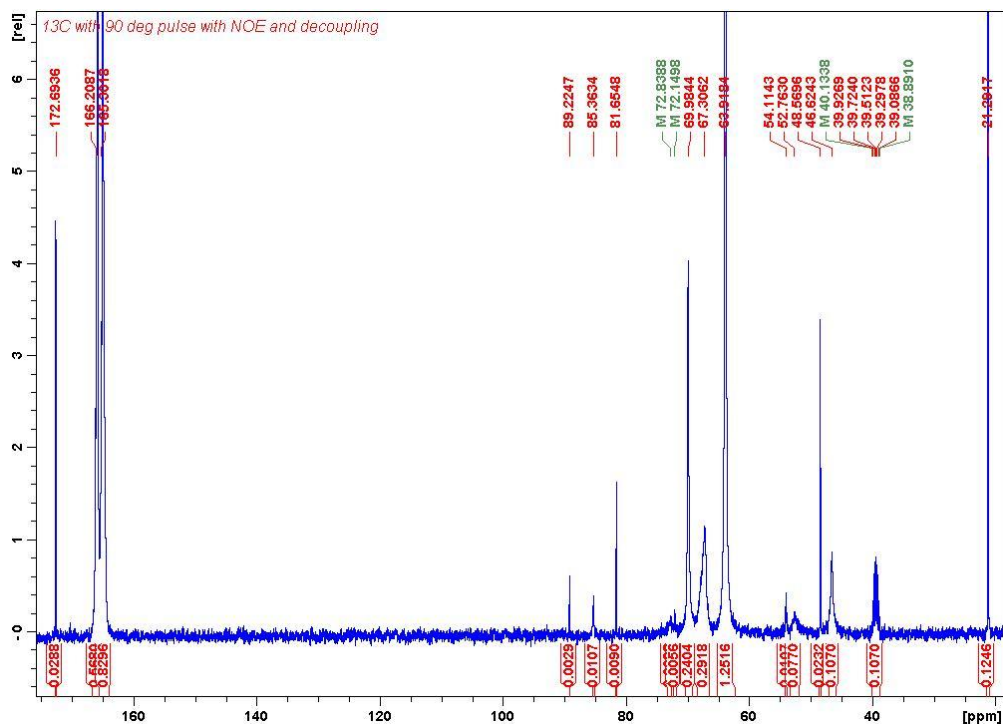
Figure 3.4 A representative spectrum of a control resin sample obtained using the qualitative (rapid) method.
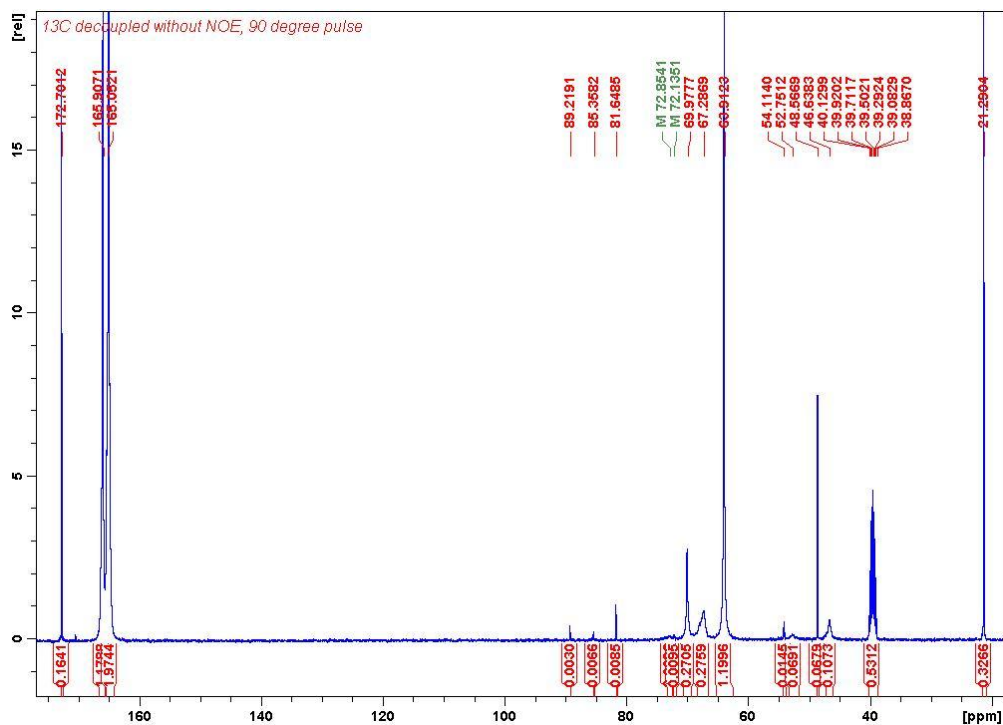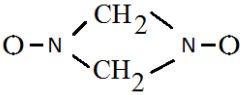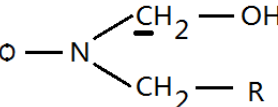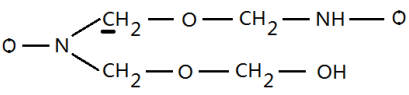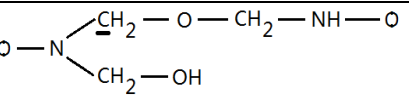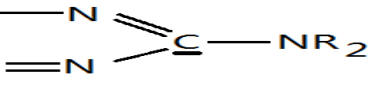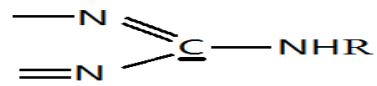
Figure 3.5 A representative spectrum of a control resin sample obtained using the quantitative (slow) method

The chemical shifts of individual resin species are assigned where possible; however there are some chemical shifts which were assigned by speculation. These assignments are given below (Table 3.1)

Table 3.1 The ^{13}C chemical shift assignments of individual melamine resin species used throughout the current investigation. (Where Ọ represents a melamine moiety, D = deuterium atom, R = CH$_2$OH, hydrogen, CH$_2$ linkage group or CH$_2$OCH$_2$ linkage group).

Chemical shift (ppm)	Functionality	Species
21.28	**CH$_3$**COOH	Acetic acid
39.50	((CD$_3$)$_2$S=O)	Dimethylsulfoxide - d6
46.72	O - NH - **CH$_2$** -NH - O	Linear methylene
48.57	**CH$_3$**OH	Methanol
52.48	O-N(CH$_2$)(CH$_2$)N-O	Branched methylene
54.09	HO-CH$_2$-O**CH$_3$**	Methoxy of hemiacetal
63.94	O - NH - CH$_2$OH	Linear methylol
67.52	O -NH - CH$_2$ - O - CH$_2$ - NH - O or O - CH$_2$ - O - CH$_2$ - OH	Linear dimethylene ether or linear hemiformal methylol
70.02	O—N(CH$_2$—OH)(CH$_2$—R)	Branched methylol
72.08	O—N(CH$_2$—O—CH$_2$—NH—O)(CH$_2$—O—CH$_2$—OH)	Branched dimethylene ether with hemiformal methylol
72.98	O—N(CH$_2$—O—CH$_2$—NH—O)(CH$_2$—OH)	Branched dimethylene ether with methylol
81.66	HO - CH$_2$ - OH	Monomeric methylene glycol
85.39	HO - CH$_2$ - O - CH$_2$ - OH	Dimeric methylene glycol
89.22	HO - **CH$_2$** - O - CH$_3$	Methylene from hemiacetal
164.86	(triazine) C—NR$_2$	Triazine carbon of melamine with tertiary amine.
166.13	(triazine) C—NHR	Triazine carbon of melamine with primary/secondary (1°/2°) amine.
172.69	CH$_3$**CO**OH	Acetic acid

A description of the specific melamine resin NMR peaks and regions which give rise to each signal are described below.[43, 46, 49]

Quaternary triazine melamine carbon region - 164-167 ppm:

Signals in this region are due to the triazine quaternary carbon of melamine directly attached to an amine group. The signals up-field of this region correspond to species with a higher degree of substitution of the associated amine groups (tertiary) (i.e. with R groups such as CH_2OH, CH_2 or CH_2OCH_2). Signals downfield of this region correspond to species with less methylol or methylene substitution (i.e. an amine NH_2). The signal detected at approximately 166.13 ppm corresponds to primary and secondary amine, the integrated range however contains signals of the melamine with no substitution due to the signals overlapping.

Formaldehyde region - 81-90 ppm:

Peaks in this region arise from the various forms of formaldehyde existing in the aqueous reaction mixture. As described before (Section 1.2.1) the species existing in an aqueous formaldehyde solution are known to be polymeric forms of formaldehyde. The signals in this region correspond to monomeric, dimeric methylene glycol and its polymeric derivatives. The polymeric form is a hemiacetal form of formaldehyde.

Methylol and ether region - 63-73 ppm:

The signals in this region arise from the methylol type carbon, directly bound to the amine group of the melamine moiety, and the mono/ dimethylene ether bridge linkage groups between two melamine moieties. The methylol carbon signals are generally further upfield in this region than the ether type carbons. The branched methylol

57

however, is further downfield than the signal arising from the linear dimethylene ether/ hemiformal methylol signal shown in Figure 3.6.
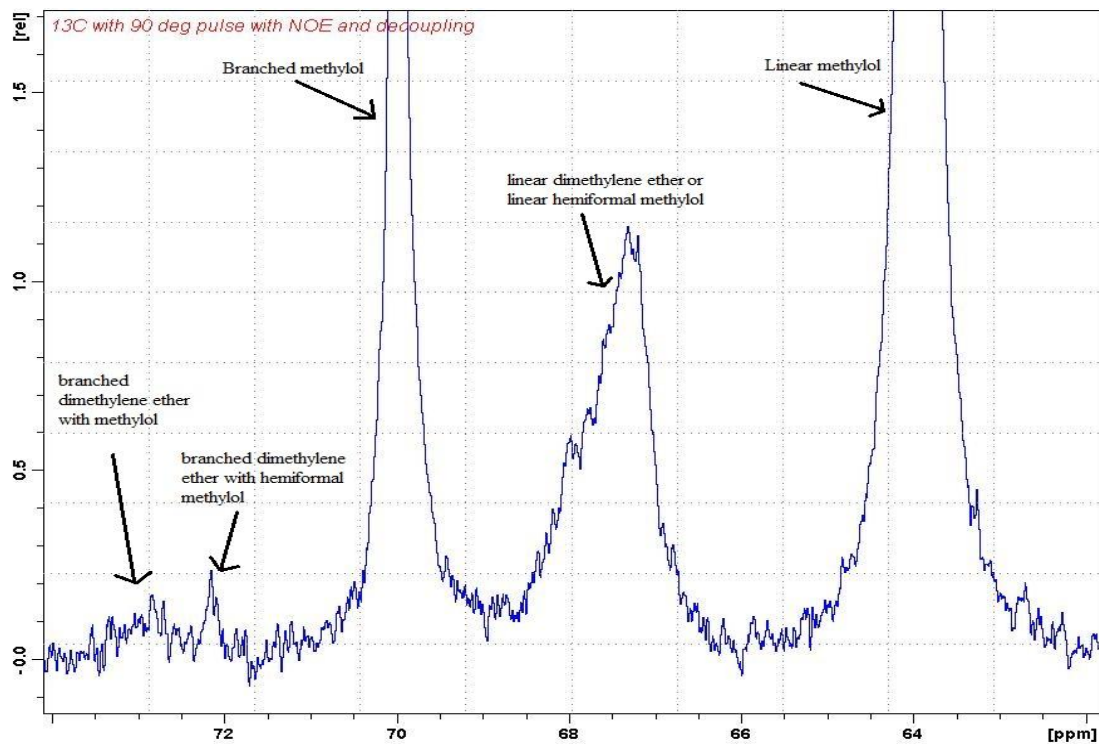
Figure 3.6 A spectrum showing the positions of the methylol and ether signals

Methoxy region - 54-55 ppm:

The methoxy carbon signal appearing in this region belongs to that of the hemiacetal group of formaldehyde.

Methylene region - 46- 53 ppm

Two signals appear in this region, the linear methylene and branched methylene peaks of the resin product.

58

3.4 Factors which influence the chemical shift

There are several factors which are likely to produce significant changes to the chemical shift values of individual resin species. The interpretation requires care when the spectrum is of a real time reaction where there are changes to factors such as pH and temperature.

The effects of temperature on the chemical shift values can be observed by overlapping spectra obtained from the real time investigation at different temperatures, using the same reference (internal insert Section 2.1.1). It should be noted that the intensities of the signals are changing over the course of reaction (Figure 3.7).
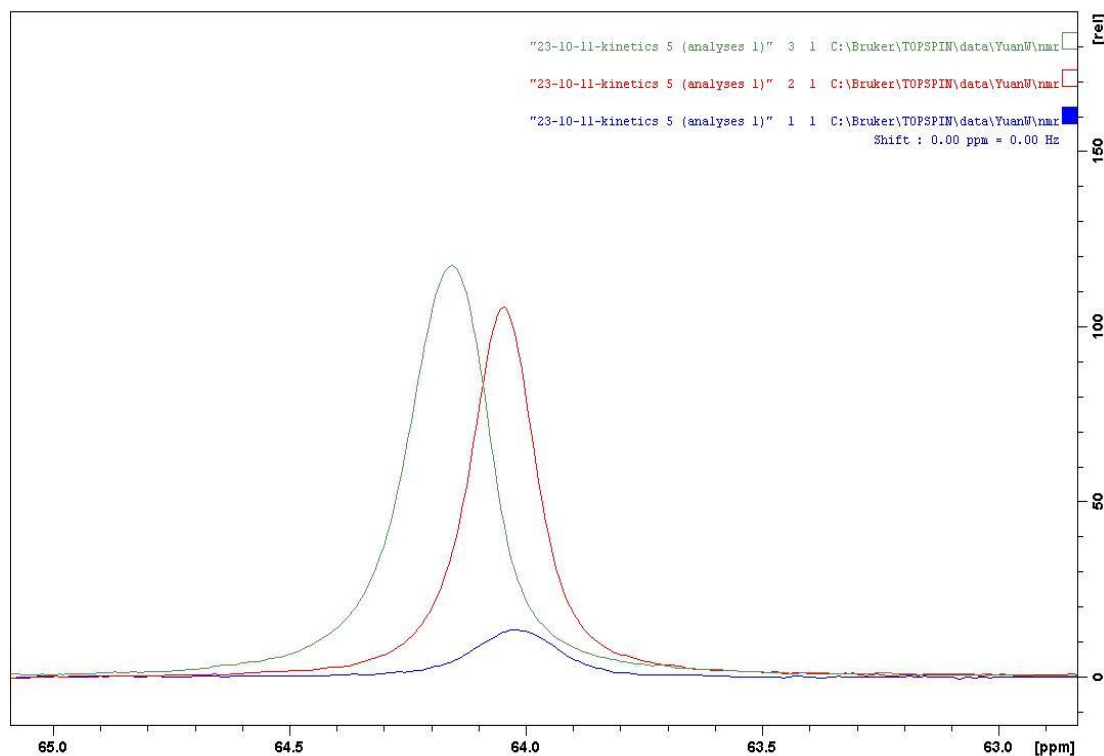
Figure 3.7 Overlaying spectra of linear methylol at 30 ℃ (green), 60 ℃ (red) and 90 ℃ (blue) noting that intensity of the peak is due to the extent of the reaction.

Due to the findings of previous studies it is known that there is a discrepancy between the variable temperature unit and the actual temperature inside the probe. It was therefore essential for the temperature inside the NMR spectrometer to be measured and managed for the determination of varying chemical shifts as a function of temperature in real time experiments.

Temperature management

A series of heating experiments was conducted to gather information on the deviation of the set temperature from the true temperature attained in the sample. The Variable Temperature Unit (VTU) was set to specific temperatures, thermal equilibration was reached within the spectrometer probe and then the actual temperature measured with a long thin thermocouple situated within the probe. This consisted of a CHY 502 K/J free standing thermometer with a K type thermocouple wire.

The following data was obtained from the investigation on the temperature within the NMR probe. (Table 3.2)

Table 3.2 A table showing the applied output power required for each of the specific set temperatures on the VTU and the corresponding temperatures of the wire thermocouple and their differences.

Max output power set (%)	Output power apply (%)	VTU set point (K)	BSMS-Temp (K)	Thermocouple (°C)	Thermocouple (K) (+273.2 °)	Difference (Thermocouple - VTU set point) (K)
5.0	2.0	300.0	302.2	27.7	300.9	0.9
5.0	4.0	310.1	302.2	38.9	312.1	2.0
8.0	6.3	320.2	303.2	50.0	323.2	3.0
10.0	8.5	330.1	305.2	60.9	334.1	4.0
13.0	10.6	340.1	308.2	71.8	345.0	4.9
15.0	12.9	350.2	311.2	82.8	356.0	5.8
15.0	13.9	355.2	312.2	88.2	361.4	6.2
17.0	14.9	360.1	315.2	93.5	366.7	6.6

Table 3.2 shows that there is a discrepancy between the temperature reading from the spectrometer and the true temperature inside the probe housing the sample.
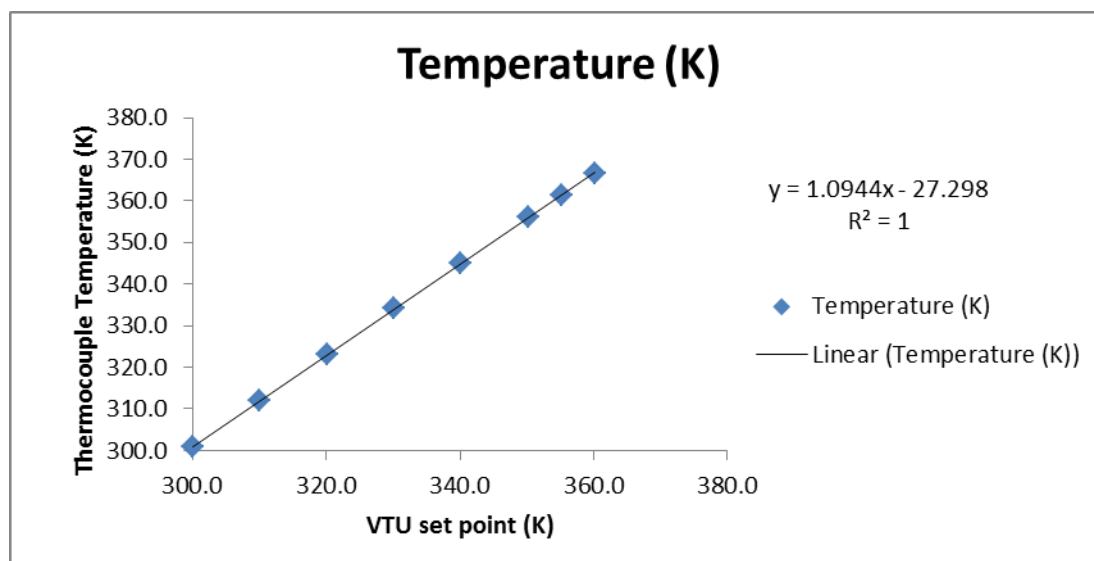
Figure 3.8 A plot showing the temperature set point of the VTU compared to the actual temperature measured with a thermocouple.
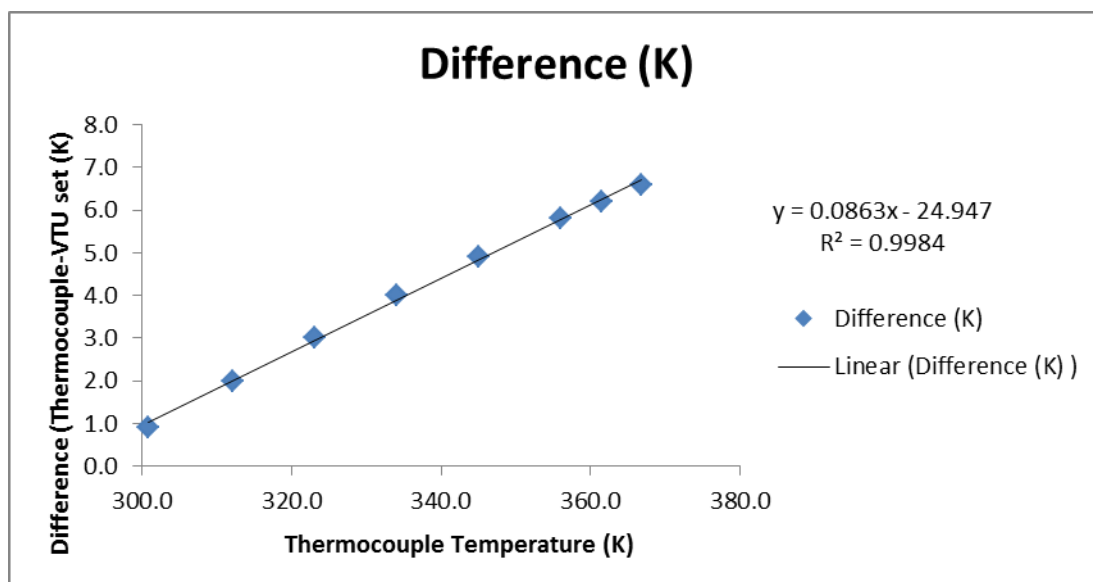
Figure 3.9 A plot showing the temperature discrepancy of the thermocouple temperature measure within the probe and the thermocouple VTU set point.

The discrepancy of temperature shows a linear trend thus using the linear equation from Figure 3.8 we can predict the true temperature since the temperature ranges used lies within the series of experiments carried out for this project. (Figure 3.8 and Figure 3.9)

For example, using the linear equation from Figure 3.8, it can be shown that the actual temperature samples were subjected to during spectra acquisition and used to acquire spectra was 303.15 K for a VTU setting of 301.95 K. Figure 3.9 shows the temperature discrepancy increases as the temperature increases.

These corrections were taken into account when running the experiment in real time to ensure that the correct temperatures were used. This ensures that the experiment would mimic the reaction industrially to the greatest possible extent so the results obtained were realistic.

In this study the chemical shifts of peaks moved approximately 0.15 ppm as the temperature increased from 30 ℃ to 90 ℃. Each resin peak shifted 0.15 ppm but the direction of shift of individual peaks was not consistent. The linear methylol signal for example, shifted downfield but the branched methylol shifted upfield by approximately 0.15 ppm, Whatever direction was taken, however, the net chemical shift of the peaks was 0.15 ppm.

In order to avoid the influences of solvent interactions between locking/reference solvents and the resin solvents , a concentric system was utilised (Figure 2.1). The lock solvent (DMSO - d6) and reference solvent ($\underline{C}H_3COOH$) were mixed and contained inside a custom made sealed glass capillary, isolating the sample from the lock and reference solvent and so preventing any spurious mixed-solvent-associated chemical shift variations. This introduced another effect where the interaction of the solvents in the internal insert and the sample solvent caused a small shift in the proton spectra compared with where resin species normally arise. The deduction of the chemical shifts was possible using literature values and the pattern with which the groups of peaks arose (see Section 3.3). The pH of the reaction mixture has also been shown to have a relatively small influence on the chemical shift values of the melamine resin species. However any effects pH had on the chemical shifts were masked by the greater effects of temperature and solvent.

3.5 Internal tube and lock solvent/reference

In this study, the internal tube is arranged concentrically (Section 2.1) (where the internal tube is inserted and centred inside the 5 mm NMR tube) and was used for the purpose of providing the deuterium lock, chemical shift reference and internal standard. The insert also prevented, as indicated earlier, any possible occurrence of side reactions between the resin and the lock and reference solvents. In this following section the internal tube and the effects it has on signal intensity, and the processes involved with selecting the NMR solvent are investigated.

3.5.1 Internal tube and optimization

Several thin walled tubes with differing external diameter were examined to determine the dimensions that would provide maximum signal intensity while maintaining the lock. Table 3.3 compares different internal tube diameters with the volume of sample used.

Table 3.3 A table showing the external diameter of the internal tube and volume of sample used.

Diameter (mm)	Volume of sample (μL)	Volume of internal solvents (μL)
~2.0	750	50
~2.1	700	100
~2.2	650	150
~2.3	600	200
~2.4	550	250
~2.5	500	300
~2.6	450	350

The dimensions of the internal tube affect the volume of sample that can be analysed within the NMR probe, thus as the dimensions increase the effective volumes in the unoccupied part of the 5 mL NMR tube which are amenable to analysis. The internal volume however provides the lock reference and integration standard therefore reducing the volume significantly can have an adverse effect on this. After consideration of various external tube diameters given in Table 3.3 above, the internal tube with the diameter of ~2.3 mm was finally chosen which allowed for adequate lock and furthermore left sufficient sample in the remaining unoccupied space around the concentric inserted tube to give adequate signal intensity for the resin species of interest.

3.5.2 Selection of solvent

The selection of solvents depends on multiple factors such as solubility, spectra interference with the analyte signals, temperature dependence, viscosity, water content, and cost. Normally the samples are dissolved in a deuterated solvent as a lock solvent but in this investigation the lock/reference solvents are sealed within the internal tube. Hence the sample and solvents are effectively separated, and this isolates the two liquid mediums negating the factors of viscosity, solubility and water content within these media

The solvent chosen must fulfill the requirements and criteria for the current investigation. The solvents will produce NMR signals, considered as "residual solvent peaks" and could mask and obstruct signals from the sample by overlapping them. Another factor to be considered is the fact that the NMR experiment is operated under a range of temperatures (30 - 90 °C) thus it is significant that the solvent's boiling points and melting points are taken into account.

To determine the appropriate locking and reference solvents for analysis of the melamine resins, common NMR solvents used in the literature were reviewed. Solvents such as $CDCl_3$, D_2O, $((CD_3)_2CO)$, CD_3CN etc do not meet the temperature requirements and solvents such as C_4D_8O and CD_2Cl_2 have peaks between 54 - 68 ppm which overlap with methoxy peaks of the hemiacetal and methylol groups therefore they were considered as inappropriate NMR solvents due to the constraints of this investigation imposed by the reagents being studied.

In contrast, DMSO-d_6 provides a septet signal at 39.5 ppm which does not overlap with any melamine resin signals, has a boiling point of 189 ℃ under atmospheric pressure (well below 90 ℃, the highest temperature used in NMR experiments) and so has a reasonably low vapour pressure over the temperature range used in the investigation. Having a relatively low vapour pressure was an important factor, since there is a variation in the temperature throughout the experiments that could lead to the relative pressure within the sealed internal tube increasing so causing possible damage to not only the NMR tube (via breakage) but also the NMR probe. This could necessitate an expensive and time consuming cleaning procedure to be carried out. Hence DMSO-d_6 was chosen as the internal lock solvent.

In terms of the reference signal coming from the insert, it was necessary to use known amounts of an internal standard spike to provide an intense signal for use as a reliable integration reference. This mixture of acetic acid and DMSO-d6 (see Section 2.1) was utilised to provide the integration reference (SR) and lock throughout this investigation

3.6 Longitudinal relaxation times, T_1

The population difference between spin states that are available to the nuclei undergoing analysis defines the observed signal in the NMR spectrum. To obtain maximum signal output, as required by quantitative analysis using a 90 degree pulse, the time between excitation pulses must be long enough to allow for complete relaxation of the nuclei.

For quantitative ^{13}C NMR analyses using a 90 degree pulse the scan repetition rate, which in a typical NMR experiment is the sum of the FID acquisition time (AQ) plus the pulse repetition delay time (D1) must ideally be longer than three times the longitudinal relaxation time (T_1) with a general recommendation of five times the T_1 time.

Hence, knowledge of the individual longitudinal relaxation times for each of the carbon species (types) in melamine formaldehyde resin was required. For the quantitative ^{13}C NMR analyses using a 90 degree pulse the minimum acceptable scan repetition rate is three (preferably five) times that of the slowest relaxing carbon species. Prior to the determination of T_1 relaxation times, it was reasoned that the slowest relaxing species were likely to be the non-protonated carbonyl species in the system being studied.

3.6.1 The inversion-recovery method

The application of a r.f. pulse can rotate the effective nuclear magnetisation away from the equilibrium position of the axis, thereby perturbing the system. The application of a 180 °pulse can invert the net equilibrium population since it is aligned in the opposite direction to that prior to the application of the 180 degree pulse. Immediately after the 180 °pulse, relaxation processes begin to return the magnetisation back to its normal state. This process, which proceeds *via* an exponential decay pathway (Figure 3.10) can be characterised by a time constant known as the spin-lattice relaxation time, otherwise known as T_1, the longitudinal relaxation time.

The inversion-recovery method is the most widely used technique for determining the longitudinal relaxation time (T_1). T_1 follows the pulse sequence: 180 °pulse, VD, 90 ° pulse and FID (AQ) acquisition. VD is a **variable** time **delay** between the 180° and 90° pulse and a fixed D1 time is used in all experiments (Figure 3.10)
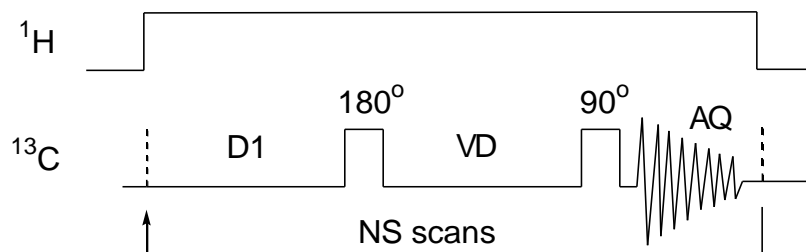
Figure 3.10 Inversion-recovery pulse sequence

A typical inversion recovery T_1 experiment data set is composed of a sequential experiment with varying values of VD (typically from longest to shortest). This series of experiments provides a set of spectra with signals effectively arising from pulse

angles between 270 ° and 90 ° depending on the length of the varied delay constants i.e. when applying a 180 ° pulse and with very small delay (small VD) then applying a 90 ° pulse is equivalent to applying a 270 ° pulse to the nuclei. If this delay becomes long enough (large VD) however, and allows the nucleus to completely relax the excitation generated by the 180 ° pulse recorded in the FID will resemble the excitation generated by a 90 ° pulse.

The time dependency of the signals detected can be plotted on a longitudinal relaxation decay curve to derive the T_1 value.

The intensity of the magnetisation vector in the z axis at time VD is given by the Bloch expression:

$$M_z = M_o (1 - 2e^{(-VD/T_1)})$$
<div align="right">**Equation 3.3**</div>

Where M_z = observed intensity for VD value

M_o = equilibrium value (long VD)

Rearrangement of this equation gives

$$M_o - M_z = 2M_o \, e^{(-VD/T_1)}.$$
<div align="right">**Equation 3.4**</div>

The integration of this equation gives

$$\ln (M_z - M_o) = \ln (2M_o)(-VD/T_1)$$
<div align="right">**Equation 3.5**</div>

Thus a plot of ln $(M_z - M_o)$ against VD will afford a straight line since T_1 and ln (2) are constants. T_1 can be manually estimated from a plot of VD vs M_z using peak areas or signal heights (intensities), by identifying the point where $M_z = 0$.

At this point the expression $M_z = M_o (1 - 2e^{(-VD/T_1)})$ becomes

$$0 = M_o (1 - 2e^{(-VD/T_1)})$$
<div align="right">**Equation 3.6**</div>

Solving this equation and rearranging of the terms leads to the expression (Figure 3.11):

$$T_1 = VD_{(Mz = 0)} / 2.303 \log 2$$
<div align="right">**Equation 3.7**</div>

$$= VD_{(Mz = 0)} / 0.693$$
<div align="right">**Equation 3.8**</div>
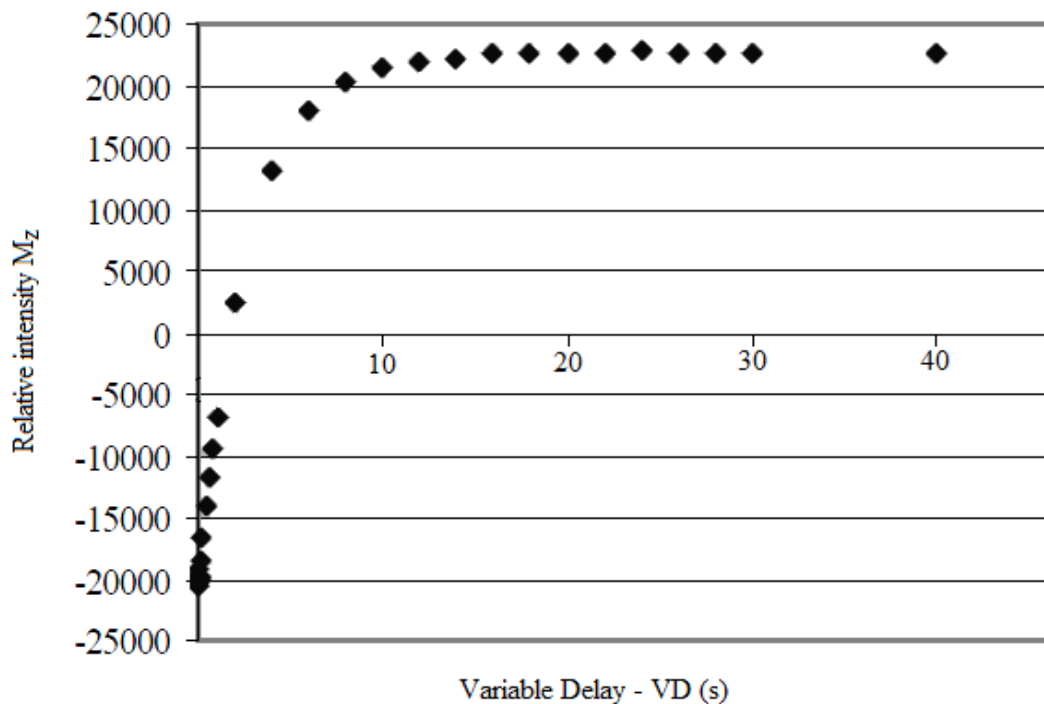
Figure 3.11 A plot of the observed intensities (M_z) against the varied delays (VD)

Alternatively a plot of ln (M_o - M_z) against VD can give a linear line from which T_1 can be ascertained by determining the VD value (= T_1) at the point where ln (M_o - M_z) = 0.

Modern NMR software such as Bruker Topspin Software can be used to iteratively fit the exponential decay curve of best fit to a series of data points. This gives a computed value of T_1 for the nucleus of interest without a user having to manually compute T_1 values as described above (Figure 3.12).
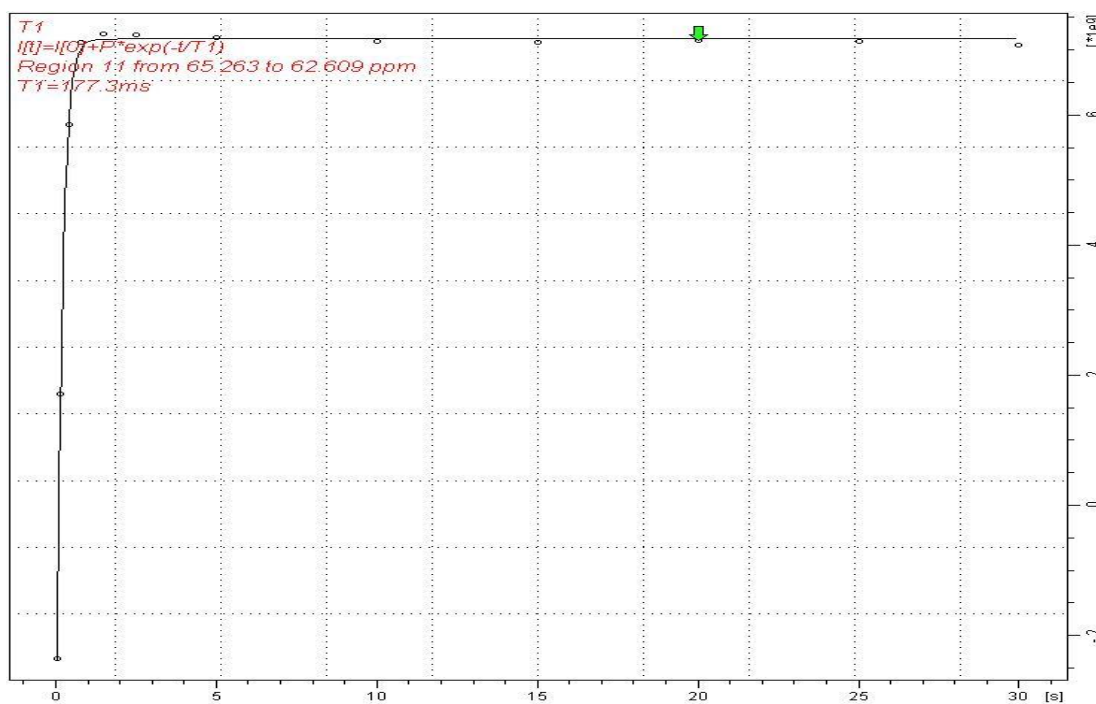
Figure 3.12 Bruker Topspin 3 T_1 profile for linear methylol.

The typical T_1 experiment was employed on the resin sample to obtain T_1 values for individual species within the resin. (Table 3.4) The parameters employed are given in Table 2.2. These T_1 values are more or less similar to the literature. [43, 44]

Table 3.4 The T_1 relaxation times measured using the Inversion Recovery Method (using commercial Bruker software) of the measurable species within the melamine formaldehyde resin sample.

Chemical shift	Chemical environment	T_1 relaxation time
179.69	CH₃**CO**OH	18.04 s
166.13	Triazine carbon with 1 ⁰/2 ° amine	1.59 s
164.86	Triazine carbon with tertiary amine	1.964 s
89.22	Methylene from hemiacetal	1.1415 s
85.39	Dimeric methylene glycol HOCH$_2$OCH$_2$OH	163.7 ms
81.66	Monomeric methylene glycol HOCH$_2$OH	1.253 s
72.98	Branched dimethylene ether with methylol	-
72.08	Branched dimethylene ether with hemiformal methylol	-
70.02	Branched methylol	165.39 ms
67.52	Linear dimethylene ether and linear hemiformal methylol	174.7 ms
63.94	Linear methylol	177.3 ms
54.09	Methoxy for hemiacetal	-
52.48	Branched methylene	2.563 s
48.57	Methanol	9.348 s
46.72	Linear methylene	180.5 ms
39.50	DMSO-d6	39.23 s
21.28	**CH$_3$**COOH	5.85 s

The D1 delay time employed was 1 s and, this was chosen for a qualitative fast experiment (see Table 2.1). This was considerably longer than the required five times T_1 value (i.e. a value as little as 0.5 s could be used), however the consequence of a short D1 if 0.3 s was used is that the degree of saturation in the quaternary carbons would substantially increase hence reducing signal intensities. This is due to the

reason that quaternary carbons (having no attached protons that aid in relaxation) have an inherently slower relaxation. Thus the use of a longer D1 is a good compromise for the signal intensity for the overall spectra shown in Figure 3.13
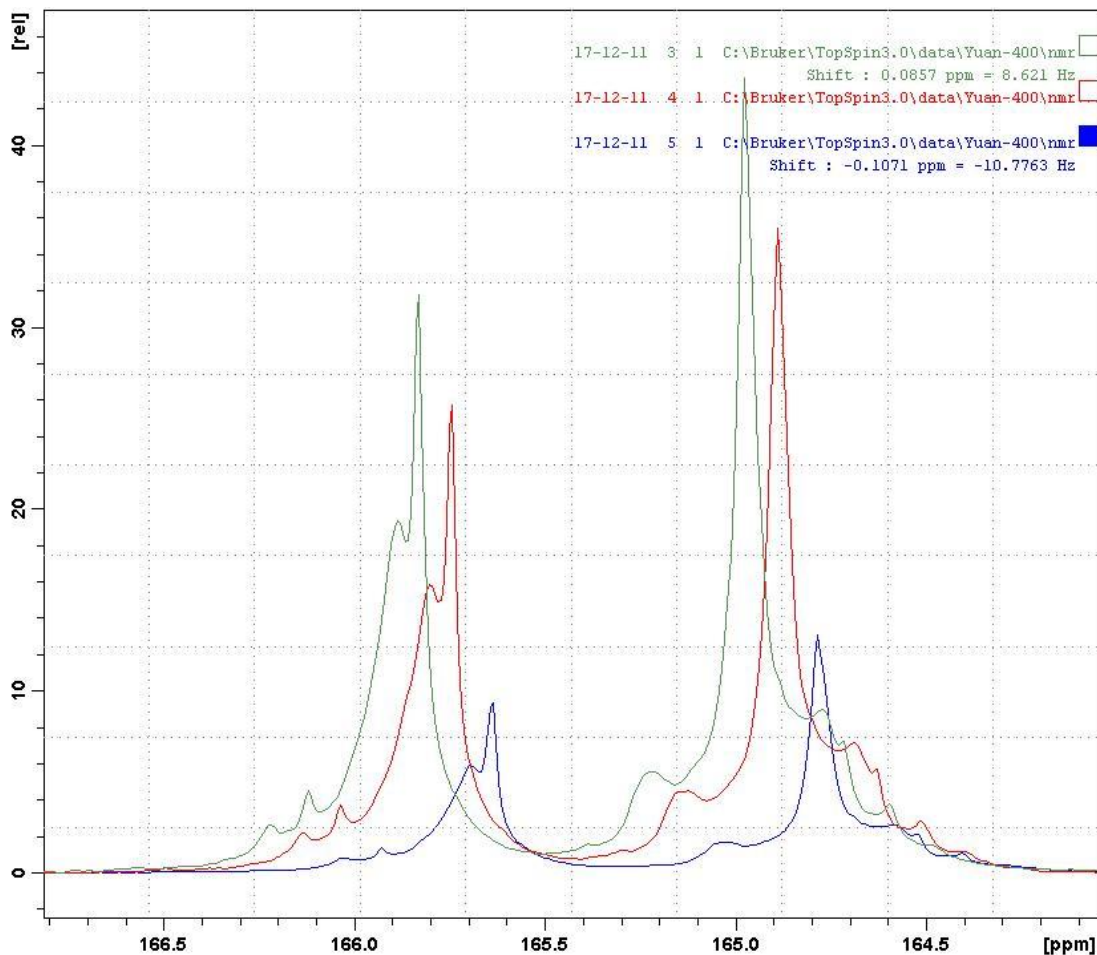
Figure 3.13 A spectra obtained using varied D1 to show the effects of saturation on quaternary carbons from left to right D1 = 2 s (green), 1 s (red), 0.5 s (blue).

3.6.2 Transverse relaxation times, T_2

The pulse program to measure transverse or spin-spin relaxation (T_2) was developed by Meiboom-Gill *via* the modification of the Carr-Purcell spin echo pulse program.[50, 51] T_2 relaxation is the rate at which the nuclei's spin system magnetisation decays to zero in the transverse plane (x-y). [50-52] The T_2 experiments were not central to the

73

main NMR study of the resin systems but were conducted as a side experiment to acquire extra NMR data to provide insight into the molecular size of the polymers under investigation. The parameters of the T_2 experiment are given earlier in (Table 2.2). The results of the T_2 experiment are presented in Table 3.5. The evaluation of the T_2's in relation to the molecular weight was outside the scope of this thesis.

Table 3.5 The T_2 relaxation times of measurable species within a control melamine formaldehyde sample.

Chemical shift	Chemical environment	T_2 relaxation time
179.69	CH$_3$**CO**OH	7.386 s
166.13	Triazine carbon with 1 º/2 º amine	78.31 ms
164.86	Triazine carbon with tertiary amine	99 ms
89.22	Methylene from hemiacetal	676.6 ms
85.39	Dimeric methylene glycol HOCH$_2$OCH$_2$OH	44.86 ms
81.66	Monomeric methylene glycol HOCH$_2$OH	3.104 ms
72.98	Branched dimethylene ether with methylol	-
72.08	Branched dimethylene ether with hemiformal methylol	-
70.02	Branched methylol	22.95 ms
67.52	Linear dimethylene ether and linear hemiformal methylol	-
63.94	Linear methylol	46.5 ms
54.09	Methoxy for hemiacetal	-
52.48	Branched methylene	-
48.57	Methanol	54.7 ms
46.72	Linear methylene	-
39.50	DMSO-d6	639.2 ms
21.28	**CH$_3$**COOH	711.1 ms

3.7 Determination of the conversion factors

Qualitative NMR is acquired with short relaxation between pulses where signal enhancements from NOE factors are included in spectra. Quantitative NMR is acquired with long relaxation between pulses with no NOE enhancement. In order to relate qualitative NMR spectra to quantitative spectra it was necessary to determine the cross calibration (Sat) factor and the NOE factor for melamine resin species within the mixture. There are two methods for determining the conversion factors which were looked into during this investigation; the one step method and the two step method. The result of both methods, provide one set of conversion factors.

3.7.1 One Step Method

The one step method is literally a one step process whereby the cross calibration (Sat) factor and the NOE factor are incorporated together. This is calculated by normalising all the resin peak integrals relative to the peak with the *shortest* relaxation time (relative peak integral) in this case the methylol species at ~64 ppm. This ensures the signal intensity are comparable between the quantitative and the qualitative methods employed. Under the conditions of both methods the chosen nucleus would have completely relaxed avoiding saturation effects. Once the peaks are normalised, the conversion factor is simply the ratio of the relative peak integrals (RPI) between the quantitative and the qualitative spectra for each signal. The following tables show the absolute intensities and the relative peak integrals of each signal of each experiment (Table 3.5 and Table 3.6)**.**

Table 3.6 Integrated signal areas and the RPI (normalised intensities to the linear methylol peak at ~64 ppm) of a quantitative spectrum

Integral	Signal	Centre	Integral [abs]	RPI
1	CH$_3$**CO**OH	172.69	337834251.2	0.158
2	Triazine carbon with 1 °/2 ° amine	166.13	1938337763	0.906
3	Triazine carbon with tertiary amine	164.86	3359871990	1.570
4	Methylene from hemiacetal	89.22	6380680.11	0.003
5	Dimeric methylene glycol HOCH$_2$OCH$_2$OH	85.39	14760748	0.007
6	Monomeric methylene glycol HOCH$_2$OH	81.66	18894248.04	0.009
7	Branched dimethylene ether with methylol	72.98	20502981.15	0.010
8	Branched dimethylene ether with hemiformal methylol	72.08	15959954.77	0.007
9	Branched methylol	70.02	418989620	0.196
10	Linear dimethylene ether and linear hemiformal methylol	67.52	317321720.9	0.148
11	Linear methylol	63.94	2140017963	1.000
12	Methoxy for hemiacetal	54.09	21693592.96	0.010
13	Branched methylene	52.48	54771497.87	0.026
14	Methanol	48.57	135034412	0.063
15	Linear methylene	46.72	127115890.5	0.059
16	DMSO-d6	39.50	996182686.2	0.466
17	**CH$_3$**COOH	21.28	665415129.1	0.311

To obtain the RPIs, one must divide the absolute integral values of each individual signal by the intensity of the linear methylol signal at ~64 ppm, effectively normalising all the signals relative to this signal. The RPI for the *branched* methylol signal (at a different ppm value to the linear methylol signal) in the quantitative run is provided as an example (Equation 3.9).

$$\text{RPI} \quad = \quad \frac{418989620}{2140017963} \quad = \quad 0.196 \,(4 \text{ s.f.}) \qquad\qquad \textbf{Equation 3.9}$$

Table 3.7 Integrated signal areas and the RPI (normalised intensities to the linear methylol peak at ~64 ppm) of a qualitative spectrum

Integral	Signal	Centre	Integral [abs]	RPI
1	CH₃**CO**OH	172.67	20727420.82	0.028
2	Triazine carbon with 1 °/2 °amine	166.20	319962465.4	0.427
3	Triazine carbon of with tertiary amine	164.84	486009125	0.649
4	Methylene from hemiacetal	89.23	2177246.11	0.003
5	Dimeric methylene glycol HOCH₂OCH₂OH	85.36	5108966.35	0.007
6	Monomeric methylene glycol HOCH₂OH	81.67	5846971.09	0.008
7	Branched dimethylene ether with methylol	73.02	7354844.19	0.010
8	Branched dimethylene ether with hemiformal methylol	72.14	4162085.08	0.006
9	Branched methylol	69.91	128850804.6	0.172
10	Linear dimethylene ether and linear hemiformal methylol	67.59	109633511.4	0.146
11	Linear methylol	63.80	748762931.4	1.000
12	Methoxy for hemiacetal	54.03	4695865.93	0.006
13	Branched methylene	52.73	18383991.57	0.025
14	Methanol	48.53	15965543.48	0.021
15	Linear methylene	46.61	36480462.37	0.049
16	DMSO-d6	39.52	43118792.49	0.058
17	**CH₃**COOH	21.27	86879709.71	0.116

The quantitative RPI is divided by the qualitative RPI from the two tables above to produce the conversion factors show in Table 3.7.

Table 3.8 Ratio of RPIs from the one step method producing the conversion factors for each signal using the results from above

Signal	RPI from Table 3.5	RPI from Table 3.6	Conversion factor (NOE+Sat)
CH$_3$**CO**OH	0.158	0.028	5.70
Triazine carbon with 1 ⅔2 °amine	0.906	0.427	2.12
Triazine carbon with tertiary amine	1.570	0.649	2.42
Methylene from hemiacetal	0.003	0.003	1.03
Dimeric methylene glycol HOCH$_2$OCH$_2$OH	0.007	0.007	1.01
Monomeric methylene glycol HOCH$_2$OH	0.009	0.008	1.13
Branched dimethylene ether with methylol	0.010	0.010	0.98
Branched dimethylene ether with hemiformal methylol	0.007	0.006	1.34
Branched methylol	0.196	0.172	1.14
Linear dimethylene ether and linear hemiformal methylol	0.148	0.146	1.01
Linear methylol	1.000	1.000	1.00
Methoxy for hemiacetal	0.010	0.006	1.62
Branched methylene	0.026	0.025	1.04
Methanol	0.063	0.021	2.96
Linear methylene	0.059	0.049	1.22
DMSO-d6	0.466	0.058	8.08
CH$_3$COOH	0.311	0.116	2.68

Quantitative and qualitative NMR experiments were carried out several times on different days with different resin batches to confirm the reproducibility and the accuracy of the conversion factors used. Statistical analysis of 8 separate experiments was carried out on the RPIs obtained from each experiment. Figure 3.14 shows the distribution of the conversion factor across the experiments.
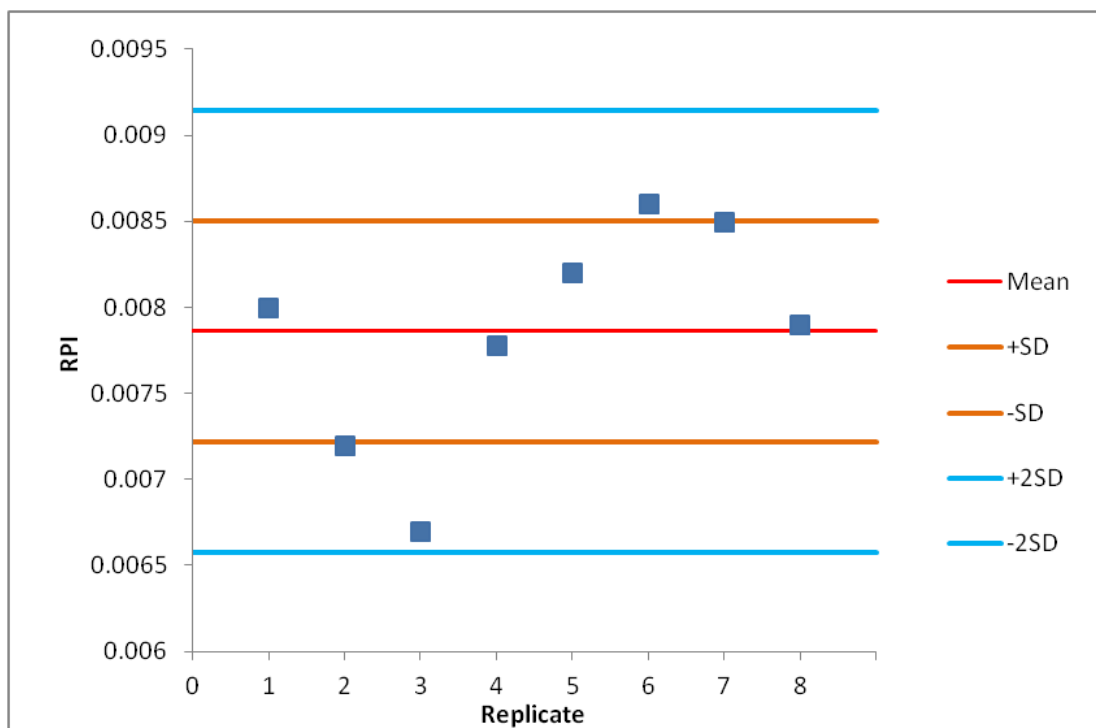
Figure 3.14 Quality control chart of 8 different replicates of quantitative NMR experiments showing the RPI of the branched dimethylene ether with hemiformal methylol (72.08 ppm)(. SD = standard deviation and 2SD = 95% confidence of a normal distribution curve.

For the majority of the signals, the first "replicate" (of the 8 done) is outside the 95% confidence interval (Appendix 1). The conditions of the experiment were optimised, after the first replicate, particularly the sample mixing and loading into the NMR tube, and consequently the remaining (7) replicates fall well within the 95% confidence interval. If the first replicate were to be excluded the standard deviation dramatically decreases, indicating that the conversion factor has a high degree of reproducibility. The first replicate has not been removed from the results in Appendix 1 so that the effect of optimization can be discerned. However, Table 3.8 summarises the mean RPIs of the qualitative (fast) and quantitiative results from 7 separate experiments (first set of data removed).

Table 3.9 The mean RPIs of the 7 NMR quantitative and qualitative experiments used for the generation of the conversion factor for all signals in melamine resin.

Integral	Chemical environment	Mean RPI of qualitative signals	Mean RPI of quantitative signals
1	CH$_3$**CO**OH	0.0274	0.1567
2	Triazine carbon with 1 ⁰/2 ° amine	0.4263	0.9095
3	Triazine carbon with tertiary amine	0.6448	1.5790
4	Methylene from hemiacetal	0.0030	0.0026
5	Dimeric methylene glycol (HOCH$_2$OCH$_2$OH)	0.0071	0.0073
6	Monomeric methylene glycol (HOCH$_2$OH)	0.0087	0.0089
7	Branched dimethylene ether with methylol	0.0087	0.0088
8	Branched dimethylene ether with hemiformal methylol	0.0062	0.0078
9	Branched methylol	0.1712	0.1956
10	Linear dimethylene ether and linear hemiformal methylol	0.1483	0.1530
11	Linear methylol	1.0000	1.0000
12	Methoxy for hemiacetal	0.0062	0.0100
13	Branched methylene	0.0364	0.0197
14	Methanol	0.0218	0.0626
15	Linear methylene	0.0487	0.0596
16	DMSO-d6	0.0606	0.4937
17	**CH$_3$**COOH	0.1144	0.3058

3.7.2 Two Step Method

The two step method in determining the conversion factor is *via* the investigation of the cross calibration factor (commonly known as the saturation factor) and the Nuclear Overhauser Enhancement (NOE). The NOE provides signal enhancement by the transfer of nuclear spin polarisation between nuclear spin populations. A total of four experiments are required to deduce these two components. These include the two experiments required for the one step method and two equivalent experiments with opposite NOE enhancements. In normal situations however, experiments would only be done with the one step method due to the fact that it only requires half the amount of time to do two experiments, rather than four. The results of the two step method from the four different pulse programs are outlined in Table 3.9.

Table 3.10 The relative peak intensities (RPI) of 5 example signals obtained from four different pulse programs used to deduce the conversion factor *via* the two step method.

Chemical environment	RPI			
	Quantitative (slow without NOE)	Qualitative (Fast with NOE)	Slow with NOE	Fast without NOE
Triazine carbon with 1 ⁄2 °amine	0.8773	0.4466	0.6678	0.6188
Triazine carbon with tertiary amine	1.5808	0.6660	1.1078	0.9163
Methylene from hemiacetal	0.0066	0.0035	0.0050	0.0045
Branched methylol	0.2233	0.2110	0.2108	0.2171
Linear methylene	0.0649	0.0802	0.0637	0.0815

The NOE factor (NOEf), Equation 3.10, is obtained by dividing the quantitative RPI by the RPI of slow with NOE (quantitative with NOE).

$$\text{NOEf} \quad = \quad \frac{\text{RPI of slow without NOE}}{\text{RPI of slow with NOE}}$$

<div align="right">**Equation 3.10**</div>

The saturation factor (Sat), Equation 3.11, is obtained by dividing the quantitative RPI by the RPI of the fast without NOE method.

$$\text{Sat} \quad = \quad \frac{\text{RPI of slow without NOE}}{\text{RPI of fast without NOE}}$$

<div align="right">**Equation 3.11**</div>

The product of NOEf and Sat is essentially the conversion factor (**Table 3.10**). Due to the increased number of steps however and the need to integrate more spectra more uncertainty is introduced into to the calculated value of the conversion factor. Therefore the application of the rapid NMR method (Section 3.8) utilises the conversion factors obtained from the **one step method**. The two-step method is hence not used.

Table 3.11 Comparison of the saturation (Sat), NOE (NOEf) factors and conversion factors of the 1 and 2 step methods.

Chemical environment	NOEf	Sat	Conversion factor -1 step	conversion factor - 2 step (Sat x NOEf)
Triazine carbon with no/mono substituted amine	1.3137	1.4177	1.9644	1.8625
Triazine carbon with di substituted amine	1.4270	1.7252	2.3736	2.4618
Methylene from hemiacetal	1.3200	1.4667	1.8857	1.9360
Branched methylol	1.0593	1.0286	1.0583	1.0895
Linear methylol	1.0188	0.7963	0.8092	0.8113

3.8 Application of the conversion factors to qualitative data.

In this section the conversion factors derived from Section 3.7 are applied to the spectral data obtained during an *in situ* melamine reaction. The results of this allow the quantitative reaction profiles of the reaction to be deduced for real time NMR analyses of the resin systems.

Based on previous research[7,17] it was predicted that the spectral data obtained from using "qualitative" experimental parameters (i.e. fast, non-qualitative data) can be reliably utilised to anticipate quantitative data, within an approximate error limit (ca. 10-15%). The results in Table 3.7 show the RPIs of a qualitative and a quantitative experiment. The ratio of the RPIs gives a conversion factor which can be applied to *in situ* real time reaction spectral data. The conversion factors given in Table 3.11 were calculated from the average of the RPIs from seven repeated quantitative and qualitative experiments obtained on separate days and different batches to ensure reproducibility. Originally eight experiments were analysed, however the first replicates were recorded before conditions were optimized. Accordingly, the RPIs from the first qualitative and quantitative experiments are not included in the conversion factor calculations.

Table 3.12 A list of reliable conversion factors for each chemical environment from using the average of the 7 repeated quantitative and qualitative experiments.

Integral	Chemical environment	Average Conversion factor
1	CH$_3$**CO**OH	5.72
2	Triazine carbon with no/mono substituted amine	2.13
3	Triazine carbon with di substituted amine	2.45
4	Methylene from hemiacetal	0.88
5	Dimeric methylene glycol HOCH$_2$OCH$_2$OH	1.02
6	Monomeric methylene glycol HOCH$_2$OH	1.03
7	Branched dimethylene ether with methylol	1.02
8	Branched dimethylene ether with hemiformal methylol	1.26
9	Branched methylol	1.14
10	Linear dimethylene ether and linear hemiformal methylol	1.03
11	Linear methylol	1.00
12	Methoxy for hemiacetal	1.61
13	Branched methylene	0.54
14	Methanol	2.87
15	Linear methylene	1.22
16	DMSO-d6	8.15
17	**CH$_3$**COOH	2.67

The average conversion factor (f_{ac}) was applied to the integrated intensities (I$_{Rr}$) of the *in situ* real time NMR analysis to produce the corrected quantitative data (I$_Q$). (Equation 3.12)

$$I_{Rr} \cdot f_{ac} = I_Q$$

Equation 3.12

Figure 3.15 shows the quantitative reaction profile of the methylene group of the hemiacetal species at 89.23 ppm after the application of the conversion factor in an *in situ* real time NMR reaction analysis.
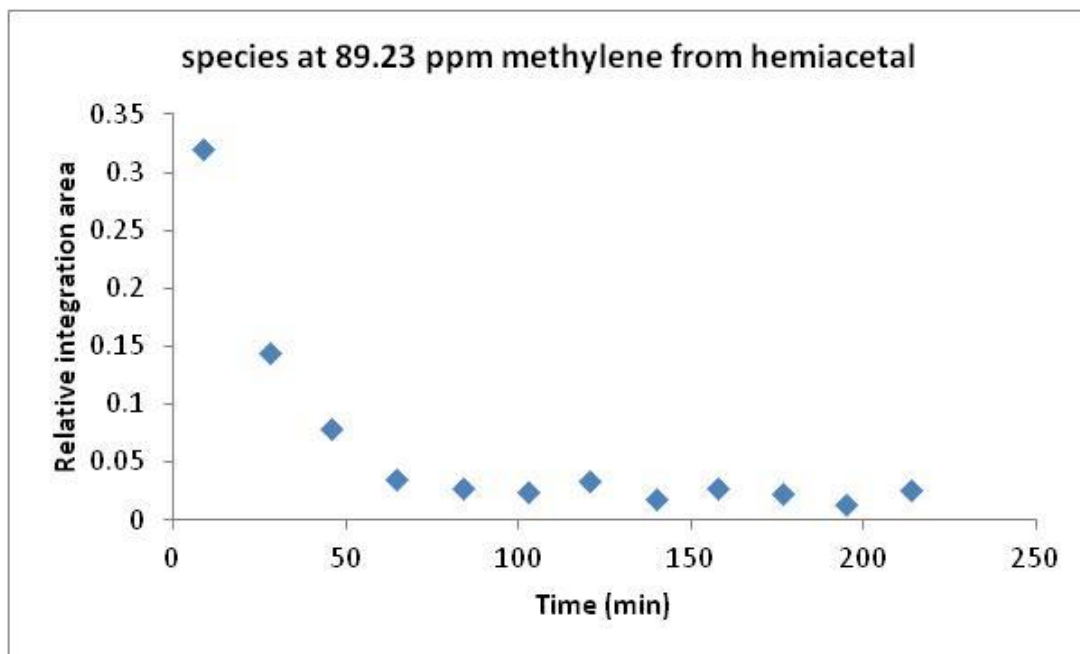
Figure 3.15 The quantitative reaction profile (after application of the conversion factor) for the integrated species of methylene from hemiacetal (89.23 ppm) generated from a real time reaction

All spectral data obtained during the real time reactions were converted into quantitative data as shown above. The reaction profiles of each species were used to monitor the formation and disappearance of transient species within the evolving resin systems during the reaction.

4 Analysis of Melamine Resin Reactions

4.1 Introduction

In this chapter, results of the *in situ* real time qualitative results converted to quantitative data are examined. They are presented in the form of quantitative reaction profiles for each of the transient species present. The progress of the changes in the transient species in the reaction was monitored throughout the duration of the reaction.

The investigation of the melamine resins using the analytical techniques of infrared spectroscopy (IR), Matrix Assisted Laser Desorption Ionisation - Time of Flight - mass spectrometry (MALDI-TOF-MS) and Electrospray Ionisation - mass spectrometry (ESI-MS) are also outlined.

4.2 NMR reaction monitoring

The qualitative NMR method was employed for the *in situ* real time monitoring of the resin formation process. The analysis of the sequential spectra obtained by this method provides information on the order of the reactions occurring during the resin synthesis.

The quantitative reaction profiles determined from Section 3.9 were used to monitor the relative concentrations of chemical species as a function of the reaction progress. This provides information on the relative rates of the formation of the melamine resin species.

Due to the demanding conditions of the qualitative method, the spectral data of the real time analysis suffers loss of resolution. To compensate for this, qualitative

signals were compared to spectra obtained using the quantitative method (high resolution). This confirms the identity of the signals related to the species being monitored.

The reaction profiles in this chapter will be discussed in two regions; region 1 is the variable temperature (VT) region and region 2 is the region for which the temperature was being held constant at 90 ℃.

4.2.1 Addition stage reactions

Addition stage reactions are known to occur between the reactant species melamine and formaldehyde (polymeric species).[20] These reactions, under alkaline conditions undergo a substitution reaction with formaldehyde species and form methylol melamines (Figure 1.5). The melamine species in the NMR region between 164 - 167 ppm gave two distinctive signals which arise at ~166.2 and 164.8 ppm. They correspond to the quaternary triazine carbons of melamine, differing with the degree of substitution of the amine group i.e. primary and secondary (A) amines gives rise to the signal at 166.2 ppm and tertiary amines (B) produce the signal at 164.8 ppm.
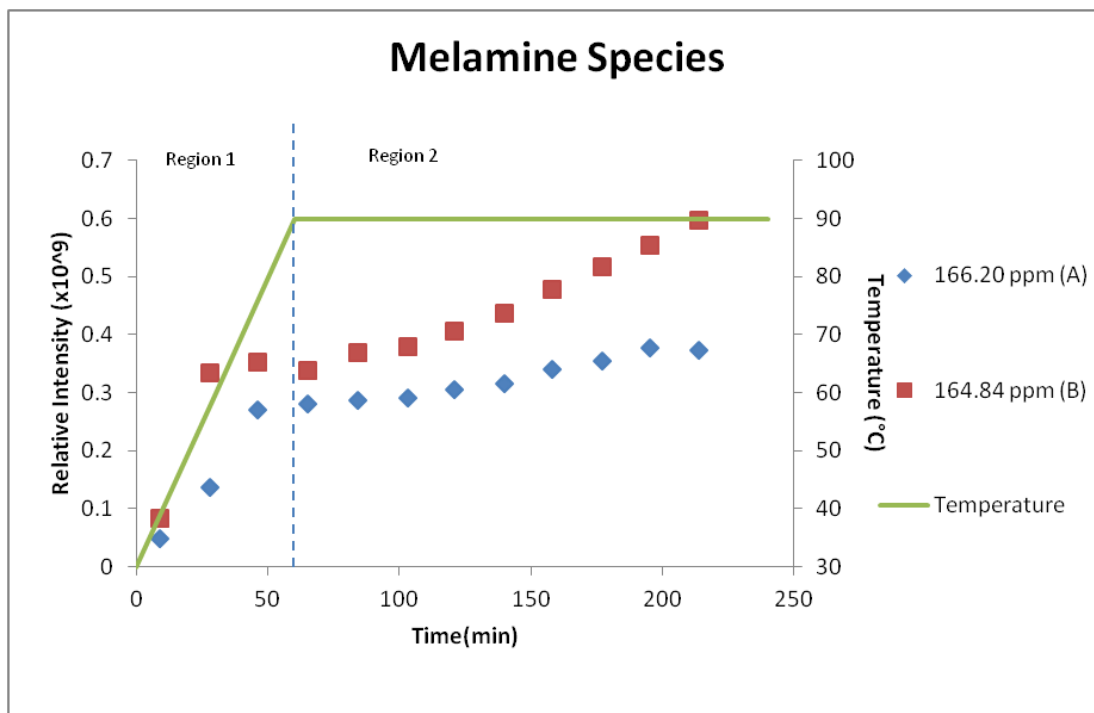
i.   Melamine species

Figure 4.1 The reaction profiles showing: secondary amine of the triazine carbon of melamine (A, 166.2 ppm) and tertiary amine of the triazine carbon of melamine (B, 164.84 ppm)

The quantitative reaction profile of the melamine species shown in Figure 4.1 can be used to describe the relative rate relationships of the melamine species. The increase in relative concentrations of species A and B in region 1, demonstrates the addition stage reaction of the melamine resin synthesis. It can be seen that in region 1, species B is twice the amount of A at approximately 30 minutes into the reaction. This means that the rate at which species B forms in the addition stage is initially twice that of species A. However, by the end of the temperature ramp the A:B ratio is 1:1.2. The significance of this is that the formation of species B has decreased dramatically, this is likely due to the high consumption of the formaldehyde species shown in Figure 4.3 and Figure 4.4. The relative rates are somewhat comparable to the research proposed by Gordon *et al.*,[53] however comparison to their research was restricted as their temperature conditions ranged only between 20 - 55 °C. The relative rates

88

observed in this study is the trend by which the reaction continues through the condensation stage up to the IRE of the resin formation process. The relative kinetics of the self condensation of melamine and formaldehyde has also in the past reported by Okano *et al.*[54] Their results relied on the assumption that no equilibrium shifts were occurring. However many investigations in the past indicate that the pH in especially alkaline conditions are highly influential to the equilibrium constant (Equation 1.4). [5, 9, 55]

ii.   Formaldehyde species

Formaldehyde species form polymers in aqueous solution. These polymeric forms can be further stabilised to hemiacetal species in the presence of methanol. Structures of the observed formaldehyde species are given in Figure 4.2.

$$HO-\underline{C}H_2-OCH_3$$

$$HO-\underline{C}H_2-O-\underline{C}H_2-OH$$

$$HO-\underline{C}H_2-OH$$

$$HO-CH_2-O\underline{C}H_3$$
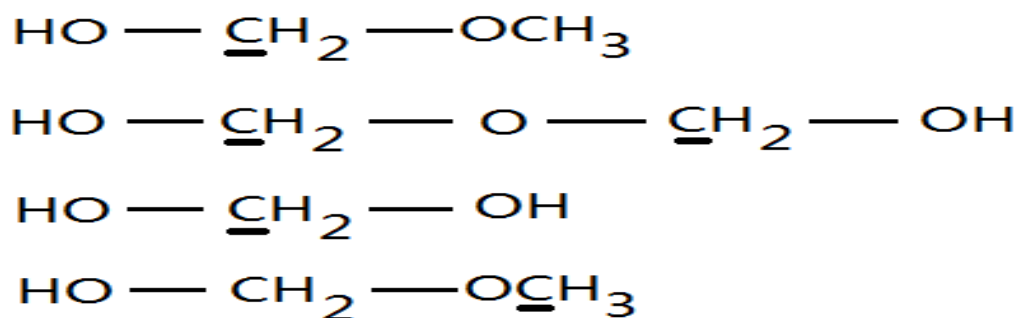
Figure 4.2 Formaldehyde species corresponding from top to bottom to: Methylene carbon of hemiacetal, dimeric methylene glycol, monomeric methylene glycol and methoxy carbon of hemiacetal

The reaction profiles of methylene glycol (Figure 4.3) and hemiacetal (Figure 4.4) species are shown below.

Figure 4.3 The quantitative reaction profile of dimeric methylene glycol (85.36 ppm) and monomeric methylene glycol (81.67 ppm)

Figure 4.4 Reaction profile of methylene carbon of hemiacetal species (89.23 ppm) and methoxy carbon of hemiacetal (54.03 ppm)

90

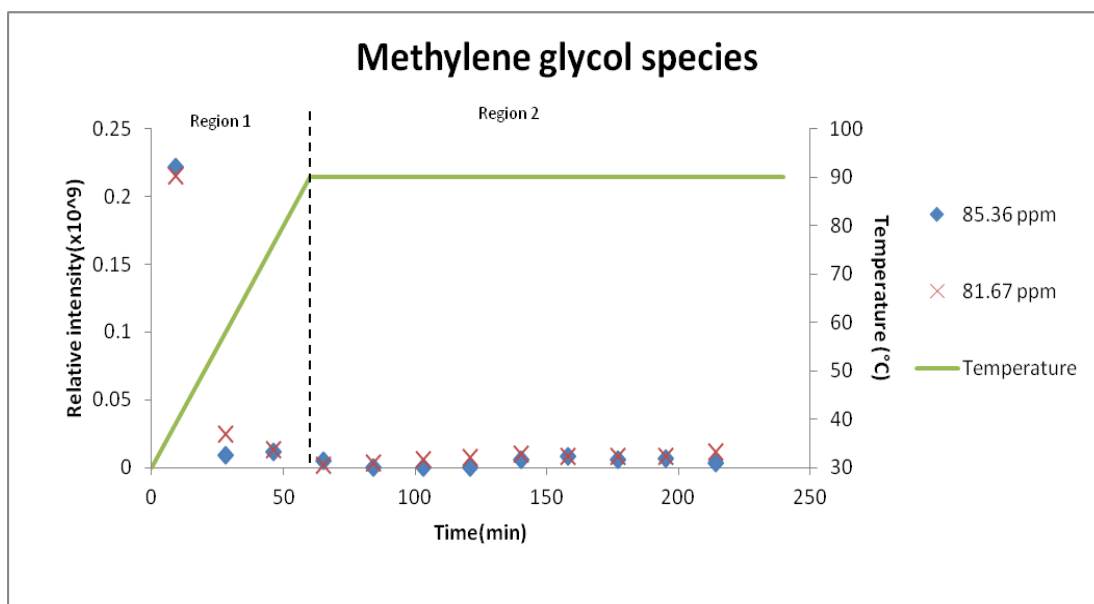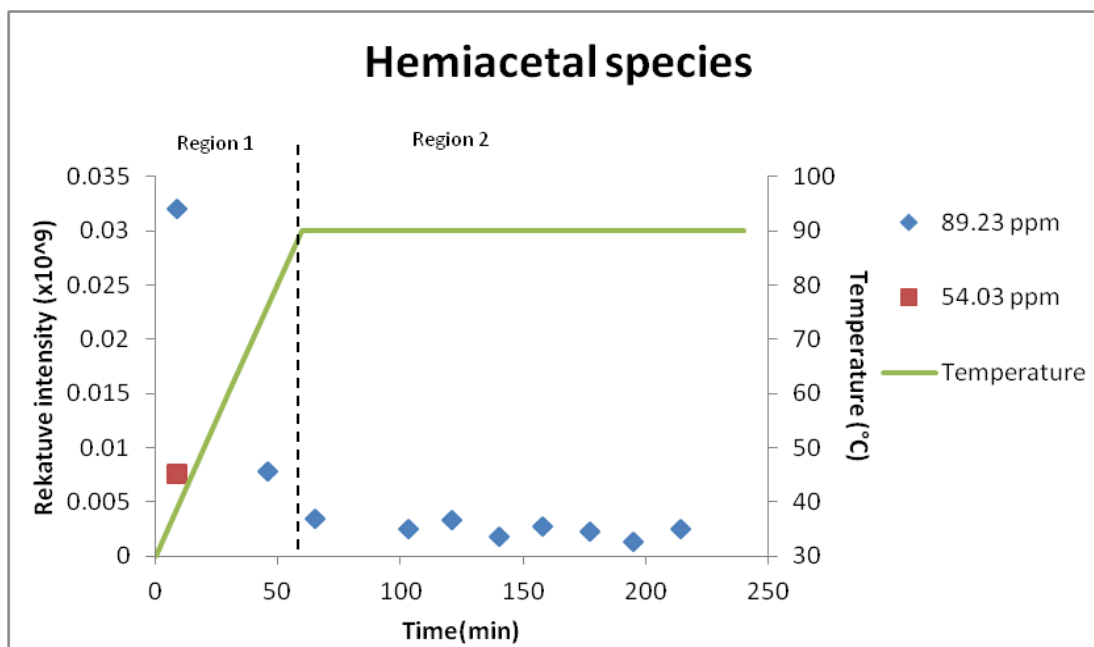Both the methylene glycol and the hemiacetal species show the same trend in region 1 (addition stage). The species rapidly decrease corresponding to a fast rate of reaction of these formaldehyde species with the melamine species discussed earlier. The methoxy at 54.03 ppm has completely disappeared during the addition stage this is possibly due to that the hemiacetal species react have reacted with a melamine losing the methoxy chemical environment. These species are consumed as the secondary and tertiary amines of triazine melamine carbon increase corresponding to the production of methylol melamines.

   iii.   Resin species

It is apparent that the linear methylol (Figure 4.5) is the major methylol species, formed at a rapid rate until the end of the temperature ramp. This is consistent with the rapid drop of the formaldehyde concentration and increase in the melamine species described earlier. This is consistent with several studies such as Scheepers *et al.*[44] and Subrayan *et al.*[43] showing the loss of methylene glycol species quantitatively as the resins are reacted.
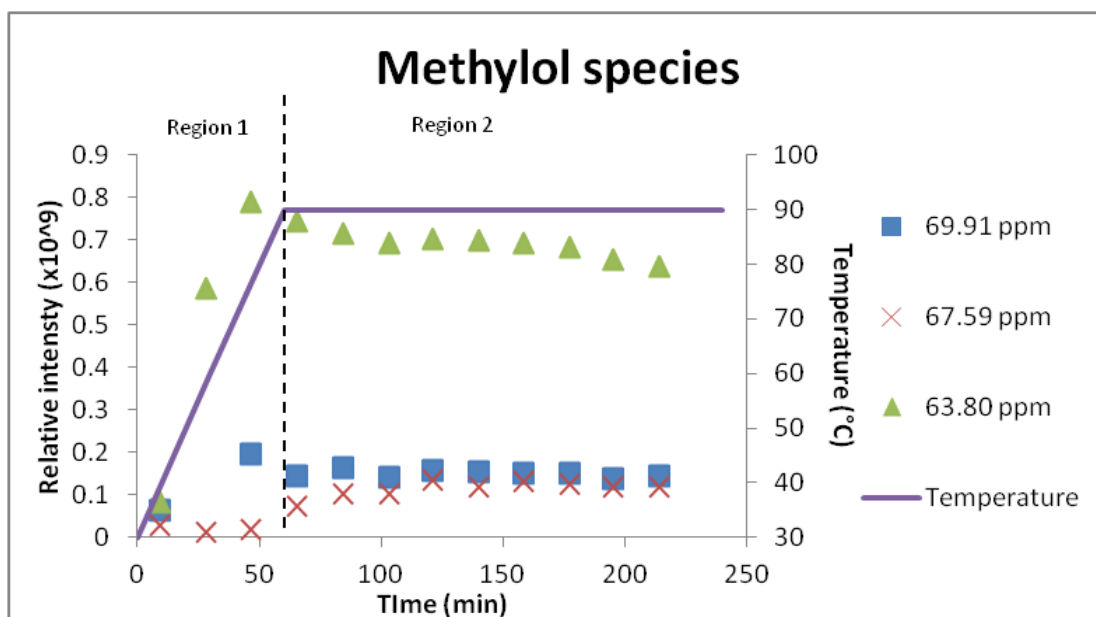

Figure 4.5 Reaction profile for linear methylol (63.80 ppm), linear hemiformal methylol (67.59 ppm) and branched methylol (69.91 ppm)

91

4.2.2 Condensation stage reactions

The condensation reactions of methylol groups to form linkages between melamine moieties correspond to the region directly after the temperature ramp (region 2).

The melamine carbons show that the condensation stages up to a reaction time of 140 min maintain an A:B ratio of 1:1.2. The significance of this is that formation of B is initially fast during the addition stage, but slows down once the temperature reaches 90 ℃. Up until 140 min the formation of A and B occurred slowly and increased at the same rate. After 150 min however, the rate at which species B increased was faster than the rate of A. The rate of formation of species A potentially decreases for two reasons; 1) the secondary amine is consumed to form tertiary amines and 2) the secondary amine is consumed to form methylene and ether linkage groups due to condensation reactions. The reaction progressed until ~225 min where the ratio of A:B is 1:1.6. This corresponds to the commercial endpoint of the reaction (the IRE) and reactions past this point have no commercial significance.

The rapid rate of methylol species formation described in the addition stage is required to support the cross linking during condensation. Cross linking is shown by the increase of methylene and ether species. (Figure 4.6 and Figure 4.7 respectively).
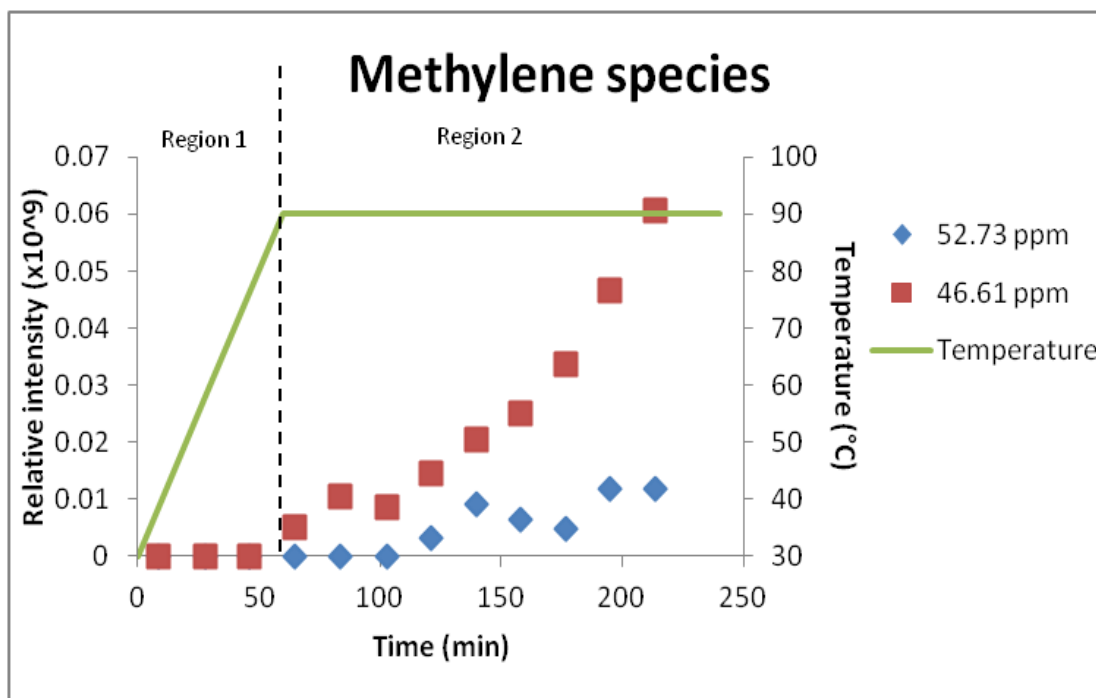
Figure 4.6 Reaction profile for linear methylene (46.61 ppm) and branched methylene (52.73 ppm)
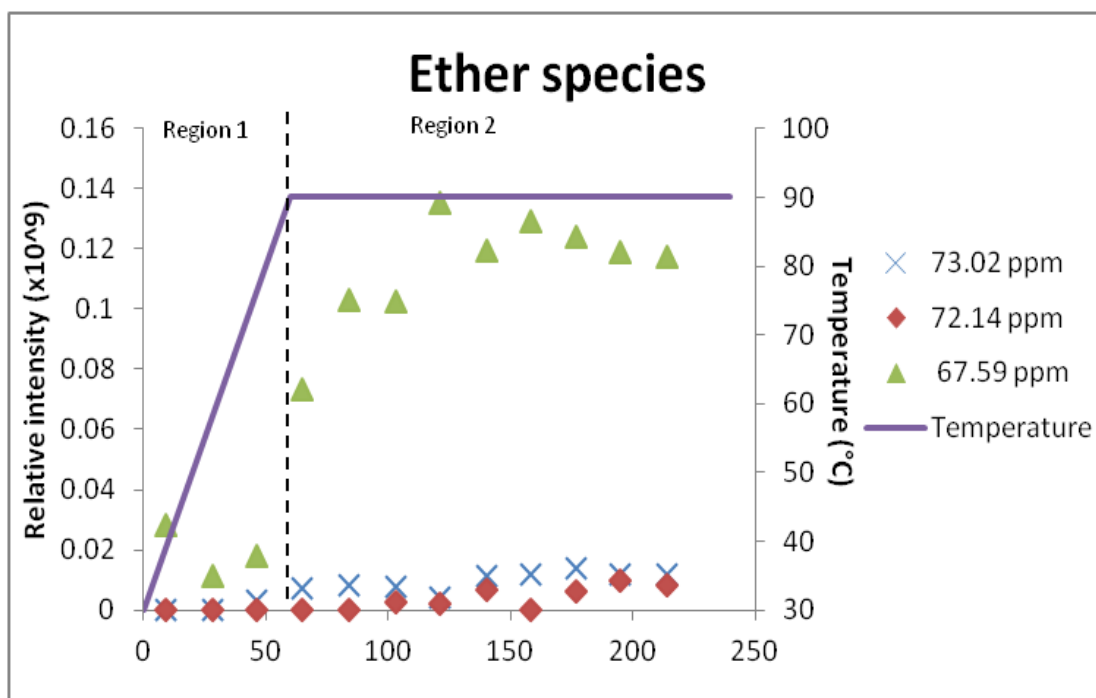

Figure 4.7 The reaction profile of linear dimethylene ether (67.59 ppm), branched dimethylene ether with hemiformal methylol (72.14 ppm) and branched dimethylene ether with methylol (73.02 ppm).

The linear dimethylene ether and the linear hemiformal methylol signal arise and overlap in the same chemical shift range. Therefore the two species provide the same reaction profile and are indistinguishable from each other. The difference between the two groups is that the ether species acts as a bridge/linkage between 2 melamine moieties and the methylol species is only attached to 1 melamine group and terminated with an alcohol group on the other end. They have very similar chemical shift because the chemical environment in the $-NH-CH_2-O-\underline{CH_2-OH}$ moiety is very much like the $-NH-CH_2-O-\underline{CH_2-NH}-$. The trend shown by the dimethylene ether reaction profile suggests that the 120 min reaction time gives the maximum amount of ether species available for linking the melamines. The profile essentially plateaus after this point and no further ether linkages are produced. Hence it is important to monitor past this point for commercial synthesis. The secondary condensation product is the methylene linkage which increases once the ether linkage possibilities are exhausted. The linear methylol profile shows a steady decrease after the ramp in region 2, indicating the consumption of the methylol species (Figure 4.5). When cross linkage occurs the hydroxide from the methylol group is removed along with a proton from an adjacent species producing water. This can account for the formation of methylene (Figure 4.6) and ether (Figure 4.7) linkage groups depending upon the nature of the adjacent species. The methylene linkages show an exponential increase after the addition stage because during condensation the production of methylene species will only increase.

In early NMR investigations many authors detected ether bridges in the resin however, did not account for any methylene linkages.[56,57] In 1992, Samaraweera *et al.*[58] published that ether links predominates over methylene linkages using ^{13}C NMR however Chang[41] contradicted their work, by presenting results obtained from liquid chromatography mass spectrometry (LC-MS)and showed strong evidence of the methylene bridging group. Under the current investigation with the techniques of real time NMR analysis of the resin, it can be concluded that both species are present within the melamine resin. The quantitative results of this investigation indicates that

preliminary stages of resin formation (addition stage) ether linkages between melamines predominate, however the condensation stage shows that the relative amount of methylene increases exponentially and if the analysis was carried through to the curing stage the possibility of methylene bridge predominating in the cured resin is relatively high.

Region 2 of the carbon with a tertiary amine B (Figure 4.1) indicates an increase in substitutions of the amine groups. The trends of this region are very similar to the trend shown by the methylene group. This strong correlation is potentially the possibility that they are indicative of the same group being formed. Figure 4. 8 shows that the commercial endpoint of the liquid resin is reached when the ratio of ether links to methylene links is 2:1.
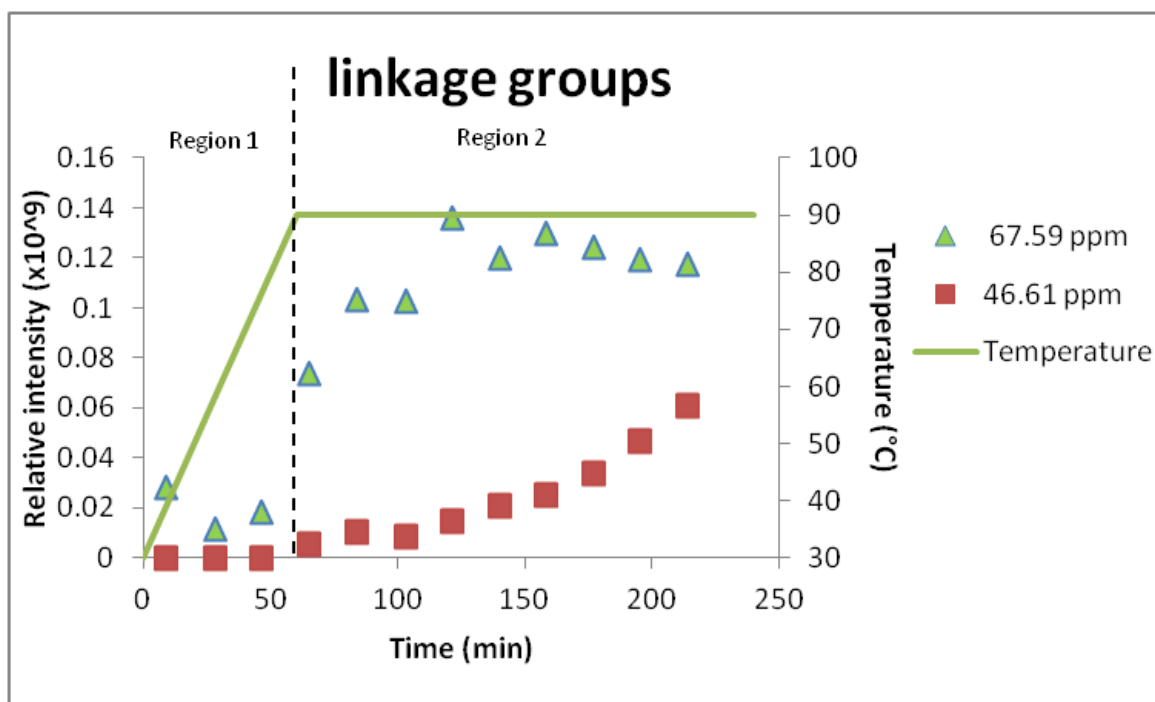

Figure 4.8 The reaction profile of the major linkage groups of the resin; linear dimethylene ether (67.59 ppm) and methylene linkage (46.61 ppm)

The summary of the analysis of real time profiles of the resin indicates that the addition stages of the resin production have a relatively quick rate followed by plateaus. This is shown by the fast increase in melamine and methylol species in the addition stage (region 1) and the exponential decay of the methylene glycol (formaldehyde) species. The condensation process promotes the production of ether linkages with the rate of formation being very rapid initially, with a plateau after 120 min of reaction. This is a crossing point of industrial significance as this is the amount of ether linkage required for this particular resin to reach the IRE. The reduction of ether formation in later stages of region 2 could possibly be due to the consumption of linear hemiformal methylol to form further cross linking products. The secondary cross linkage group is the methylene group. The methylene profile shows that it does not form during the addition stage and increases at an exponential rate once the condensation stage is reached. This is supported by the reduction of methylol species and increase in the melamine carbon with tertiary amine substitute. The IRE of the melamine resin in this research shows that the cross linking end point of the final liquid resin requires that the methylene to ether linkage ratio is 1:2.

Quantitative measurements of the ether and methylene bridging groups have been measured in the past. [43, 44] However, experiments were constricted to reactions occurring outside the NMR subsequently once the reaction has progressed to a desired stage inject into the NMR for analysis therefore the observations of species reacting could not be acquired. This investigation forms the basis of monitoring of melamine resins quantitatively in a real time *in situ* NMR analysis, this technique allows the transient reaction profiles of each species to be observed. Future work using the technique developed in this study for quantitative NMR analysis should possibly exploiting the industrial parameters including stoichiometry, temperature and pH to see what the effects of changing these parameters has on the final resin products.

4.3 Results from the additional techniques used to study the melamine formaldehyde resin systems

4.3.1 Solid state NMR spectroscopy

Solid state NMR spectroscopy was included in this study to see if additional information can be obtained for the melamine formaldehyde resin system. The solid state NMR pulse programs of cross polarisation and high powered decoupling were utilised to acquire spectra for these investigations.
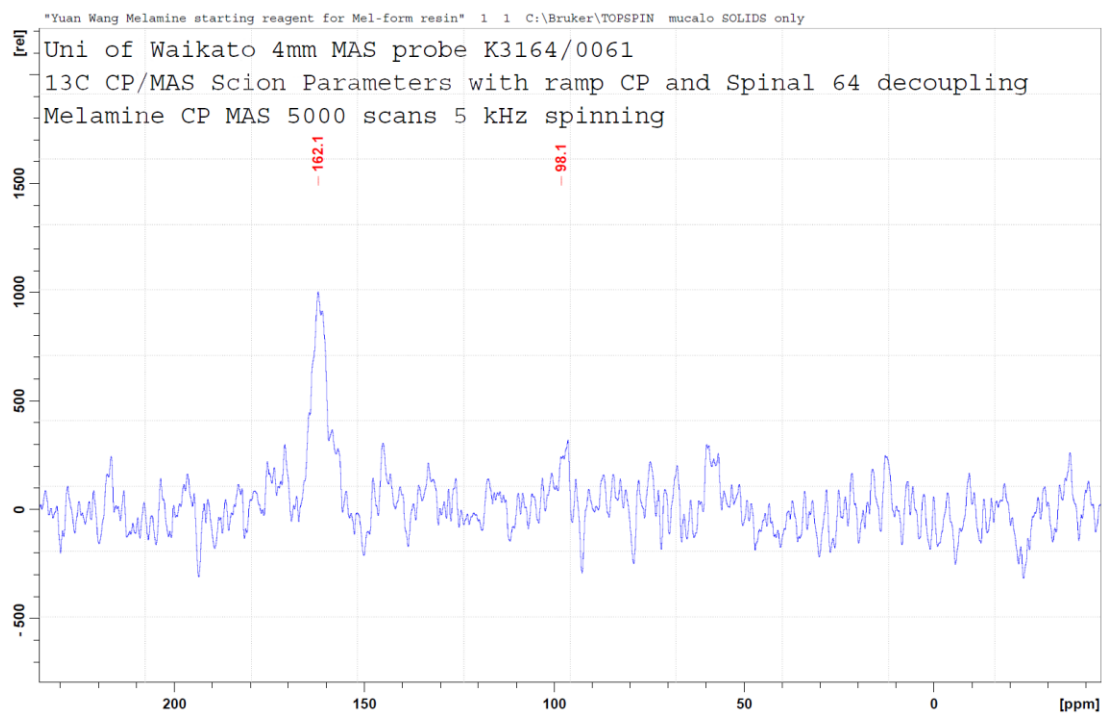

Figure 4.9 Solid State NMR spectrum of melamine using CP pulse program with 5000 scans

The spectrum of melamine shown above was obtained with CP pulse program . There was only 1 significant peak observed as expected corresponding to the triazine carbon of the melamine at 162.1 ppm.
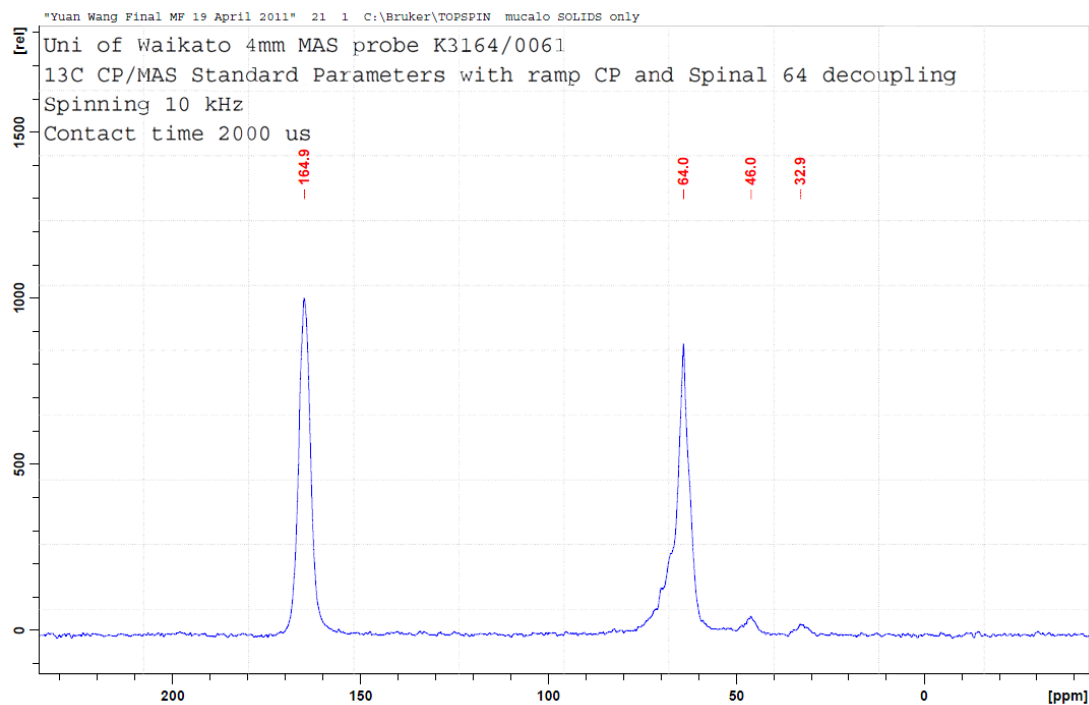
97

Figure 4.10 Solid state NMR spectrum of freeze dried melamine formaldehyde final resin (control) using CP puse program with contact time of 2000 μs

The spectrum of MF resin obtained with CP pulse program, the spectrum shows the melamine triazine peak arising at 164.9 ppm, and the broad CH_2-O peaks arising around 64 ppm. The peak arising at ~46 ppm is assigned as the methylene linkage peak however uncertainties arise from the possibility that it was a spinning side band from another signal. It is important to note the peak at 32.9 ppm are the spinning side band of the 164.9 signal (10 kHz displaced from the 164.9 ppm peak). The broadness of the ether peak is due to either, multiple chemical environments (e.g. methylol and ether linkage) or reflects on the different levels of molecular motion in the resin (i.e. flexible chains versus crystalline).[59] Solid state NMR peak widths are sensitive to these factors and what is observed spectrally depends strongly on acquisition conditions used.
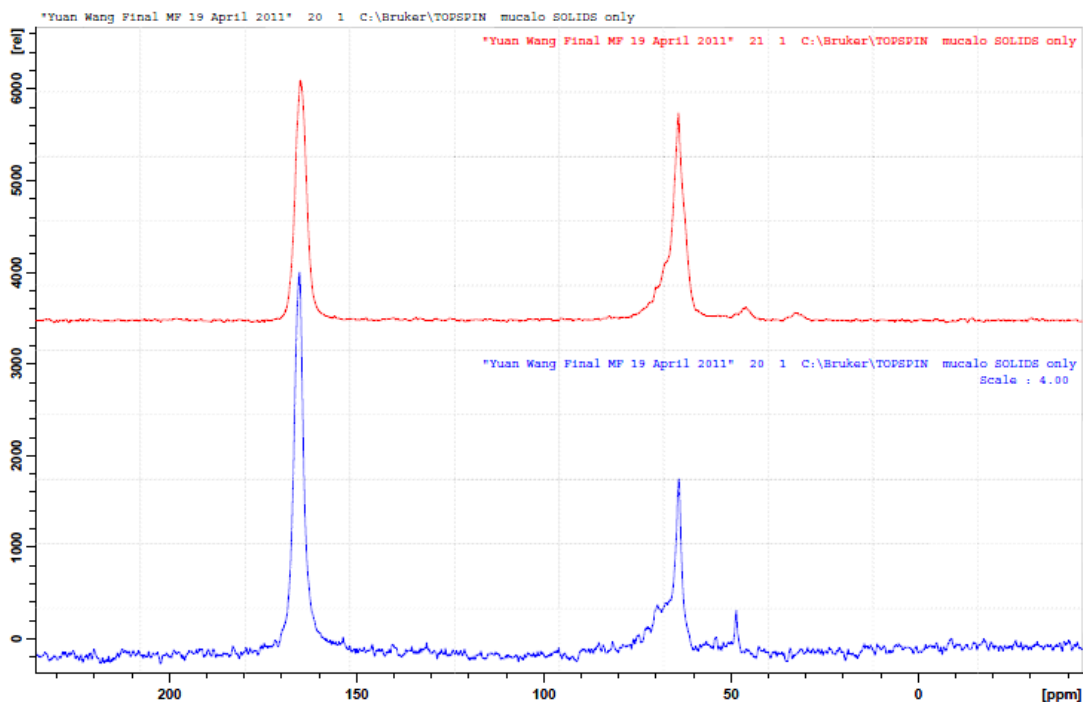
Figure 4.11 Overlaid spectra of the final resin (control) sample acquired under the CP (red, top) and the HP DEC (blue, bottom) pulse programs.

The comparison of the final resin samples acquired using the CP and the HP decoupling pulse programs confirm that the peak at 48 ppm is not a spinning side band therefore it is very likely the signal produced by the methylene linkage. The technique of solid state NMR is not quantitative thus these are shown merely as confirmation of the linkage groups present in the resin system.

4.3.2 Fourier transform infrared spectroscopy

Fourier transform infrared spectroscopy (FT-IR) was employed on samples of melamine and the final melamine formaldehyde resins as a complementary technique to NMR. Several FT - IR methods were carried out including thin film, ATR, microscope and KBr disk.

The techniques of thin film, ATR and microscope produced spectra which were not optimum, however the spectra obtained from KBr disks provided spectra which showed clearly the changes of absorption patterns between melamine and the melamine formaldehyde resins.

The representative IR spectrum of melamine, melamine formaldehyde resin and both spectra overlaid for comparison is given in Figure 4.12, Figure 4.13 and Figure 4.14 respectively.
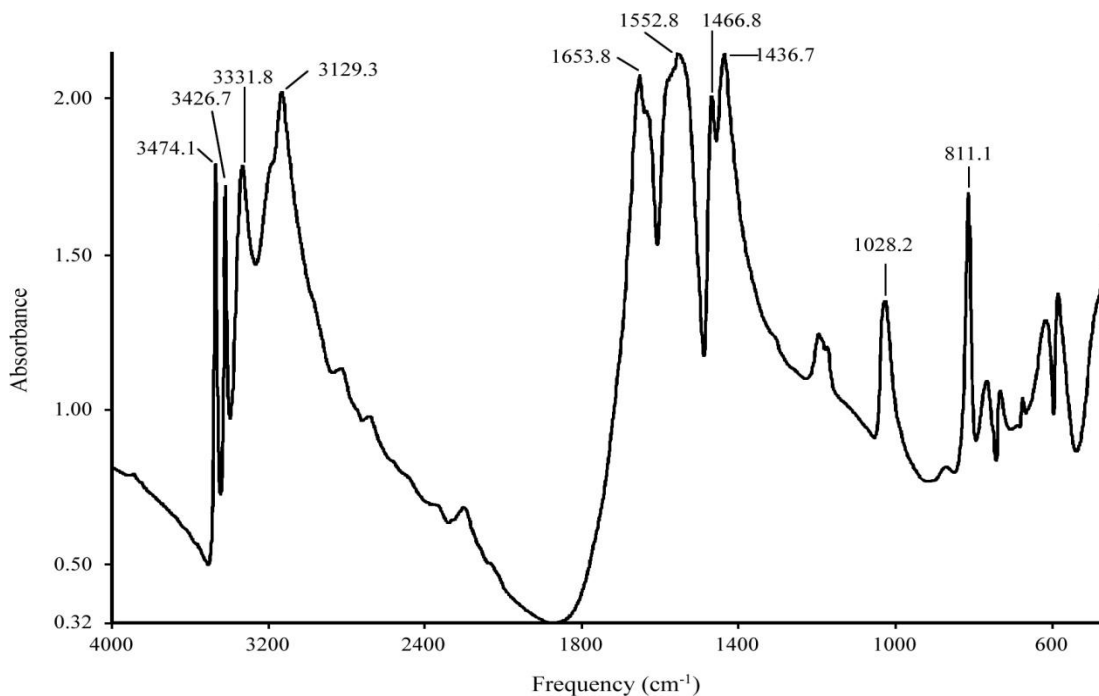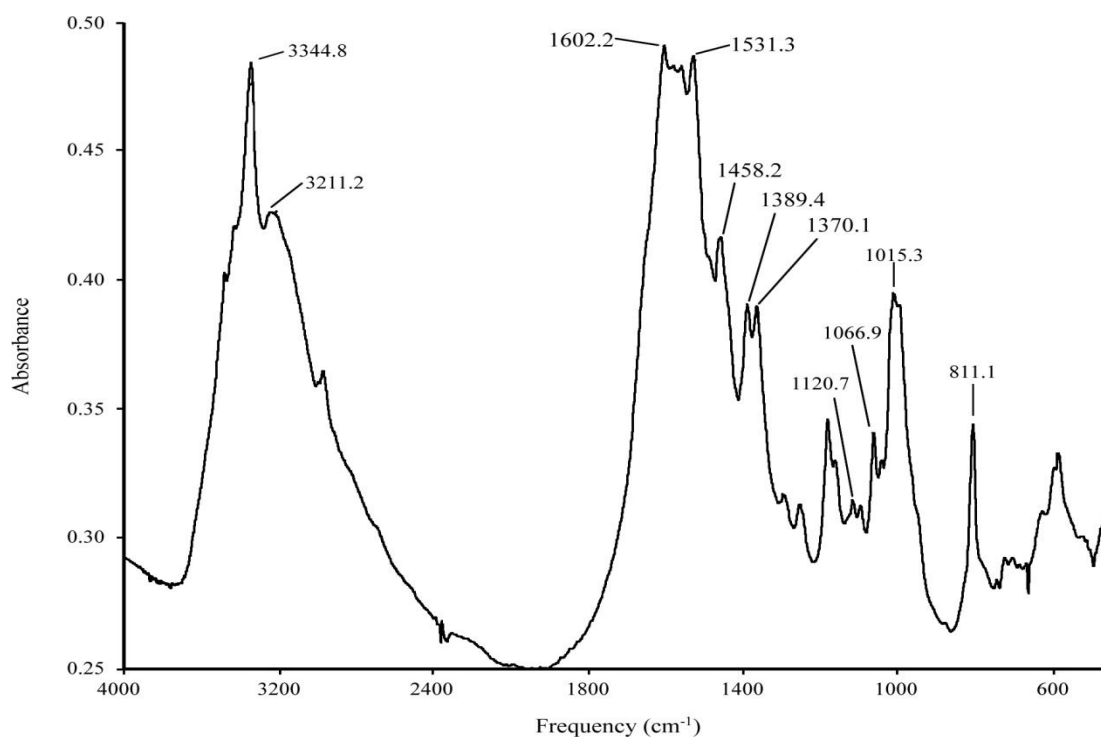

Figure 4.12 Representative FT - IR spectrum of melamine

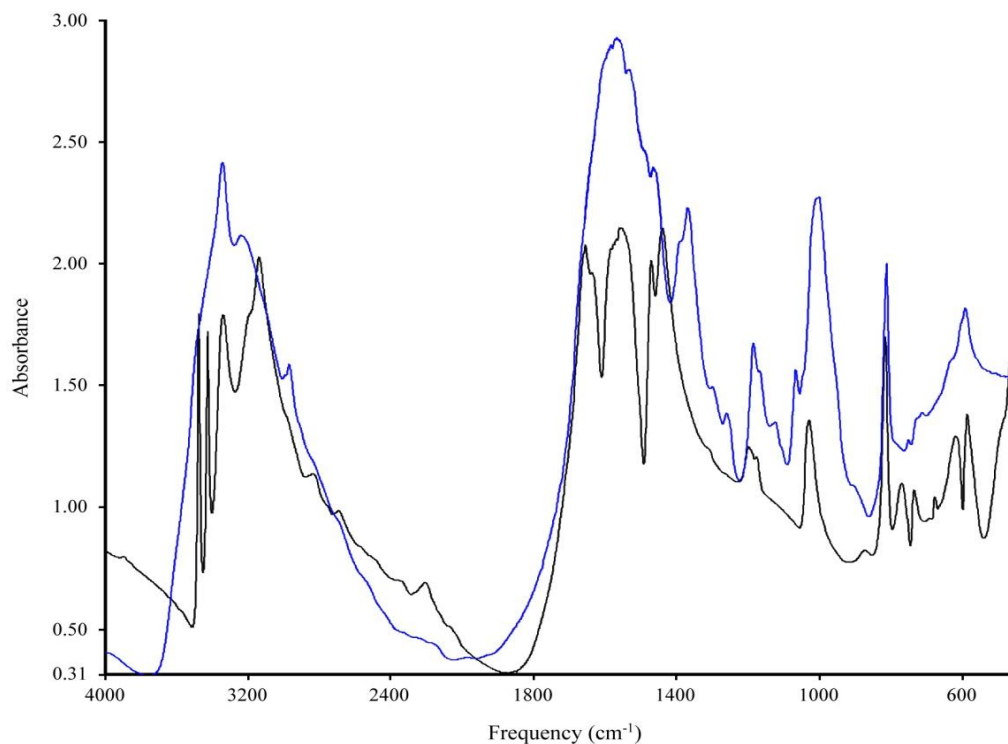**Figure 4.13 Representative spectrum of melamine formaldehyde resin**

Figure 4.14 Overlapped FT - IR spectra of melamine (black) and melamine formaldehyde spectra (blue)

101

All the major absorption signals of melamine and melamine resin were assigned according to the literature values.[34, 60- 62] The assignments of peaks in melamine and melamine formaldehyde resin are shown in Table 4.1 and Table 4.2 respectively.

Table 4.1 The infrared absorptions of melamine corresponding to the nature of the assignments

Wave number (cm^{-1})	Assignment	Nature
3500 - 3400	NH$_2$ stretch	Primary amine
3300 - 3100	NH stretch	Melamine
1650 - 1400	C=N stretch	Triazine ring of melamine
1015 - 1030	C-N stretch	Primary amine
810 - 820	Triazine out of plane bend	Triazine ring of melamine

Table 4.2 The infrared absorptions of melamine formaldehyde resin corresponding to the nature of the assignments

Wave number (cm^{-1})	Assignment	Nature
3300 - 3100	NH stretch	Secondary symmetric and asymmetric amines
1650 - 1450	C=N stretch	Triazine ring
1330-1400	C-N stretch	Secondary and tertiary amine
1120	C-O-C stretch	Ether linkage group
1066	C-O stretch	Ether linkage group
1015	C-N stretch	Primary amine
810 - 820	Triazine out of plane bend	Melamine

Description of the major absorptions observed are provided below

Melamine IR spectrum:

The several sharp narrow peaks ranging from 3500 - 3400 cm^{-1} can be assigned as the primary amine group (NH$_2$) on the melamine spectra. A broad peak ranging from 3300 - 3100 cm^{-1} is assigned as the secondary (NH) and tertiary amine stretch. The broad absorption band in the range of 1650 - 1400 cm^{-1} is attributed to the stretching vibrations of the C=N bonds in the triazine ring of melamine. 1021 cm^{-1} is assigned as the C-N stretch with primary amines and tertiary carbon.

MF resins:

A broad peak ranging from 3300 - 3100 cm^{-1} is assigned as the secondary (NH) and tertiary amine stretch. Another broad peak in the region of 1650 - 1500 cm^{-1} arises due to the C=N stretch in the triazine ring. The weak absorption band between 1300 - 1400 cm^{-1} is the C-N stretch of the secondary and the tertiary amine groups. The two very weak absorption bands at 1120 and 1066 cm^{-1} correspond to C-O-C (ether) stretch and C-O stretch due to the dimethylene ether. The medium intensity of 1015 cm^{-1} is assigned as the C-N primary amine stretch.

When the melamine reacts with formaldehyde, the primary amine (NH$_2$) stretch is no longer observed. This confirmed by the increase in the intensity of C-N stretch corresponding to secondary and tertiary amine group. The presence of C-O-C is also observed in the resin spectrum indicating the presence of cross linkage. The results show good agreement with the absorptions reported by Chen *et al.*[34] and Chiu *et al.*[60]

Although major differences are seen between the melamine and the resin product, the FT - IR spectra appears to be highly overlapped with common signals making interpretation less reliable.

4.3.3 MALDI-TOF-MS

MALDI - TOF analysis was conducted due to its potential ability to observe the oligomers present within the final resin sample.[63] ESI - MS analysis was also carried out on the final resin however, results were unreliable. Figure 4.12 shows the MALDI spectrum of the final resin resin, with the use of dithranol as the matrix.
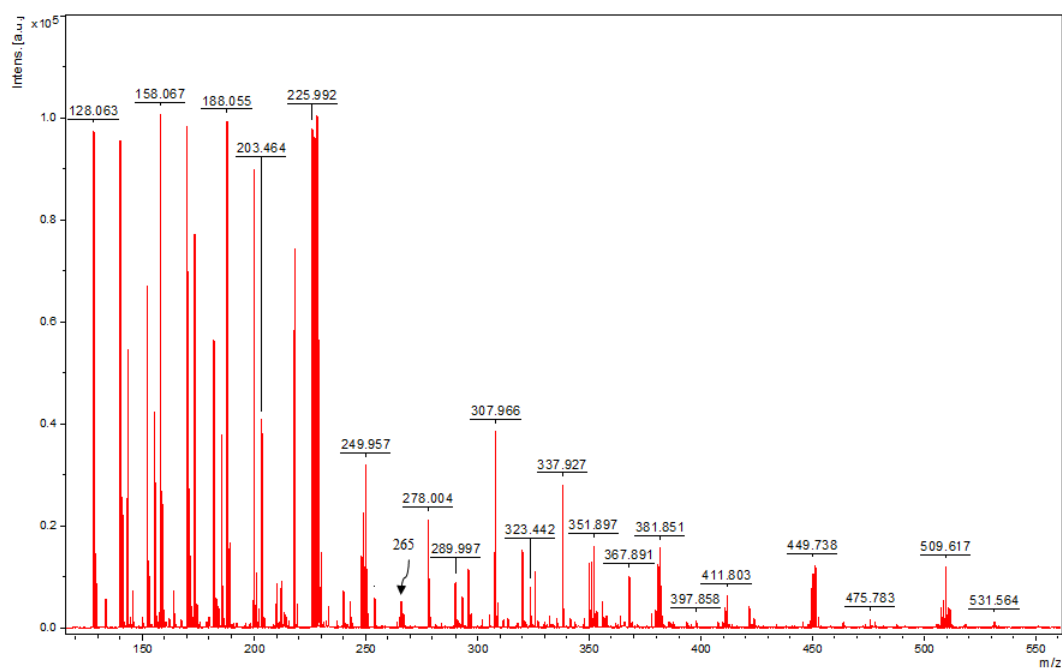

Figure 4.15 MALDI - TOF spectrum of sample with dithranol as a matrix

Table 4.3 The area and intensity of the mass peaks of interest

m/z	Intensity	Area
128.063	107384.6	12237
140.065	104306.5	15270
158.067	113043.5	14732
170.063	108006.4	17848
188.055	110670.4	12949
200.053	96369.01	11388
218.024	77095.33	6865
264.905	2092.74	219
295.967	11875.7	1206
325.928	11057.91	1167
355.895	5042.71	547
385.877	1169.57	181
415.846	371.33	41
445.82	1261.71	142
475.783	1480.3	210

The series of peaks with *m/z* values 140,170 and 200 Da could possibly result from $M\text{-}CH_2^+$ or $M\text{=}CH_2$, $OHCH_2\text{-}M\text{-}CH_2^+$ and $CH_2\text{=}M\text{-}(CH_2OH)_2$ fragments respectively. If the mass difference of 1 Da is disregarded then this set of data is comparative to Zanetti *et al.*[45]

Table 4.4 Mass to charge ratio of substituted melamine determined by MALDI - TOF

	Mass to charge ratio (*m/z*)		
	Mass	**[M+H]⁺**	
		Observed	**Expected**
Melamine	126	128	127
Monomethylol melamine	156	158	157
Dimethylol melamine	186	188	187
Trimethylol melamine	216	218	217

The mass peaks corresponding to two melamine molecules with different link group(s) were also observed. The peak at *m/z* 265 corresponds to the two melamines linked by

a CH_2 group, i.e. M-CH_2-M, whereas *m/z* 325, 355, 385, 415, 445 and 475 are the signals that result from ether linkages (X = CH_2OCH_2 or H) between the two melamine groups, shown in Figure 4.11 (where n = 1-7).
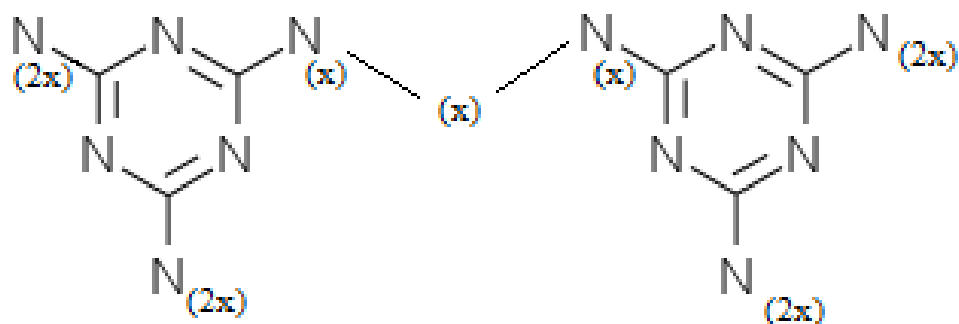
where x = CH_2OCH_2 or H
n = no. of x which is CH_2OCH_2

Figure 4.16 The structure of 2 melamine molecules with different numbers of linkage groups

Although the MALDI-TOF analysis method is not a quantitative technique, the intensities of the mass peaks of the ether species compared to the methylene species suggests that there are more ether species in the final resin. This supports the results from the NMR section whereby the ratio of ether linkages is higher than that of the methylene linkages.

5 Conclusion and Recommendations

5.1 Conclusion

This investigation of melamine formaldehyde resin showed *in situ* formation reactions can be monitored with a 400 MHz NMR using a 5 mm probe, despite the reduced sample size compared with the NMR methods previously employed by Zeng and Woolley to obtain quantitative results through the use of a qualitative NMR acquisition method.

The main parameter that was required when applying these methods to melamine formaldehyde resins was the determination of the longitudinal relaxation time (T_1) of all species in the reaction. Once the T_1s were deduced, the repetition times of the quantitative and the qualitative NMR acquisition methods could be established.

It was found that the sequential addition of melamine followed by formaldehyde was not the best way of sample preparation for NMR real time analysis since the NMR spinning of 20 Hz did not adequately mix the reagents. Vigorous premixing of all the reagents prior to introduction into the NMR for analysis provided results which were not affected as much.

NMR methods were developed in this study, which allow the identification and quantification of the chemical species involved in the formation reaction. The monitoring of the reaction *via* reaction profiles of each species shows the relative concentration changes of these species during a real time *in situ* NMR experiment of melamine formaldehyde resins.

The results of real time monitoring by the reaction profile shows that the requirement of the relative ratio of cross linkage between the melamine for a resin which has reached the IRE is ether to methylene ratio of 2:1. This information can contribute to

further research in the field of quantitative real time reaction monitoring of melamine formaldehyde resins for the plywood and LVL industries

5.2 Future development

Future development could include variation of resin synthesis parameters such as pH, stoichiometry, addition of catalyst and temperature to investigate the structural changes and compare them to the physical properties of the effects of each parameter.

The enrichment of ^{15}N to the resins could enable ^{15}N NMR studies This could offer new information on the structure since the backbone of melamine resins contain high levels of nitrogen.

More work needs to be carried out on using MALDI - TOF - MS and ESI - MS to confirm the results acquired and provide further details to the sub reactions during the reaction course.

Since there are a wide range of mixed melamine resins, including melamine urea formaldehyde (MUF) and MUF with a portion of phenol added to it (PMUF). The parameters obtained from this research can be used as a guide, and further adapted for *in situ* real time quantitative analysis of the reaction process of these resins.

6 References

1.   Bray, P. S.; Anderson, K. B., Identification of carboniferous (320 million years old) class IC amber. *Science* **2009,** *326* (5949), 132-134.

2.   Grimaldi, D., Pushing back amber production. *Science* **2009,** *326* (5949), 51-51.

3.   Theophrastus. In *The Penny Cyclopedia of the Society for the Diffusion of Useful Knowledge*, Long, G., Ed. Knight, C: London, 1842; Vol. 24, pp 332-334.

4.   Sayed, Z. E. Queen Hatshepsut's expedition to the land of the punt: The first oceanographic cruise? http://ocean.tamu.edu/Quarterdeck/QD3.1/Elsayed/elsayedhatshepsut.html (accessed 3-9-2012).

5.   Brydson, J. A., *Plastics Materials*. Sixth ed.; Butterworth-Heinemann: Oxford, 1995; p 2-874.

6.   May, C. A., *Epoxy Resins Chemistry and Technology*. 2nd ed.; Marcel Dekker Inc: Watsonville, 1988.

7.   Woolley, S. L. Real time NMR analyses of phenolic resin reactions. MSc, University of Waikato, Hamilton, 2008.

8.   Gardziella, A.; Pilato, L. A.; Knop, A., *Phenolic Resin, Chemistry, Applications, Standarization, Safety and Ecology*. 2nd ed.; Springer-Verlag: Berlin, 2000.

9.   Saunders, K. J., *Organic Polymer Chemistry*. 2nd ed.; Chapman & Hall: Bristol, 1988; p 349-357.

10.   Weldon, *SRI: The Founding Years*. Publishing Services Center: distributed by W. Kaufmann: Los Altos, California, 1980; p 97.

11.   Chanda, M.; Roy, S. K., *Industrial Polymers, Specialty Polymers, and their Applications*. Taylor & Francis: Boca Raton, 2009.

12.   Diem, H.; Matthias, G., Amino resins and Plastics. In *Ullmann's Encyclopedia of Industrial Chemistry*, Sixth ed.; Wiley-VCH: Weinheim, 1998.

13.   Williams, L. L., Amino resins and plastics. In *Kirk-Othmer Encyclopedia of Chemical Technology*, John Wiley and Sons Inc: Electronic release, 2002; Vol. 2, pp 618-652.

14.   Pizzi, A., Melamine Formaldehyde Adhesives. In *Handbook of Adhesive Technology*, Second ed.; Pizzi, A.; Mittal, K. L., Eds. Marcel Dekker: New York, 2003; pp 653-680.

15.   Binder, W. H.; Dunky, M.; Jahromi, S., Melamine resins. In *Kirk-Othmer Encyclopedia of Chemical Technology*, John Wiley & Sons, Inc.: New York, 2000; Vol. Vol 15, pp 1-30.

16.   Pizzi, A., *Advanced Wood Adhesives Technology*. Marcel Dekker Inc: New York, 1994.

17.   Zeng, H. Studies of the formation and properties of urea-formaldehyde resin adhesives Ph.D., University of Waikato, Hamilton, 2001.

18.   Rätzsch, M.; Bucka, H.; Ivanchev, S.; Pavlyuchenko, V.; Leitner, P.; Primachenko, O. N., The reaction mechanism of the transetherification and crosslinking of melamine resins. *Macromolecular Symposia* **2004,** *217* (1), 431-443.

19.   Hesse, W., Phenolic resins. In *Ullmann's Encyclopedia of Industrial Chemistry*, Wiley-VCH Verlag GmbH & Co. KGaA: 2000.

20.   Williams, L. L., Amino resins. In *Encyclopedia of Polymer Science and Technology*, John Wiley 2002.

21.   Snyder, D. M.; Vuk, T. J., Self-condensation of aqueous hexa(methoxymethyl) melamine: Effects of concentration, pH, and alcohol content. *Journal of Applied Polymer Science* **1992,** *46* (7), 1301-1306.

22.   Field, L. D.; Sternhell, S., *Analytical NMR*. John Wiley: Chichester, 1989.

23.   Günther, H., *NMR spectroscopy*. 2nd ed.; John Wiley and Sons: Chichester, 1995; p 581.

24. Friebolin, H., *Basic One- and Two-Dimensional NMR Spectroscopy*. Fourth ed.; Wiley: Weinheim, 2005; p 406.

25. Derome, A. E., *Modern NMR Techniques for Chemistry Research*. Pergamon Press: Oxford, 1987; Vol. 6.

26. Sanders, J. K. M.; Hunter, B. K., *Modern NMR Spectroscopy*. Oxford University Press: New York, 1986; p 308.

27. Akitt, J. W.; Mann, B. E., *NMR and Chemistry- An Introduction to Modern NMR Spectroscopy*. Fourth ed.; Stanley Thornes: UK, 2000; p 400.

28. Jacobsen, N. E., *NMR spectroscopy explained simplied theory, applications and examples for organic chemistry and structural biology*. John Wiley & Sons, Inc.: Hoboken, New Jersey, 2007; p 668.

29. Irrgeher, M.; Schmidt, H.; Bretterbauer, K.; Gabriel, H.; Schwarzinger, C., Synthesis, characterisation, and polymerisation of vinylmelamines. *Monatsh Chem* **2011,** *142* (8), 849-854.

30. Scheepers, M. L.; Meier, R. J.; Markwort, L.; Gelan, J. M.; Vanderzande, D. J.; Kip, B. J., Determination of free melamine content in melamine-formaldehyde resins by Raman spectroscopy. *Vibrational Spectroscopy* **1995,** *9* (2), 139-146.

31. Jahromi, S., Storage stability of melamine-formaldehyde resin solutions, 1. The mechanism of instability. *Macromolecular Chemistry and Physics* **1999,** *200* (10), 2230-2239.

32. Ji, S.; Crews, G. M.; Pittman, C. U.; Wang, Y.; Ran, R., Ammeline–melamine–formaldehyde resins. Preparation and properties. *Journal of Polymer Science Part A: Polymer Chemistry* **1996,** *34* (13), 2543-2561.

33. Kohlmayr, M.; Zuckerstätter, G.; Kandelbauer, A., Modification of melamine-formaldehyde resins by substances from renewable resources. *Journal of Applied Polymer Science* **2012,** *124* (6), 4416-4423.

34. Chen, W.-C.; Wu, S.-Y.; Liu, H.-P.; Chang, C.-H.; Chen, H.-Y.; Chen, H.-Y.; Tsai, C.-H.; Chang, Y.-C.; Tsai, F.-J.; Man, K.-M.; Liu, P.-L.; Lin, F.-Y.; Shen, J.-L.; Lin, W.-Y.; Chen, Y.-H., Identification of melamine/cyanuric acid-containing nephrolithiasis by infrared spectroscopy. *Journal of Clinical Laboratory Analysis* **2010,** *24* (2), 92-99.

35.   Kandelbauer, A.; Despres, A.; Pizzi, A.; Taudes, I., Testing by fourier transform infrared species variation during melamine–urea–formaldehyde resin preparation. *Journal of Applied Polymer Science* **2007,** *106* (4), 2192-2197.

36.   Sato, K.; Maruyama, K., Studies on formaldehyde resins, 18. Kinetics of acid-catalyzed hydrolysis of bis(hydroxymethyl)melamine. *Die Makromolekulare Chemie* **1981,** *182* (8), 2233-2243.

37.   Sato, K.; Yamasaki, K., Studies on formaldehyde resins, 15. Base-catalyzed hydrolysis of bis(hydroxymethyl)melamine. *Die Makromolekulare Chemie* **1978,** *179* (4), 877-885.

38.   Widmer, G., *Paint, oil and chemical review*. Trade Review Co.: 1949; Vol. 112, p 18,26,28,30,32.

39.   Hirt, R. C.; King, F. T.; Schmitt, R. G., Detection and estimation of melamine in wet-strength paper by ultraviolet spectrophotometry. *Analytical Chemistry* **1954,** *26* (8), 1273-1274.

40.   Blank, W. J., Reaction mechanism of amino resins. *Coatings Technology* **1979,** *51* (656), 61-70.

41.   Chang, T. T., Characterization of (methoxymethyl)melamine resins by liquid chromatography/mass spectrometry. *Analytical Chemistry* **1994,** *66* (19), 3267-3273.

42.   Tomita, B.; Ono, H., Melamine–formaldehyde resins: Constitutional characterization by Fourier transform 13C-NMR spectroscopy. *Journal of Polymer Science: Polymer Chemistry Edition* **1979,** *17* (10), 3205-3215.

43.   Subrayan, R. P.; Jones, F. N., 13C-NMR studies of commercial and partially self-condensed hexakis(methoxymethyl)melamine (HMMM) resins. *Journal of Applied Polymer Science* **1996,** *62* (8), 1237-1251.

44.   Scheepers, M. L.; Adriaensens, P. J.; Gelan, J. M.; Carleer, R. A.; Vanderzande, D. J.; De Vries, N. K.; Brandts, P. M., Demonstration of methylene-ether bridge formation in melamine-formaldehyde resins. *Journal of Polymer Science Part A: Polymer Chemistry* **1995,** *33* (6), 915-920.

45.   Zanetti, M.; Pizzi, A.; Beaujean, M.; Pasch, H.; Rode, K.; Dalet, P., Acetals-induced strength increase of melamine–urea–formaldehyde (MUF)

polycondensation adhesives. II. Solubility and colloidal state disruption. *Journal of Applied Polymer Science* **2002,** *86* (8), 1855-1862.

46. Angelatos, A. S.; Burgar, M. I.; Dunlop, N.; Separovic, F., NMR structural elucidation of amino resins. *Journal of Applied Polymer Science* **2004,** *91* (6), 3504-3512.

47. Egger, C. C.; Schadler, V.; Hirschinger, J.; Raya, J.; Bechinger, B., H-1-C-13 CPMAS and T-2 relaxation solid-state NMR measurements of melamine-based polycondensed chemical gels. *Macromolecular Chemistry and Physics* **2007,** *208* (19-20), 2204-2214.

48. Pretsch Erno; Buhlmann, P.; Badertscher, M., *Structure Determination of Organic Compounds*. 4th ed.; Springer: Berlin, 2009; p 433.

49. Tomita, B.; Matsuzaki, T., Cocondensation between resol and amino resins. *Industrial & Engineering Chemistry Product Research and Development* **1985,** *24* (1), 1-5.

50. Müller, K., NMR spectroscopy of polymers. *Acta Polymerica* **1995,** *46* (1), 86-86.

51. Mirau, P. A., *A Practical Guide to Understanding the NMR of Polymers*. Wiley-Interscience: New York, 2005.

52. Koenig, J. L., *Spectroscopy of Polymers*. 2nd ed.; Elsevier Science Inc: New York, 1999.

53. Gordon, M.; Halliwell, A.; Wilson, T., Kinetics of the addition stage in the melamine–formaldehyde reaction. *Journal of Applied Polymer Science* **1966,** *10* (8), 1153-1170.

54. Okano, M.; Ogata, Y., Kinetics of the condensation of melamine with formaldehyde. *Journal of the American Chemical Society* **1952,** *74* (22), 5728-5731.

55. Simmonds, R. J.; Dua, G., The geometry of N-hydroxymethyl compounds. Part 5. Studies on ground-state geometry and reactions of N-(hydroxymethyl)pentamethylmelamine and related compounds using MNDO calculations. *Journal of the Chemical Society, Perkin Transactions 2* **1995,** (3), 469-476.

56.   Huang, Y.; Jones, F. N., Synthesis of crosslinkable acrylic latexes by emulsion polymerization in the presence of etherified melamine-formaldehyde (MF) resins. *Progress in Organic Coatings* **1996,** *28* (2), 133-141.

57.   Bauer, D. R., Melamine/formaldehyde crosslinkers: characterization, network formation and crosslink degradation. *Progress in Organic Coatings* **1986,** *14* (3), 193-218.

58.   Samaraweera, U.; Gan, S.; Jones, F. N., Enhanced reactivity of melamine–formaldehyde resins by fractionation. Crosslinking at ambient temperature. *Journal of Applied Polymer Science* **1992,** *45* (11), 1903-1909.

59.   Mathias, L. J., *Solid State NMR of Polymers*. Plenum Press: New York, 1991.

60.   Chiu, H.-T.; Huang, Y.-C.; Chiang, C.-H., Curing behavior of anionic poly(urethane urea) dispersions crosslinked with partially methylated melamine formaldehyde. *Journal of Applied Polymer Science* **2007,** *106* (2), 849-856.

61.   Glowacz-Czerwonka, D.; Kucharski, M., New melamine-formaldehyde-ketone resins. VI. Preparation of filled molding compositions and compression-molding materials from reactive solvents based on cyclohexanone. *Journal of Applied Polymer Science* **2010,** *116* (5), 2802-2807.

62.   Singh, M.; Kumar, V., Preparation and characterization of melamine–formaldehyde–polyvinylpyrrolidone polymer resin for better industrial uses over melamine resins. *Journal of Applied Polymer Science* **2009,** *114* (3), 1870-1878.

63.   Braun, D.; Unvericht, R., Model investigation of the co-condensation of melamine and phenol components in MPF thermoset moulding materials. *Die Angewandte Makromolekulare Chemie* **1995,** *226* (1), 183-195.
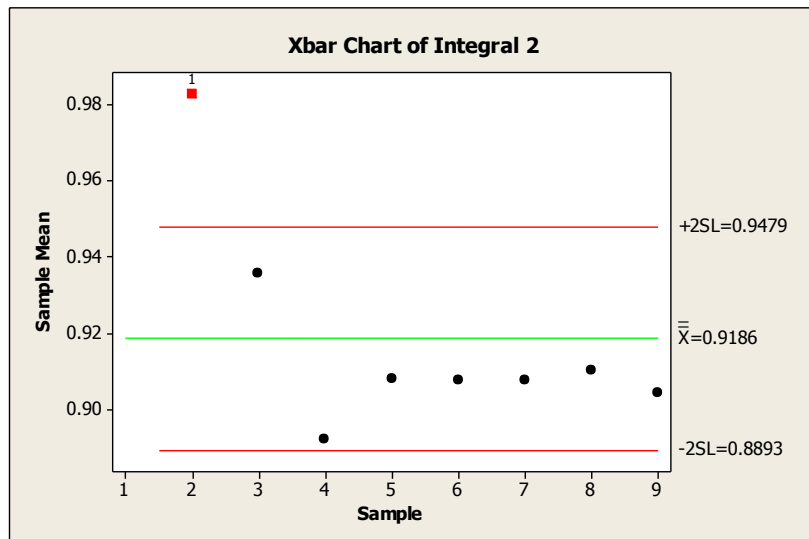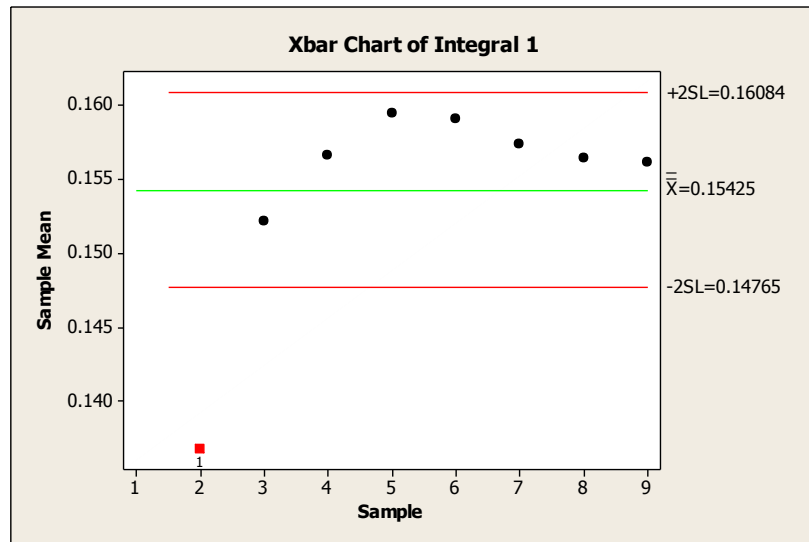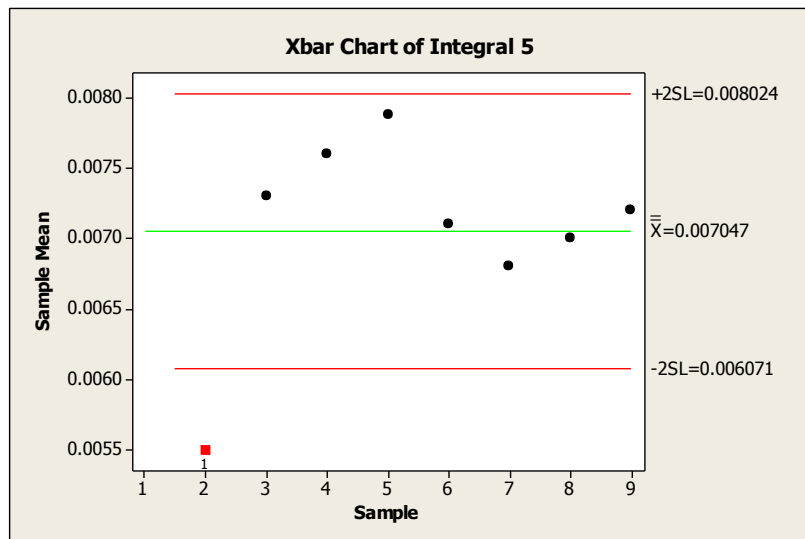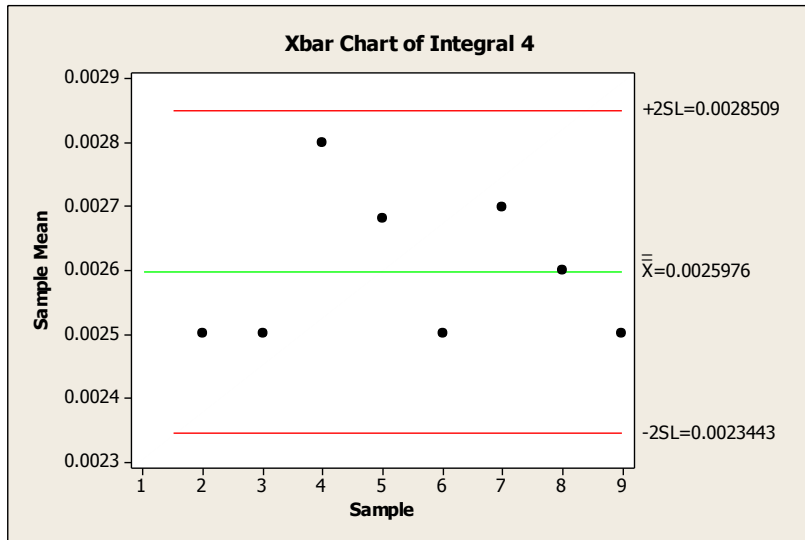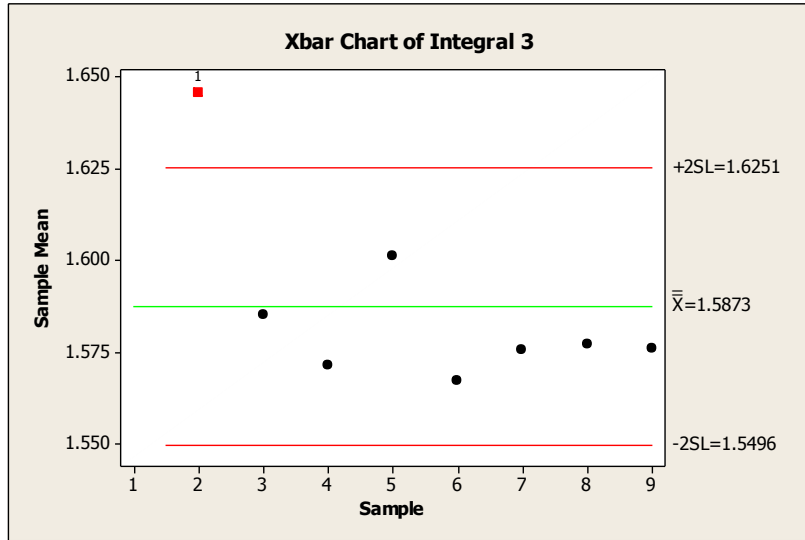
7 Appendix 1

The quality control charts of all the species carried out using quantitative and qualitative conditions. Integrals represent different species specified below
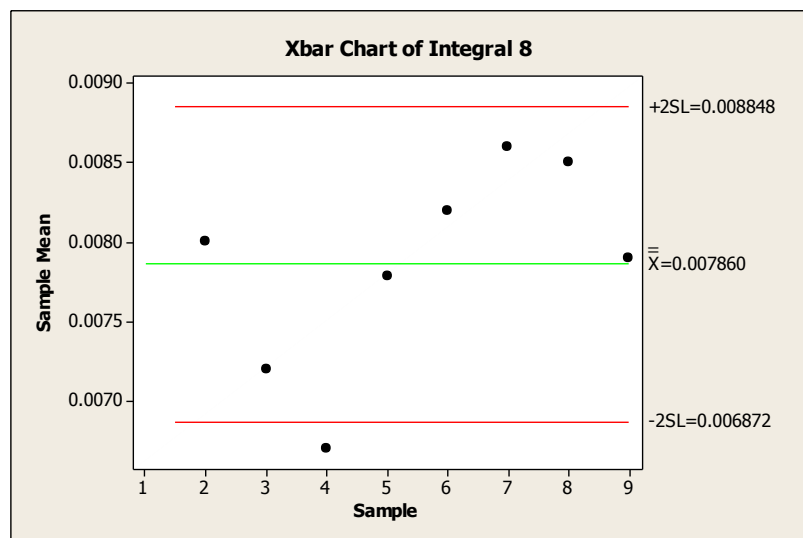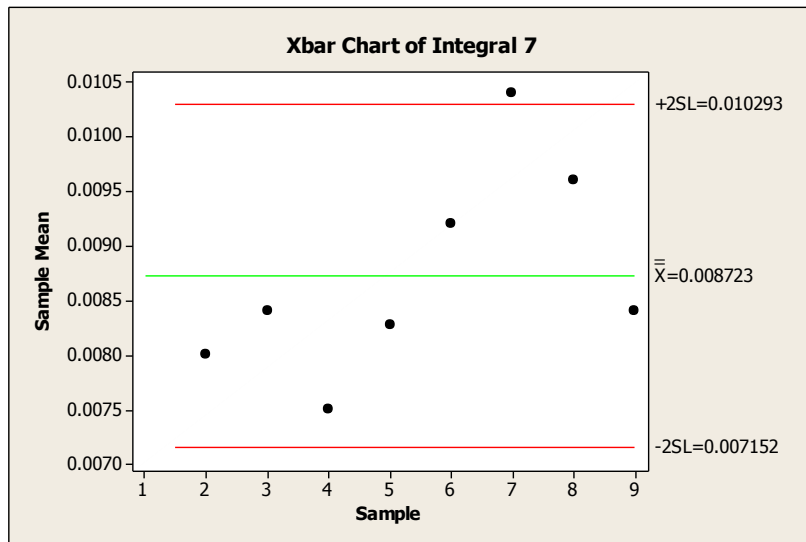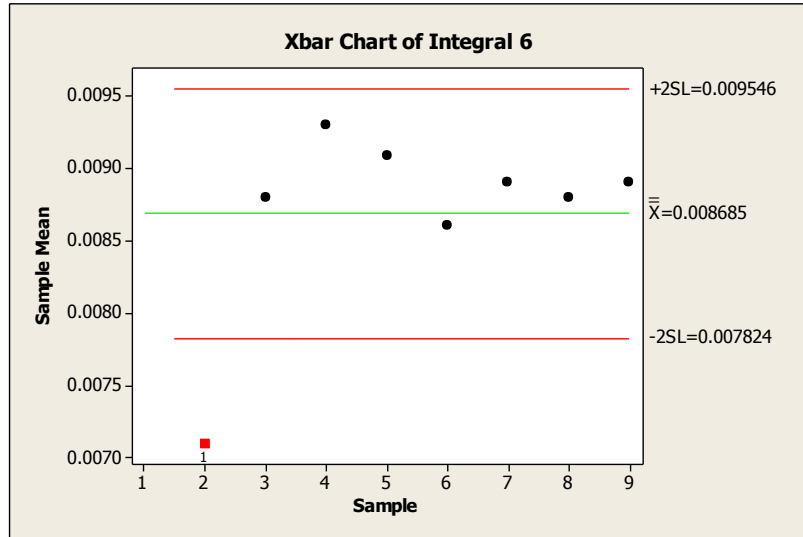
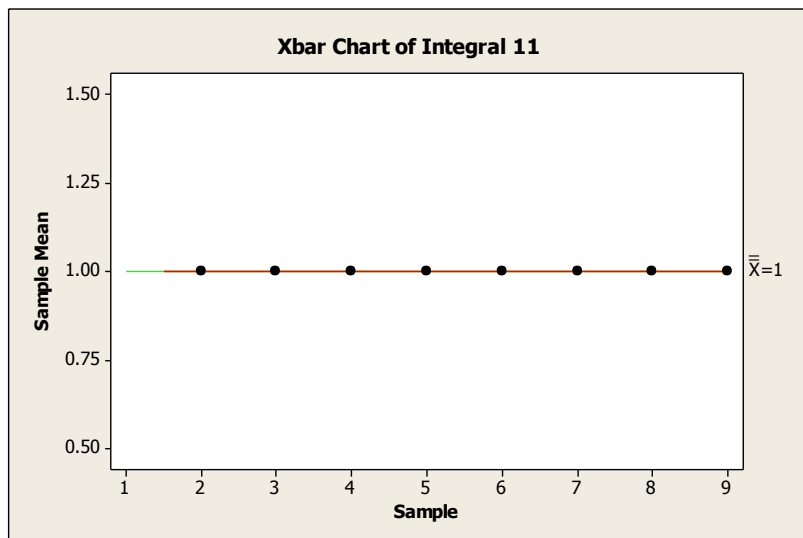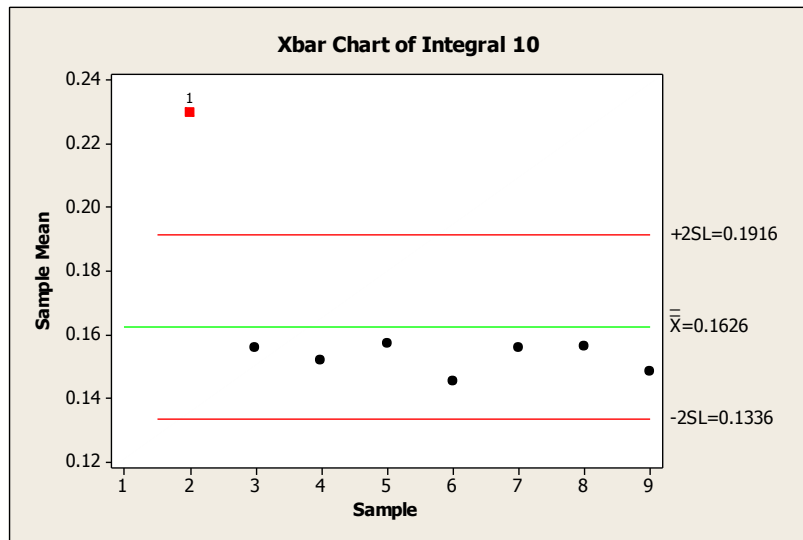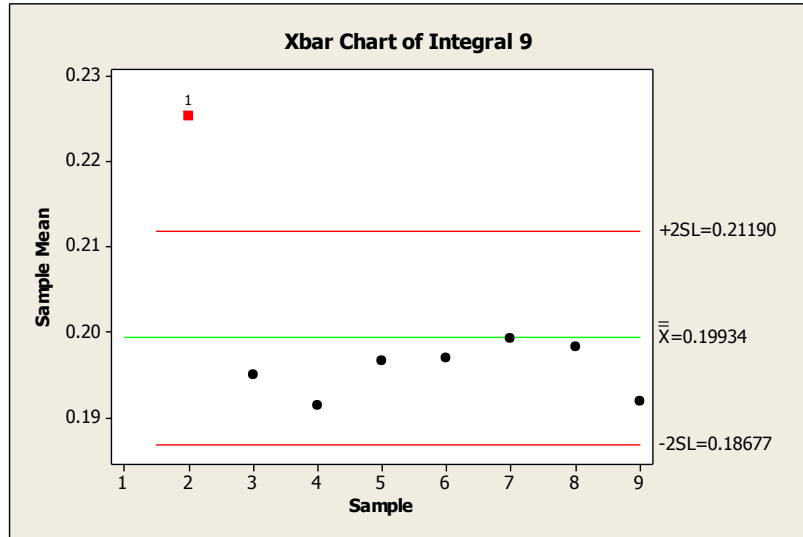| Integral	Signal
1	CH$_3$**CO**OH
2	Triazine carbon with 1 °/2 ° amine
3	Triazine carbon of with tertiary amine
4	Methylene from hemiacetal
5	Dimeric methylene glycol HOCH$_2$OCH$_2$OH
6	Monomeric methylene glycol HOCH$_2$OH
7	Branched dimethylene ether with methylol
8	Branched dimethylene ether with hemiformal methylol
9	Branched methylol
10	Linear dimethylene ether and linear hemiformal methylol
11	Linear methylol
12	Methoxy for hemiacetal
13	Branched methylene
14	Methanol
15	Linear methylene
16	DMSO-d6
17	**CH$_3$**COOH

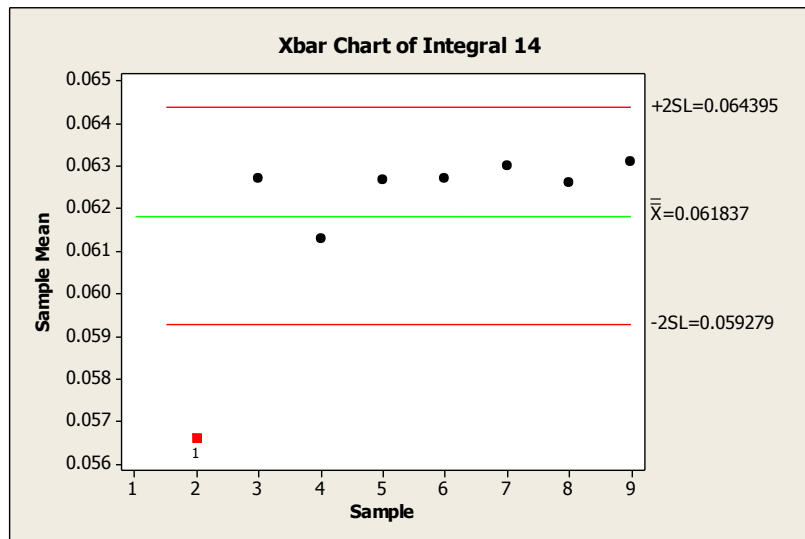(SL on the quality control charts represent the 95% confidence intervals (2SD)

Quantitative quality control charts

Xbar Chart of Integral 1

+2SL=0.16084
$\bar{\bar{X}}$=0.15425
-2SL=0.14765

Xbar Chart of Integral 2

+2SL=0.9479
$\bar{\bar{X}}$=0.9186
-2SL=0.8893

Xbar Chart of Integral 3

+2SL=1.6251

$\bar{\bar{X}}$=1.5873

-2SL=1.5496

Xbar Chart of Integral 4

+2SL=0.0028509

$\bar{\bar{X}}$=0.0025976

-2SL=0.0023443

Xbar Chart of Integral 5

+2SL=0.008024

$\bar{\bar{X}}$=0.007047

-2SL=0.006071

Xbar Chart of Integral 6

+2SL=0.009546
X̿=0.008685
-2SL=0.007824

Xbar Chart of Integral 7

+2SL=0.010293
X̿=0.008723
-2SL=0.007152

Xbar Chart of Integral 8

+2SL=0.008848
X̿=0.007860
-2SL=0.006872

118

Xbar Chart of Integral 9

Xbar Chart of Integral 10

Xbar Chart of Integral 11

Xbar Chart of Integral 12

Xbar Chart of Integral 13

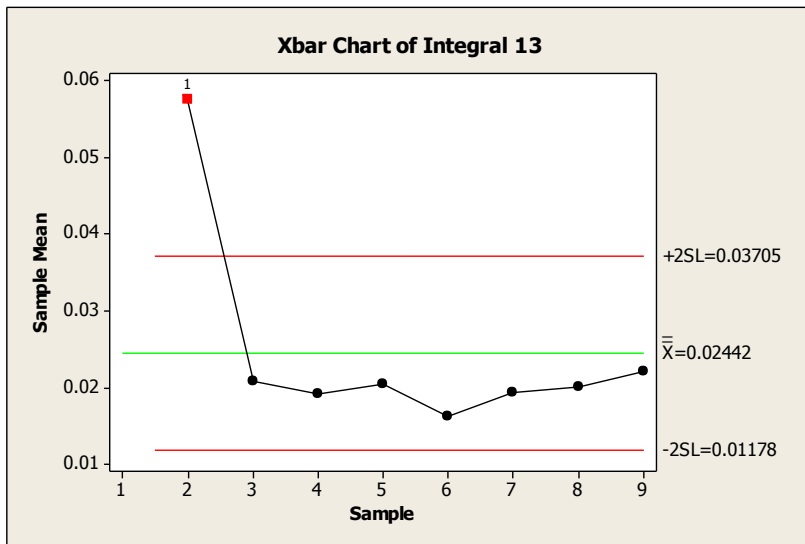Xbar Chart of Integral 14

Xbar Chart of Integral 15

Xbar Chart of Integral 16

Xbar Chart of Integral 17

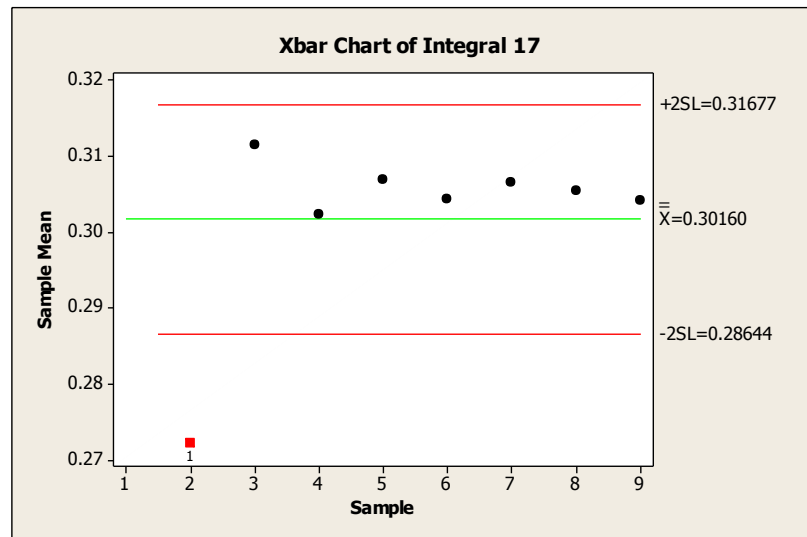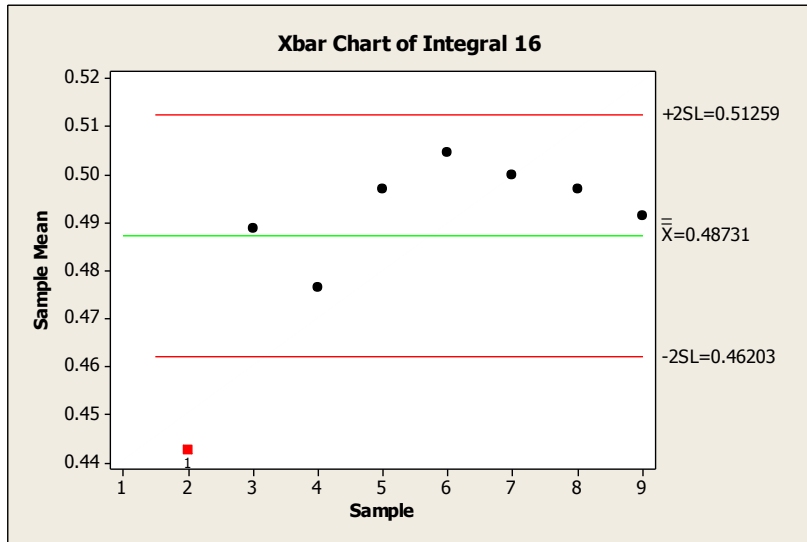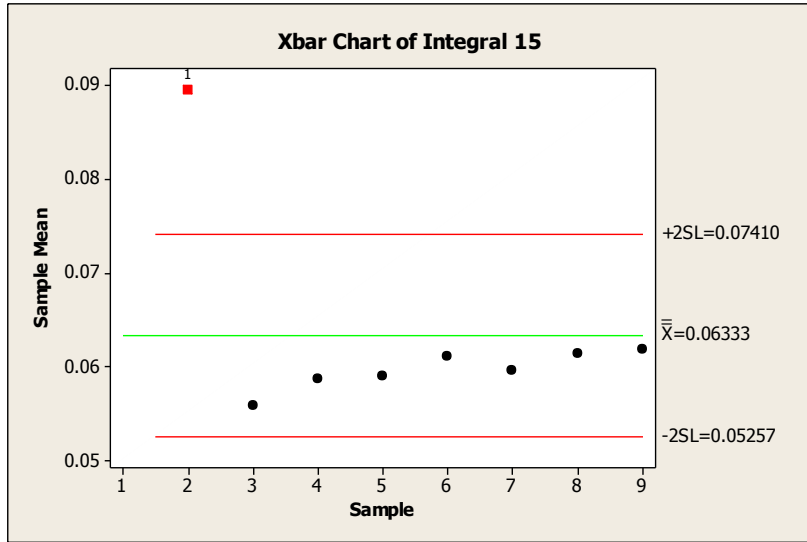# Qualitative quality control charts

Xbar Chart of Integral 3

Xbar Chart of Integral 4

Xbar Chart of Integral 5

Xbar Chart of Integral 6

Xbar Chart of Integral 7

Xbar Chart of Integral 8

Xbar Chart of Integral 9

Xbar Chart of Integral 10

Xbar Chart of Integral 11

Xbar Chart of Integral 12

Xbar Chart of Integral 13

Xbar Chart of Integral 14

Xbar Chart of Integral 15

Xbar Chart of Integral 16

Xbar Chart of Integral 17